Purpose-designed technogenic materials for sustainable urban greening

vorgelegt von:
M.Sc.
Flores Ramírez, Eleonora
geb. in Distrito Federal, Mexico

von der Fakultät VI - Planen Bauen Umwelt
der Technischen Universität Berlin
zur Erlangung des akademischen Grades

Doktorin der Naturwissenschaften
- Dr. rer. nat.-

genehmigte Dissertation

Promotionsausschuss:
Vorsitzender: Prof. Dr. Gerd Wessolek
Gutachter: Prof. Dr. Martin Kaupenjohann
Gutachterin: Prof. Dr. Christina Siebe Grabach
Gutachter: Prof. Dr. Jean Louis Morel

Tag der wissenschaftlichen Aussprache: 6. Oktober 2017

Berlin 2018

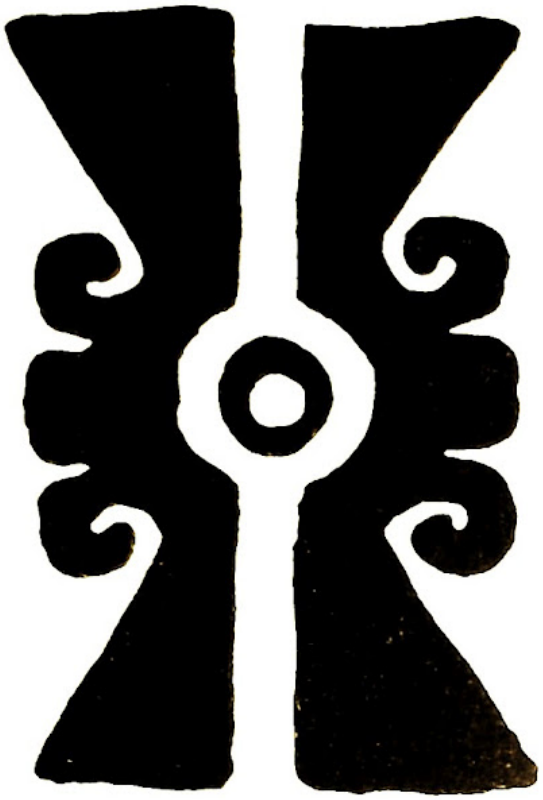

La ciudad no cuenta su pasado, lo contiene como las líneas de una mano, escrito en las esquinas de las calles, en las rejas de las ventanas.

Italo Calvino, Las ciudades invisibles, 1972

Acknowledgements

I would like to warmly thank:

- ⊙ Prof. Martin Kaupenjohann, for supervising my thesis, for his constructive discussions, for his long-term academic support, and his confidence in my work.
- ⊙ Dr. Thomas Nehls, for inviting me to the SUITMA community, for his constant academic support and constructive discussions, and for his valuable contribution to Chapter 4. But above all, for his friendship.
- ⊙ Dr. Stefan Abel, for his constructive discussions and valuable contribution to Chapter 4. For his love and support translated in a diversity of ways. For staying in the long journey.
- ⊙ Dr. Peter Dominik, for sharing his knowledge and his fascination for Fe (hydr)oxides. For his valuable contribution to the development of this thesis.
- ⊙ Dr. Christina Siebe, for sharing so enthusiastically her knowledge about soils, for accepting the SUITMA Congress challenge, and for being the link between Berlin and Mexico. For reviewing this thesis.
- ⊙ Dr. Jean Louis Morel, for the warm welcome to the SUITMA community, and for reviewing this thesis.
- ⊙ Christine Beusch, for proof reading and helping with the bureaucracy process of the thesis. Mais principalmente por ser minha amiga, e compartilhar escritório, risadas e conversas desde o começo.
- ⊙ Katja Kerber and Wilhelm van Husen, for sharing laughs beyond the uni.
- ⊙ The laboratory staff members of the Department of Soil Science Maike Mai, Sabine Dumke & Rautenberg, Claudia Kuntz, Monika Rohrberck, and Iris Pieper, for their patience and kind assistance with the laboratory procedures.
- ⊙ Martin Kern, for his support with all related with computers and for all the shared blaue Donnerstage.
- ⊙ The German Academic Exchange Service (DAAD), for funding (A/10/80578).
- ⊙ The Abel Stiftung, for the long and kind support.
- ⊙ Isabel, Luis, Tania, Melina e Iliusi, por compartir andanzas y amistad en Berlín. It is so good that you are here.
- ⊙ A Margarita, por todo su gran amor, con todo mi gran amor.
- ⊙ A Leonardo, porque siempre está conmigo, aunque no esté.

↬ Berlin

Abstract

Background Urban green areas provide a number of desirable ecosystem services for the environment and city dwellers. However, the substrate preparation for the greenery installation mostly implies the mining a Technosol based on a mixture of mainly recycled materials, to sustain vegetation and to lower the environmental impacts in the production of growing media. In particular, the proposed design aims to cope with water stagnation risk of the soil due to a high precipitation regime. Accordingly, the crucial points of the Technosol design are to have a high hydraulic conductivity and simultaneously retain water and nutrients for proper plant growth. In this specific case, a sandy soil with a dispersed clay fraction is more likely to lead to waterlogging and clogging of technical drainage systems. Instead of clay or silt within the soil matrix, an artificial addition of Fe (hydr)oxides on sand can fulfil necessary chemical characteristics of the soil, and the addition of coarse porous materials in the soil profile can retain enough plant available water while clogging is avoided.

Methods A simple technique to coat and stabilize a synthesized Fe (hydr)oxide (2-line ferrihydrite, 2L-FH) on quartz sand was developed. Afterwards, locally available and recycled ferrihydrites were characterized to reproduce the coating and stabilization process on an dredged sand. Separately, the hydraulic properties of six commercially available coarse porous materials were characterized, pure and mixed with sand. A variety of measurement techniques were used to obtain high-resolution data and a good parametrization of water retention models.

Results The stabilized coated sand is homogeneously covered with ferrihydrite, it is mechanically resistant, and it is effectively P-adsorptive. From the tested recycled ferrihydrites, two out of three ferrihydrites were suitable to develop a stable coating. One ferrihydrite has a high pH due to its high $CaCO_3$ content, and sand coated with it may be used as an amendment for acidic clayey soils. Regarding the characterized commercially available coarse porous materials, four out of six were not effective to retain an appropriate volume of plant available water. However, a theoretical water retention optimum can be achieved, applying a ratio of 1:1 of sand and porlith for the substrate.

Conclusion The desired functionalities of high hydraulic conductivity and simultaneous readily available water for plants can be achieved by a simple design of the growing media. Effective and simple sand coating and ferrihydrite-coating stabilization processes were developed. Further, recycled materials were used to reproduce the processes and successfully obtain an affordable coated sand with low environmental impacts in production, with the potential to be further improved. The resulting functional technogenic material has a chemical reactive surface and a high hydraulic conductivity. Two out of four characterized coarse porous materials are recommended for practical application, as they presented a good performance retaining plant available water, while the other materials showed a rather low water retention. The use of the materials favouring the water retention is recommended, in particular in combination with ferrihydrite coated sand. The composite substrate can fulfill the crucial chemical and hydraulic soil functions intended for a further practical implementation with vegetation.

Zusammenfassung

Hintergrund Urbane Grünflächen stellen eine Vielzahl wünschenswerter Ökosystemdienstleistungen für Umwelt und Einwohner von Städten bereit. Allerdings geht die Bereitstellung von Substraten für die Neuentwicklung urbaner Grünflächen mit dem Abbau wertvoller natürlicher Böden einher.
Um dem entgegenzuwirken, ist das Ziel dieser Arbeit ein künstliches Bodensubstrat zu erzeugen, dessen Herstellung möglichst geringe Umweltauswirkungen besitzt und auf der Verwertung von überwiegend recycelten Materialien basiert. Das Substrat muss speziellen bodenkundlichen Anforderungen entsprechen, welche sich aus dem späteren Einsatz als Pflanzensubstrat, aber auch von klimatischen Einflussgrößen ableiten lassen. So sollte es eine möglichst hohe pflanzenverfügbare Wasserhaltekapazität und ein hohes Nährstoffspeicherungsvermögen aufweisen und gleichzeitig eine ausreichende Wasserleitfähigkeit besitzen um die Entstehung von Staunässe zu vermeiden. Die beiden ersteren Eigenschaften sind bei bindigen Substraten gegeben, jedoch besteht die Gefahr von Staunässe und die Beeinträchtigung der technischen Entwässerungselementen durch einen hohen Feinkornanteil an Ton und Schluff. An Stelle von Ton oder Schluff in der Bodenmatrix kann ein mit Eisen(hydr)oxiden ummantelter Sand die notwendigen chemischen Charakteristika eines Bodens erfüllen, mit der Beimischung von porösen Materialien ein ausreichend hohes pflanzenverfügbares Wasserspeicherungsvermögen gewährleisten werden, während ein Zusetzen des Entwässerungssystem vermieden wird.
Methoden Mit einer einfachen Methode wurde Sand mit synthetisierten Ferrihydriten ummantelt und stabilisiert. Im Anschluss wurden lokal verfügbare und recycelte Ferrihydrite charakterisiert und der Ummantelungs- und Stabilisierungsprozess mit einem Flusssand, welcher als Baggergut anfiel, wiederholt.
Parallel wurden die hydraulischen Eigenschaften von sechs kommerziell erhältlichen, grobkörnigen porösen Materialien unter Anwendung hochauflösender Messmethoden bestimmt. Gleiches erfolgte für die Materialien in Kombination mit Sand. Die Ergebnisse wurden für die Parametrisierung eines Wasserretentionsmodell verwendet.
Ergebnisse Der Sand konnte homogen mit Ferrihydrit ummantelt werden. Die Ummantelung erwies sich als mechanisch stabil und konnte effektiv P adsorbieren. Von den drei analysierten recycelten Ferrihydriten waren zwei geeignet eine stabile Ummantelung zu erzeugen. Ein Ferrihydrit wies aufgrund seines hohen $CaCO_3$-Gehaltes einen hohen pH auf, hiermit ummantelter Sand kann zur Verbesserung von sauren, tonigen Böden verwendet werden.
Die grobkörnigen porösen Substrate zeigten mehrheitlich ein mäßiges pflanzenverfügbares Wasserspeicherungsvermögen. Optimale hydraulische Eigenschaften können nur bei einen entsprechend hohem Anteil der grobkörnigen porösen Materialien in sandigen Substraten erreicht werden.

Schlussfolgerung Die gewünschte Funktionalität von hoher Wasserdurchlässigkeit bei gleichzeitig pflanzenverfügbarer Wasserspeicherung wurde durch ein einfaches Design des Bodensubstrats erreicht. Darüber hinaus konnte eine einfache und effektive Methode für die stabile Ummantelung von Sanden mit Eisen(hydr)oxiden entwickelt werden. Mit dem Einsatz von recycelten Ausgangsmaterialien wurde ein nachhaltiges Pflanzensubstrat geschaffen, welches positive Adsorptionseigenschaften und eine ausreichend hohe Wasserleitfähigkeit besitzt. Die Mehrzahl der grobkörnigen porösen Materialien wies ein mäßiges Wasserspeicherungsvermögen auf, deren sinnvoller Einsatz als kommerzielles Pflanzensubstrat in Bezug auf die Verbesserung von Bodeneigenschaften ist somit fraglich. Nichtsdestotrotz, für die Materialien mit hohem Wasserretentionsvermögen ist der praktische Einsatz durchaus positiv zu bewerten. Besonders in Kombination mit Eisen(hydr)oxid-ummantelten Sanden werden die wichtigsten Eigenschaften, die ein fruchtbares Pflanzensubstrat definieren, erfüllt. Insgesamt zeigt sich somit, dass bei optimalen Mischungsverhältnissen der einzelnen Materialien ein Pflanzensubstrat hoher Qualität erzeugt werden kann. Weitere Untersuchungen sind nötig, um die Laborergebnisse in der Praxisanwendung zu verifizieren.

Contents

List of Tables

List of Figures

1. General Introduction

1.1. Urbanization and soils

Urban areas have an important role for humans since the beginning of the civilizations. Urban settlements have allowed the flourishing of populations in cultural and economic aspects. Cities are cultural hot spots, centralize the government activities, transportation, commerce and usually concentrate also a large number of health centres. But, the consequence of such development always implies a drastic human-made modification of the local environment along with a huge consumption of resources to set up the urban infrastructure and to satisfy the demand of basic services of the population (e.g. housing, food, water).

Therefore, the current expansion of the cities is a growing concern since the projected global population living in cities by 2050 will reach 66 %, and it already reaches 73% and 80 % in Europe and Latin America, respectively (United Nations Population Division 2014). Those facts turn the planning and development of sustainable cities into a worldwide priority.

Among many affections, the urbanization process specifically entails a severe degradation of soils. But highly anthropized soils are not exclusively a phenomenon occurring inside urban areas. The concept of urbanization can be widened to include also the processes that enable the development of the urban areas that happen not necessarily within cities (Lehmann and Stahr 2007). For instance, there is an increasing pressure on the agricultural areas for food supply. Another example can be the supply of raw materials, like metals, and their industrial transformation, which imply the modification and erosion of the mined area, as well as the installation of the roads to carry the metals to the factories. The factories, in turn, modify and pollute their own and surrounding areas, and are more likely to be located in the outskirts of the cities.

In the highly anthropized soils human activity has become the main driver of pedogenesis, participating not only in the modification of the soils but also in their formation (Morel et al. 2014; Huot et al. 2015). Soils modified by the urbanization process are predominantly located in urban, industrial, traffic, mining and military areas, and thus can be joined under the acronym of SUITMA (proposed by W. Burghardt in 1998; Morel et al. 2014). The study of SUITMAs is recent, despite their interdependence with a large percentage of the human population and their severe modifications. The first systematic study of an anthropogenic urban

soil has been registered in 1847, but it was until the 1970s that the number of studies increased, and boosted in the 1990s (Lehmann and Stahr 2007; Burghardt et al. 2015). Nowadays there is a SUITMA Working Group that belongs to the International Union of Soil Sciences (IUSS), Division III–Soil Use and Management.

SUITMAs can present little or no alterations in comparison to the local natural soil –as it is the case of natural soil of protected areas and pseudo-natural soils of large old parks–, or can be completely modified. A gradient of soils in between these two extremes can be found in urban areas simultaneously. Consequently, SUITMAs are modified in very different ways and levels, and present a high horizontal and vertical heterogeneity (Lehmann and Stahr 2007; Rossiter 2007).

SUITMAs can contain different amounts of technogenic materials or artefacts[1]; ranging from few or no artefacts, to a complete anthropogenic composition. According to the World Reference Base for Soil Resources (WRB), soils containing large amounts (>20 % w:w), or made exclusively of artefacts are classified as Technosols, (Lehmann 2006; Rossiter 2007; IUSS Working Group WRB 2015), including the soils sealed by technic hard rock (hard material created by humans, having properties unlike natural rock).

Examples of Technosols can be found at dumping sites, roads, industry settling ponds, but also urban green roof facilities, or archaeological buried areas. In spite of the widespread presence of Technosols, the monitoring of their early stages to mid and long term pedogenesis is scarce (Jangorzo et al. 2013), although is recently increasing (Capra et al. 2015). Huot et al. (2015) analysed the available studies and found that, despite the different and diverse origin of the artefacts that compose the Technosols, the pedological processes occurring can be compared with the ones of natural soils, but tend to be more intense and rapid, specifically at the first stages, while the reactive technogenic materials reach equilibrium. Additionally, the diversity of artefacts within one Technosol that act as parent materials leads

[1] The artefacts (from Latin *ars*, art, and *facere*, to make) are defined by the World Reference Base for Soil Resources, or WRB (IUSS Working Group WRB 2015), as solid or liquid substances that:
1. are one or both of the following:
(a) created or substantially modified by humans as part of an industrial or artisanal manufacturing process; or
(b) brought to the surface by human activity from a depth where they were not influenced by surface processes, with properties substantially different from the environment where they are placed; and
2. have substantially the same properties as when first manufactured, modified or excavated. Examples of artefacts are bricks, pottery, glass, crushed or dressed stone, industrial waste, garbage, processed oil products, mine spoil and crude oil.

to the coexistence of pedogenic processes, that would rarely occur simultaneously in natural soils.

For example, in the research of Séré et al. (2012), even within a three years lapse, processes related to the initial constituent materials were observed, as the leaching of soluble compounds (e.g. vast dissolution of gypsum), loss of constitutive water, as well as aggregation. Scalenghe and Ferraris (2009) monitored for 40 years an Haplic Regosol in which the newly deposited debris differentiated into A/C horizons after four years, and differentiated into O/A/AB/Bw/BC/C horizons by the end of the monitoring. In this same work, the authors emphasize that vegetation colonization was directly related to the topography and the nutrient retention capacity of the soil.

Along with the fast pedological changes, Technosols are either compacted or loose, having extreme densities that ranges from <0.5 to $>1.6\,\mathrm{g\ cm^{-3}}$ (Morel et al. 2014), which lead to modification in the pore system architecture and consequently in the water retention capacity of the soil (Jangorzo et al. 2013). They also have extreme pH values, coarse textures, and, mostly, are highly polluted by both organic and inorganic contaminants (Morel et al. 2014; Huot et al. 2015). Some SUITMAs also face erosion and nutrient depletion. All these alterations of the land cover modify the natural soil functioning. For instance, the sealing or high compaction of large extensions of soil surface –one of the most extended and drastic alterations– have the direct consequence of the loss of vegetation and biodiversity (Burghardt 2006), though it provides stability for urban infrastructure. Additionally, the sealing disables the gas interchange between soil and atmosphere, avoids the water recharge of the aquifers and at the same time it increases the water run-off and the risk of floods. In turn, the loss of vegetation and the soil sealing decreases the rate of evapotranspiration, avoiding the air temperature regulation, which rises the average temperature in the cities, contributing to the so called heat island effect (Santamouris 2001; Burghardt 2006; Scalenghe and Marsan 2009; Albanese and Cicchella 2012). All this in conjunction impacts negatively the welfare of the urban citizens, the costs of urban management, and interferes with the environmental nutrient cycling (Lorenz and Lal 2009).

In spite of their general bad quality, the urban soils generate a wide range of ecosystem services (Bolund and Hunhammar 1999) dependent on their gradient of anthropization. The more vegetation they sustain, the more ecosystem services they provide (Morel et al. 2014). Many studies demonstrate how cities benefit from taking care of the existing green areas and investing in green infrastructure

(De Sousa 2003; Tzoulas et al. 2007). The vegetated soil areas provide services such as micro-climate regulation, air filtration, lower wind speed, lower vulnerability to soil erosion, increase of biodiversity, more effective rainwater drainage that lowers the risks of runoff and flooding, supply of clean water and food, sewage and noise reduction, and other recreational and cultural values (Bolund and Hunhammar 1999; Morel et al. 2014). Consequently, there is a reduction of the urban heat island effect (Wong and Yu 1995; Weng et al. 2004).

1.2. Technosols for greening purposes

Despite their desirability, the installation of new large green areas in densely populated cities is not an easy task. The number of free areas is quite limited and many of them have an inadequate soil quality to sustain vegetation, as mentioned before. In order to cope with this problem, alternative available spaces that were not intended to be vegetated (secondary urban greening; Nehls et al. 2015) are generally used, such as facades and building roofs. Another alternative is to either rehabilitate or reclaim, in the ecological sense, the bad quality available soils. While rehabilitation of a site implies the change to an intermediate state between the degraded and the original state of the area, the reclamation implies a substitution of the degraded state not intended to be like the original state of the area, but a rather functional (Bradshaw 1997). Common techniques of reclamation are drastic and imply the excavation of the degraded soil for the most severe cases and its substitution with other substrates or natural soil (although it is very expensive). Rehabilitation commonly implies the addition of amendments to restore the soil functionality (Katsumi 2015).

Despite the adversities to install urban green areas, fertile substrates have been used to sustain vegetation inside the cities since the antiquity, as testify the iconic ancient Babylonian gardens. Nowadays we can find the same expression, more refined, in the vegetated roofs. Extensive or intensive roof greening intend to provide basic soil functioning through a mixture of substrates, but modern techniques use a large list of highly industrialized and/or costly materials (natural and technogenic, such as geomembranes) and technical facilities, specially for drainage systems.

Another side of the urban greening are the gardens producing food. For instance, Berlin, Germany (Bendt et al. 2013), and Cuba (Altieri et al. 1999) are outstanding examples of the proliferation of civil projects using mixtures of mineral and organic (mainly or sometimes exclusively compost) materials to produce food in the city,

using pots, roofs, small orchards, and other spaces. A further possibility of secondary greening is found in the construction of new large green areas, such as parks or green belts installed in reclaimed or rehabilitated areas. Representative examples can be the large Berlin-located Gleisdreieck park installed over a former marshalling yard (Berlin Senatsverwaltung für Umwelt, Verkehr und Klimaschutz), or the enlargement and covering of the highways A7 in Hamburg, Germany (*Hamburger Deckel*; Melchior 2016), and M-30 in Madrid (*Madrid Río project*; Hernández et al. 2016), both establishing public parks on the top of their roofs.

All these mentioned greening expressions still have deficiencies and counterparts. One is a high consumption of natural soil (Rokia et al. 2014), a non-renewable resource, mostly obtained from the surrounding forested and arable land (Haraldsen and Petersen 2003). Also, many sophisticated materials used for green roofs are expensive and their production involve a considerable investment of energy, although the knowledge about their physical and chemical characteristics is often basic or limited. In contrast, the substrates used for the orchards are mainly economic mixtures composed by mineral amendments and a large proportion of compost, mixed mostly empirically, resulting in a sub-optimal soil structure and performance (e.g. excess of nutrients).

One way to lower the demand of natural soil and to improve the deficiencies mentioned above is to rehabilitate or reclaim the scarce available areas (even if they are highly compacted or sealed) establishing special Technosols composed of well-characterized alternative materials. The traditional removal reclamation process of non-functional soils and its consequent disposal problem can be avoided if a new deep soil profile is directly installed on their top surface.

Applying the current pedogenic knowledge, special Technosols can be constructed. They can be specifically designed to perform the basic soil functioning to sustain vegetation according to the local environmental conditions (*purpose-designed Technosols*), which is based on its potential to provide bioavailable water, nutrients and oxygen, favourable physical and chemical soil conditions (e.g. rootability, CEC, pH, eC), to buffer hazardous substances, and to infiltrate precipitation.

Beside lowering the natural soil consumption, purpose-designed Technosols can reduce the resource and energy input that the use of highly processed materials imply if the Technosols are preferably composed of locally available or waste materials. Thus, installation costs, the pressure of material extraction in nature, and the urban waste disposal problems can considerably be diminished (Séré et al. 2008; Yakovlev et al. 2013; Rokia et al. 2014; Nehls 2015). Following this approach,

some research groups have chosen technogenic materials to develop diverse fertile substrates and construct Technosols using recycled materials like rubber, paper-mill sludge (Rokia et al. 2014), biochar, and bricks (Nehls et al. 2013).

Nevertheless, recycled materials require a more intensive analysis, not only considering their physical properties, but in order to quantify their contamination status, and the risk for human health once used for food production or greenery. If such extra analysis has to be omitted for any reason (e.g. time, costs), then alternative conventional materials can be used. Materials of natural origin (e.g. brown coir or coconut fibre, porlith, lava stones) or further processed (e.g. perlite, clay and schist thermically expanded) are commonly used as amendments in fertile substrates to improve their water availability (Earth Pledge 2005; Oberndorfer et al. 2007; Zhang et al. 2009). Nowadays there are many brands and providers. However, only few materials have been properly characterized. The current available information about the physical and chemical properties of the natural, processed and recycled materials –specially their hydraulic properties– is non-existing or it is often obtained from low resolution measurements which do not deliver detailed information. Thus, the knowledge of their full performance range, and their behaviour when combined with other materials, is not completely understood, and that fact often leads to a sub-optimal use or a misuse of the materials.

Therefore, the extensive characterization of each intended Technosol component will increase the quality of knowledge-based design and construction of Technosols. It will also allow the creation of fully-functional and affordable mixtures of materials, counteracting the sub-optimization. Purpose-designed Technosols then will require less resources, infrastructure and energy, leading to a high functionality via low-tech investment.

1.3. The Hamburger Deckel - a case study

1.3.1. Current project

In order to contribute to the knowledge-based design of Technosols for greening purposes, in this work I propose a basic mixture of materials to be used in a Technosol able to sustain a park installed on a concrete impervious surface. It comes up more specifically as an alternative proposal for the projected park at the roof of the highway A7 in Hamburg, Germany, (*Hamburger Deckel*). As mentioned above, the highway will be expanded and covered with a roof in three separated sections

of the road as it crosses the city. On the roof of the tunnel a large public park mixed with a communal orchard is planned. It will connect neighbourhoods formerly separated by the highway, providing them with many ecosystem services, e.g. noise reduction, connectivity among dense populated areas and green patches, food production and wind speed reduction. The projected three sections of the park will run along 3.5 km in total, with a final extension of 25 ha. In order to cover such area, between 1.5 and 2 $\times$ 10^3 kg m^{-3} of soil is needed, if the maximum weight load calculated for the soil (including water saturation) is 20 kN m^{-3}, according to Melchior (2016).

As the numbers reflect, the soil extraction impact in the case of this project will be severe, unless it is reduced by using soil excavated from other construction sites. Nevertheless, an extracted natural soil always turns into an allochthonous material and loses structure and other properties when removed and installed in a different place. But that is not the only problem. Hamburg has a precipitation regime with a constant basal rain, and marked peaks in summer and winter (Table 1.1). Therefore, clay and silt content of most natural soils would significantly lower the hydraulic conductivity needed in events of heavy rain (>50 mm h^{-1}), and can also clog the drainage facilities due to their small sizes (<0.063 mm for silt), leading to stagnation problems, and possible flash flooding.

Table 1.1. Annual mean temperature and precipitation of Hamburg. In years with abundant precipitation the annual mean can reach 838 mm (Deutscher Wetterdienst)

	Jan	Feb	Mar	Apr	May	June	July	Aug	Sept	Oct	Nov	Dez	Year
T (°C)	0.5	1.1	3.7	7.3	12.2	15.5	16.8	16.6	13.5	9.7	5.1	1.9	8.6
pp (mm)	61	41	56	51	57	74	82	70	70	63	71	72	770

T is for temperature, and pp for precipitation

In order to test this premise, a simulation of the water fluxes using specific recommendations for the *Hamburger Deckel* soil profile was made. The data were obtained from the proposal written by Prof. Eva-Maria Pfeiffer (Institute of Soil Science of the Hamburg University) and Dr. Thomas Vollmer (Büro für angewandte Geowissenschaften), as well as the article written by Dr. Stefan Melchior (melchior + whittpohl Ingenierugesellschaft; Melchior 2016).

The software HYDRUS 2D was used for the modelling with the following data: a planned soil profile height of 120 cm, the weather data from 1st of January 2006 to 31st of December 2008, and the soil texture. The planned *Hamburger Deckel* profile has three horizons: 30 cm of a sandy-loam mixture, classified as Sl3/Sl4

(10–40 % of silt and 8–17 % of clay; Ad-Hoc-AG 2005) containing 4 % of organic matter, 70 cm of Sl3/Sl4 without organic matter, and 20 cm of sand at the bottom as a drainage layer. Ten observation nodes running in two parallel columns from bottom to top were defined to calculate their water content.

The general results of the modelling show a high water saturation degree of the simulated soil profile (Fig. 1.1). Although the four upper observation nodes ranged between pressure heads of 0.5 m and 1 m (corresponding to matric potentials of pF 1.7 and 2.0, respectively), almost the whole studied period the lower layers were below a pressure head of 0.5 m (pF 1.7), and the bottom of the second and the third layers were always between pressure heads of 0 and 0.25 m (pF 1.4). The worst scenario can be observed at the period corresponding to the end of winter and beginning of spring 2007. Then, the model shows that more than 90 days the whole profile presented pressure heads corresponding to pF $<$1.7 at the highest four observation nodes, while the six lower observation nodes reached and exceeded total saturation ($\geq$0 m pressure head). A breakdown in the simulation was reached in a heavy rain event at summer 2007.

Considering that the water stored at matric potentials between pF 0 to 1.8 is gravitational water, and from pF 1.8 (field capacity) up to 4.2 (permanent wilting point) is the range of available water content (AWC) for plants (Veihmeyer and Hendrickson 1931), then, at pF $<$1.7 even the largest pores ($>$60 µm) are filled with water, leading to stagnation. Additionally, in a period of more than 90 days of saturation at depths near the surface, the root drowning is imminent (Fig. 1.2). The threat of saturation is not only related to plant drowning, but also to flash flooding eroding rapidly the soil, as well as anaerobic conditions in the soil horizons (reduction of vulnerable cations as nitrate, manganese, ferric iron compounds, and sulphates; Schaetzl and Thompson 2015). For these reasons, the proposed soil profile is not adequate for the given environmental and facilities conditions.

1.3.2. Technosol improved performance

As an alternative to solve the stagnation problems, the proposal of this work is to design a Technosol mainly able to effectively drain water excess while accomplishing the pedogenic functions to sustain vegetation. This work is developed taking the environmental and technical conditions given in the specific case of the project *Hamburger Deckel* as a representative reference comprising many places with similar conditions, overcoming a case study.

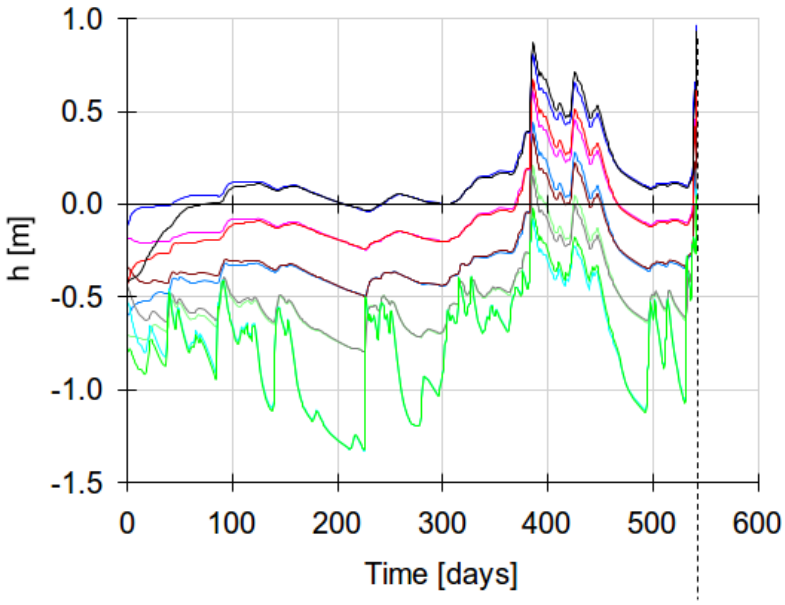

Figure 1.1. Simulated pressure heads of the observation nodes (ten paired nodes) in the *Hamburger Deckel*s projected substrate during the whole studied period (01.01.2006 to 31.12.2007). The lower lines correspond to the upper nodes of the upper soil layer, and vice versa. Pressure heads (h) are given in meters. Zero imply total saturation and positive values exceed it. It can be observed at around day 370 (winter) a drastic increase of the pressure heads of all the observation nodes, where many reach and exceed saturation. The dashed line at the end corresponds to a heavy rain event at summer 2007, which HYDRUS 2D was not able to model

The crucial point of this aim is to guarantee a high hydraulic conductivity in the soil profile and simultaneously retain enough available water for continuous plant growing.

As water stagnation is the main risk given the environmental and infrastructural conditions, I propose a sandy soil profile, agreeing with the *Hamburger Deckel* project. Sand has the highest hydraulic conductivity within the soil texture classes. However, sand has a low surface chemical reactivity needed in the soil solid phase to retain nutrients and enhance the aggregation. Also, its water retention capacity is very low (Sumner 1999). In natural soils these functions rely mainly on the clay fraction. Some of the functions positively influenced by clay are water retention, cation exchange capacity, and aggregation (Blume et al. 2009). Clay additionally contains a considerable amount of pedogenic iron (oxides, oxihydroxides and hydroxydes named also Fe (hydr)oxides; Sumner 1999) which has also an important role for the stability of soil structure (Duiker et al. 2003) and the surface chemical reactivity of the soil solid phase (Jambor and Dutrizac 1998; Cornell and Schwert-

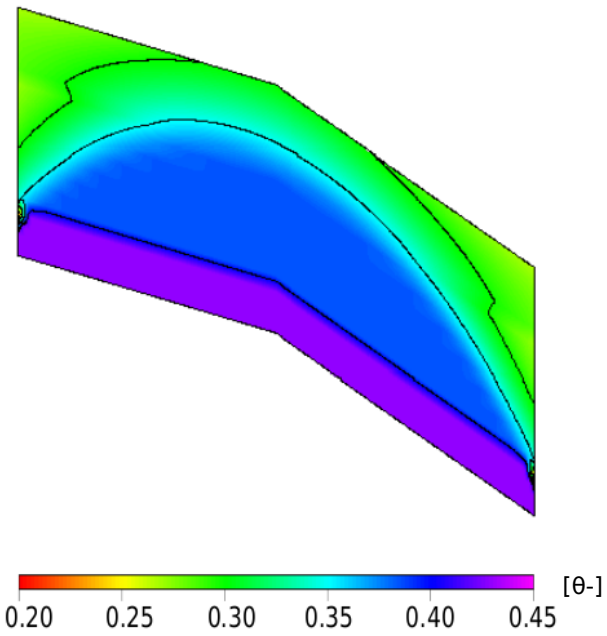

Figure 1.2. Soil profile frontal plane of the simulated water content with HYDRUS 2D at day 394 (29.01.2007). The suction values are given in Θ [-]. Below the green line, saturation is reached

mann 2003). Nevertheless, in contrast with the *Hamburger Deckel* project, I do not recommend the use of a dispersed clay fraction, as it is not adequate due to the threat of clogging the draining system due to its small size (<0.002 mm; Fig. 1.2). As the clay fraction in the soil has a large list of core functions, it is necessary to find efficient substitutes.

The core part of the Technosol construction is to design the subsoil, which could be comparable with a B-horizon, able to accomplish the water retention-conductivity balance needed by means of a correct mixture of materials. Later, an equivalent A-horizon has to be created by mixing the subsoil-material with organic matter. This organic fraction can easily be introduced as compost until reaching 4–6 % of organic matter. In the case of Hamburg, this is an easy task, as the country cooperates with the German Federal Compost Association (Bundesgütegemeinschaft Kompost e.V., BGK). The BGK guarantees the quality of the compost, and analyses the nutritional and pollutant levels of the local production. A third layer at the bottom that works as a drainage layer is needed. The material used can be pure gravel in order to avoid root growth and clogging of the system, or a similar lighter material. The proportionality among the layers proposed in the *Hamburger Deckel* project is appropriate, given the 120 cm soil depth: 30 cm of upper soil enriched with organic

matter, 70 cm of subsoil, and 20 cm of drainage layer (Fig. 1.3). However, as mentioned above, the basic knowledge for the commercially available materials is not sufficient to purpose-design such a soil profile.

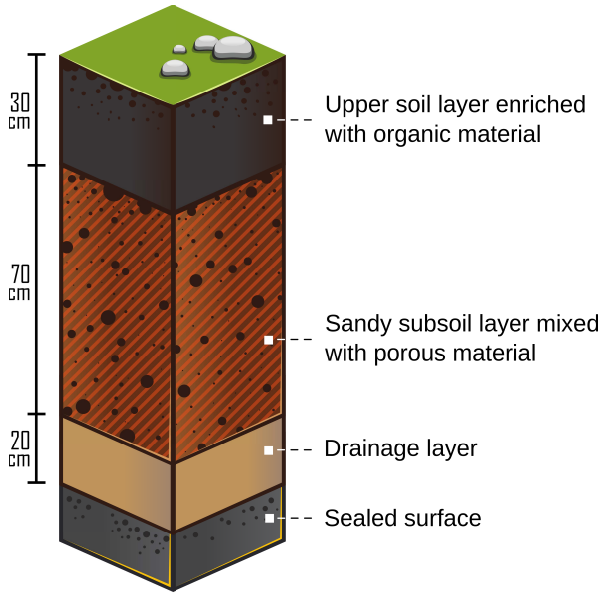

Figure 1.3. Scheme of the proposed soil profile. The sandy subsoil has to have a high hydraulic conductivity, and simultaneously retain enough plant available water. The upper layer can be composed by the same mixture of materials of the sandy subsoil, including 4–6 % of organic matter. A drainage layer can be composed by pure coarse sand

1.4. Objectives of the thesis

Derived from the background described above, the general aim of this thesis is to increase the knowledge basis for the design and construction of Technosols for greening purposes. Specifically, the aim is to improve the basis of the proposed sandy Technosol and to cover the lacks that a dispersed clay fraction absence implies in order to avoid stagnation risks.

Thus, I propose: (a) the inclusion in the sand of an Fe (hydr)oxide fraction, which will increase mainly the chemical functionality of the soil, and (b) the inclusion in the soil profile of large grain size porous materials able to retain enough plant available water, while avoiding clogging. The topics can, therefore, be separated in these two main sections from now on.

In order to accomplish the proposals, the following questions are addressed in the thesis:

- ↬ How to stably combine sand with Fe (hydr)oxides?
- ↬ Once knowing the adequate process, how to optimize the sand and Fe (hydr)-oxides combination in terms of sustainability and economic feasibility?
- ↬ What kind of materials can store enough plant-available water to be used mixed with sand in the construction of the fast-drainage Technosol?

To answer the question of the combination between sand and Fe, I developed a simple technique to obtain a sand coated with an amorphous Fe (hydr)oxide, a 2-line ferrihydrite (2L-FH). Detailed information about the materials, methods, and the functionality and resistance of the coated sand obtained is given in Chapter 2.

Later, local, recycled and economic materials were characterized to achieve an affordable sand coating process. Thus, Fe (hydr)oxides from different sources were collected, analysed and combined with sand extracted from the Hamburger harbour of the Elbe river. The results of the coating possibilities with these diverse materials are explained in detail in the Chapter 3.

In order to chose the material or materials which, combined with the Fe coated sand, could store enough water available for plants, six different commercially available porous materials were characterized, with a special emphasis on their hydraulic properties. In combination with sand, a variety of measurement techniques were used to obtain high resolution data and a good parametrization of water retention models. Details of the materials chosen, the methods and results on their water holding capacity are discussed with detail in the Chapter 4.

2. Novel ferrihydrite sand coating process as a first step for designed Technosols[1]

Abstract

Purpose The production of Technosols to remediate polluted or sealed urban soils to sustain new green areas is mainly empirical. For this, our research aims to contribute with the scientific knowledge base for purpose designing of Technosols. Since iron minerals play an important role for many different functions of soils, we simplified a technique to incorporate and stabilize iron minerals in a substrate: a sand coated with an amorphous iron (hydr)oxide, a 2-line ferrihydrite (2L-FH).

Materials and methods The 2L-FH was precipitated by neutralization of a concentrated $FeCl_3$ solution. The suspension was homogeneously mixed with the sand and the mixture was dried at 35 °C. The mechanical stability of the 2L-FH-coated sand was determined by shaking the aggregates in water for 0, 1, 10, 100 and 1000 min. The degree of coating detachment and the properties of the coating after shaking were characterized through (a) Fe content, (b) zeta-potential and particle size of the detached particles, (c) the specific surface area (SSA) of the coated sand, and (d) its surface structure using scanning electron microscopy (SEM). A phosphate adsorption isotherm was performed to measure the P-sorption capacity of the shaken samples and to test the 2L-FH-quartz attachment stability against the surface charge reduction of the 2L-FH associated with P adsorption.

Results and discussion A reduced Fe loss (30 %) and smaller sizes of the coating detached particles in the sample shaken for 1000 min indicate that a fractioning and reattachment of these aggregates occurred during the agitation process, resulting in a smoother surface (SEM), and a larger SSA and P-sorption capacity. The coated shaken samples showed P-adsorption capacities (5.3–6.34 µmol P g^{-1}) comparable to high loadings of phosphate in soils, and low detachment of Fe (7–14 %) in spite of negativity surface charge increase.

Conclusions The practical novel coating process along with the 1000 min shaking produced a mechanical resistant and P-adsorptive effective coated sand that could sustain the needs of plants in further experiments.

2.1. Introduction

In urban agglomerations soils of formerly open spaces are removed, sealed, and polluted along with the establishment of the build urban environment (Burghardt 2006; Brabec et al. 2002; Albanese and Cicchella 2012). The severe detriment of the ecosystem services that soils naturally perform in urban areas (Bolund and

[1] This is a postprint version of an article published by Springer: Flores-Ramírez, E., Dominik, P., and Kaupenjohann, M. (2016). Novel ferrihydrite sand coating process as a first step for designed technosols. *Journal of Soils and Sediments*, 1-11. DOI:10.1007/s11368-016-1450-1. Republished with permission of Springer. The publication is available on SpringerLink.

Hunhammar 1999; Scalenghe and Marsan 2009) can be partly counteracted if new green infrastructure is established (Weng et al. 2004; Makhelouf 2009).

Shrinking cities have everyday large vacant tracts of land belonging to former heavy industries, which often falls idle, and expanding cities have the need to integrate new green areas to their territory. This opens opportunities to communities for the creation of new green infrastructure in modern cities, like parks, green playgrounds, and urban agriculture. However, the soils on these properties are often sealed, compacted, low in organic matter, contain various amounts of construction debris and pollutants, which all decrease their value as a growing medium.

Generally to solve this, either the soils are remediated or they are excavated and substituted by other substrates, which may be specifically designed for various purposes (Séré et al. 2008; Yakovlev et al. 2013). These constructed or manufactured soils classify as Technosols according to the World Reference Base for Soil Resources (IUSS Working Group WRB 2015).

The production of these artificial soils by mixing various inorganic and organic compounds is mainly empirical, relying on experience. Target-oriented, knowledge-based design is the exception, although the research on new substrates for constructed soils with specific characteristics to provide nutrients, porosity, and water holding capacity is a developing scientific area (Nehls et al. 2013; Rokia et al. 2014). Our work aims at the creation of the knowledge base for the purpose-designed substrates for urban use.

Among others, soil functioning is based on the potential of soils to provide bioavailable water, nutrients, and oxygen to buffer hazardous substances and to infiltrate precipitation. Soil structure and the properties of the solid soil phase determine these potentials. Pedogenic iron (Fe) minerals (oxides, oxihydroxides, and hydroxides, summarized as Fe (hydr)oxides) play a crucial role for both the stability of soil structure and the surface chemical reactivity of the soil solid phase and can be found ubiquitously in soils and sediments (Sumner 1999). They contribute to the aggregation by cementing clay minerals and quartz particles (Wang et al. 1993) or other soil minerals into stable aggregates (Duiker 2003). Further, these (hydr)oxides with a large specific surface area (McLaughlin et al. 1981; Borggaard 1983; Cornell and Schwertmann 2003) adsorb oxyanions, heavy metals, viruses, and bacteria as well as organic molecules, and thereby play an important role for the dynamics of nutrients and pollutants in soils.

Accordingly, iron minerals should be one of the essential components of artificial soils, next to organic matter and nutrient-containing inorganic compounds. Thus,

the specific aim of this study is to provide an easy-to-use method for the incorporation of Fe minerals into artificial soils.

Some substrate mixtures of constructed soils (such as green roofs or gardens) include a dispersed clay fraction, which contributes to water retention, cation exchange capacity and contains Fe (hydr)oxides. But, designed Technosols with a high risk of stagnation should not use any dispersed clay fraction to prevent clogging. In order to keep a high hydraulic conductivity and at the same time incorporate Fe minerals into artificial soils, this study proposes the use of sand as the main fraction of a designed Technosol due to its advantages of availability and texture, but modified with an amorphous iron (hydr)oxide coating.

Beside the soil functions, sand and other substrates coated with Fe (hydr)oxides (diatomaceous earth, Lukasik et al. 1996; clays, Sakurai et al. 1990; fiber glass or polyester, Kumar et al. 2008) have received attention due to their effective adsorption capacity of diverse anions of health interest from waste or drinkable water. Hazardous viruses (Farrah and Preston 1991; Scott et al. 2002), bacteria (Lukasik et al. 1996), arsenic (Thirunavukkarasu et al. 2003; Kumar et al. 2008), and heavy metals (Lai et al. 2000; Trivedi and Axe 2001; Xu and Axe 2005) have been adsorbed with good results. Although, in spite of the wide use of the Fe (hydr)oxide coated materials, the coating procedures used are sophisticated and too expensive to coat large amounts of substrate.

Our coating technique was planned to be as simple as possible. This would allow to have affordable large amounts of substrate to be used in the field, with natural soil average levels of anion adsorption and mechanical stability when installed outdoors.

For this, a 2-line ferrihydrite was synthesized to further coat a quartz sand. Ferrihydrite, widely found in natural soils and one of the mayor Fe (hydr)oxides (Cornell and Schwertmann 2003), presents a broad 2-line or a 6-line X-ray diffraction pattern as a result of its low crystallinity, being the 2-line the most amorphous.

The mechanical stability of the coating was tested through heavy shaking with water. The stability level was quantified in relation of the detached Fe. These Fe outgoing particles were characterized by zeta-potential, particle size, and pH. Additionally, another stability test was performed adding large amounts of phosphate (P) to the coated sand in an adsorption experiment. The aim was to quantify the dispersion of coating Fe due to the increasing surface charge along with P-adsorption (Ilg et al. 2008).

Sand, as an important element of substrate mixtures for greening or germination, is widely used since centuries ago. Also, other Technosols include Fe deposits or fractions in their constitution (Huot et al. 2014), but not any work uses a sand with Fe (hydr)oxides as a substrate transformed specifically for a designed Technosol.

2.2. Materials and methods

2.2.1. 2L-ferrihydrite synthesis

A 2-line-ferrihydrite (2L-FH, 5 Fe_2O_3 × 9 H_2O; Fleischer et al. 1975) was synthesized by neutralization of a 420 g L^{-1} solution of $FeCl_3$ with NaOH at room temperature.

In order to obtain a 2L-FH which contains 0.25 mol Fe, 67.58 g of $FeCl_3$ × 6 H_2O were dissolved in 1.25 L of deionized water (DI water). While stirring vigorously, a 1 M NaOH solution was added slowly but continuously. The suspension was stirred for 30 min more to yield a final pH of 7.6 (Knick 761 Calimatic). The Fe (hydr)oxide suspension was centrifuged (10 min at 1 300 g; Beckman Coulter Optima L-90k Ultracentrifuge), decanting the supernatant and re-dispersing the precipitate three times with DI water (about 10–fold volume of the sediment, respectively) to be rid of salt excess. The final 2L-FH suspension contained 52 g of Fe per litre and was stored at 4 °C to avoid crystallization. The structure of the 2L-FH obtained was controlled with an X-ray powder diffraction (XRD; Panalytical PW 1710, Cu anode, 5–80 ° measurement range, scanning speed of 0.01 ° 2Θ/ min) obtaining the characteristic two broad peaks pattern (one between 30 and 40 2Θ, the second at 60 2Θ).

2.2.2. Sand coating

Sixty mililiters of this dense sludge were hand-mixed with 1 kg of quartz sand (0.5–1 mm, Sand Schulz®, >96 % SiO_2, C 0,14 %, N 0.014 %, S 0.06 %) until a visually homogeneous cover was reached. The coated sand was spread on a tray to a height less than 1 cm and dried for 12 h at 35 °C. Thereafter, the coated sand was wet sieved (with DI water through a 63 µm sieve) until the effluent was visually clear in order to exclude free iron particles as well as weakly attached coating particles. Afterwards, the coated sand was dried again at 35 °C for 12 h.

2.2.3. Mechanical stability of the coating

A mechanical abrasion test was conducted using 50 g of the coated sand with 16.6 ml of DI water in 120 ml Nalgene bottles (in triplicate). The samples were shaken for 1, 10, 100, and 1000 min, respectively, at 250 rpm in a horizontal shaker (Janke & Junkel KS501). An additional sample was not shaken. All samples were washed with DI water through a sieve (63 µm), until the effluent was visually clear. Thereafter, the samples were dried at 35 °C. In order to determine the Fe loss level due to mechanical abrasion, the total Fe content in the coated sand was analysed by citrate-bicarbonate-dithionite (Fe_d) extraction according to Mehra and Jackson (1958). The concentrations of Fe in the Fe_d extracts were measured by atomic adsorption spectrophotometry (Perkin Elmer 1100B AAS). The same method was used to determine the original Fe content of the uncoated sand, and its value was subtracted from all the correspondent calculations.

The corresponding amount of ferrihydrite in the coated sand was calculated as 1.7 times the measured Fe concentration. This factor is the relation among the molecular weight of the ferrihydrite per Fe and the Fe (95 and 55.85, respectively). Because ferrihydrite has been proposed to have different structures due to its low degree of order and the difficulty to establish a precise separation of structural OH and H_2O from adsorbed water (Cornell and Schwertmann 2003; Michel et al. 2007), the formula $5\,Fe_2O_3 \times 9\,H_2O$ (Fleischer 1975; Schwertmann and Taylor 1989) was used. This formula gives a molecular weight of 96.2 per Fe, but we assumed 95 to get an approach of a ferrihydrite less hydrated.

A repetition of the mechanical abrasion test described above was performed to obtain and characterize only the two samples that detached the lowest and the highest amount of Fe particles, together with the sample only washed. In the washing step, the first 200 ml of this washing water were collected to characterize the suspended Fe (hydr)oxide. The shaken samples were used to further test the effect of the mechanical abrasion on the coating particles as well as the stability against detachment by inverting surface charge by P adsorption.

2.2.4. Characterization of the coated sand

The washing water containing the detached particles was analysed through the following measurements: Fe_d content (according to Mehra and Jackson 1958), turbidity of the water (1:10 dilution, Hach 2100P ISO), zeta-potential (Malvern

Z-Seizer 2000), particle size (by laser diffraction with Sympatec Helos H0541), and pH (Knick 761 Calimatic).

Morphology and topography of the coated sand surfaces were observed with the scanning electron microscope (SEM) and the backscattered electron detector (BSE) using a Zeiss Leo 982. For this, the samples were mounted dry and coated with a 25 nm carbon film using an Edwards-E12E4 Vacuum Coating Unit.

The specific surface area (SSA) of the sand was calculated (value below the detection limit) using its particle size distribution. The specific surface of each sieving fraction (0.06, 0.1, 0.2, 0.3, 0.4, 0.5, 0.6 and 1.0 mm) was calculated assuming a spherical shape of the sand grains (SS_{frac}):

$$SS_{frac}[m^2\,g^{-1}] = 6/(\varnothing \times 1000 \times \rho_{sand}) \quad (1)$$

where $\varnothing$ is the mean diameter of each sand fraction in mm, and $2.63\,g\,cm^{-3}$ is the sand density (ρ_{sand}). Afterwards, the SSA of the sand (SS_{sand}) was calculated as the sum of the SS_{frac}:

$$SS_{sand} = \sum(SS_{frac} \times Frac\%) \quad (2)$$

where Frac% is the particle percentage of each fraction. Because sand is not completely spherical, a roughness adjustment factor of 7 was used (White 1995).

The SSA of the coated sand samples was quantified with a nitrogen gas adsorption isotherm of 11 points using the BET equation (Quantachrome Autosorb 1 surface analyzer). Thereafter, the SSA of the 2L-FH that coats the sand was calculated by subtracting the specific surface of the (uncoated) sand from the SSA of the coated samples, and dividing by the concentration of ferrihydrite in the coated sand:

$$SSA_{2L-FH}[m^2\,g^{-1}] = (SSA_{coatedsand} - SS_{sand})/2L - FHg\,g^{-1} \quad (3)$$

2.2.5. Batch experiment

A batch experiment was performed to determine the P-adsorption characteristics of the coated sand and to test if a change of the zeta-potential to negative values would induce a detachment of the 2L-FH coating.

A range of initial phosphate concentrations was calculated with the SSA of the 2L-FH and different maximum sorption capacity (q_{max}) values: 2.50 µmol P m^{-2} for crystalline Fe (hydr)oxides –specifically goethite (Strauss et al. 1997)–, to 12 µmol P m^{-2}. From these calculations, four concentrations logarithmically equidistant were chosen. Samples with four grams of sand were shaken with 25 ml of a 10 mM KNO_3 solution containing 0, 60, 234, 907, or 3 530 µM H_2KPO_4, respectively. The samples were shaken at 2 rpm end-over-end for 24 h at 20 °C. Thereafter, the samples were turned upside down every 6–12 h by hand (to minimize mechanical detachment of the coating) for 4 days (McLaughlin et al. 1981; Borggaard 1983).

A 4 ml aliquot of the suspension was ultracentrifuged at 100, 000 g for 18 min, and the supernatant used for phosphate determination either with the continuous flow analyzer (CFA, Seal Analytical AA3, ortho-P; detection level of $<0.5\,mg\,L^{-1}$) or with an inductively coupled plasma mass spectrometer (ICP-OES, iCAP 6000 Thermo Scientific 6300 DUO; detection level of $>0.5\,mg\,L^{-1}$). The amount of P sorbed was calculated as the difference between the amount of P added (C_{ini}) and the P amount in solution at the equilibration (C_{eq}). The experimental results were analysed with the Langmuir and Freundlich models using the QtiPlot software (version 0.9.8.7). The Langmuir equation is expressed as:

$$C_{ad} = K_l \times q_{max} \times C_{eq}/1 + K_l \times C_{eq} \tag{4}$$

where C_{ad} is the adsorbed P $\mu mol\,g^{-1}$, K_l is the Langmuir coefficient (the intensity of the adsorption isotherm), C_{eq} $\mu mol\,L^{-1}$ is the concentration at equilibrium in the solution, and q_{max} is the maximum sorption capacity expresed in $\mu mol\,g^{-1}$. The Freundlich equation is:

$$C_{ad} = K_f\,C_{eq}^{n} \tag{5}$$

where K_f is the Freundlich average affinity constant and n is the adsorption intensity factor.

Additionally, the supernatant was further characterized by Fe_d content, zeta-potential, and pH.

2.3. Results and discussion

2.3.1. Fe-coating

Fe coating process

The performed sand coating process has less steps and wastes less energy compared with other traditional processes. Other procedures usually add the material to be coated into a concentrated $FeCl_3$ solution. Then, Fe precipitates *in situ* by neutralization with NaOH at different high heating temperatures, when more crystalline forms are obtained, stirring or shaking end-over-end for several hours. Further steps can involve different drying temperatures (sometimes as high as 110 °C or 550 °C), one or more washing steps to be rid of salts, or even subsequent coatings (Scheidegger et al. 1993; Schwertmann and Cornell 2008; Kumar et al. 2008; Rusch et al. 2010).

In this work, the 2L-FH was synthesized at room temperature (amorphous coatings are obtained at low temperatures; Lo et al. 1997). When coating, the pH does not need to be adjusted, nor the ionic strength, and the mixing time is less than 30 min. Additionally, drying the coated sand at 35 °C avoids structure affections against the high percentage of H_2O physically adsorbed (9 % at 30–125 °C) that ferrihydrite has. Ferrihydrite presents a peak of weight loss at 92 °C (Wang et al. 2013b).

Fe loading

Iron concentrations increased notably, from 0.32 mg Fe_d g^{-1} in the original sand to an average maximum loading of 2.31 mg Fe_d g^{-1}, after the coating process (Table 2.1). These concentrations are within the broad range of values reported by other authors using different processes for the coating of sand with Fe (hydr)oxides synthetically produced. Previously reported values vary due to the method, the size of the sand, and the kind of Fe (hydr)oxide used, although the latter is not always reported. Xu and Axe (2005) obtained a loading range of 0.67–8.5 mg Fe g^{-1}. The data given by Scheidegger et al. (1993, 6 mg Fe g^{-1}), Jerez and Flury (2006, 4.4 mg Fe g^{-1}) and Chang et al. (2012, 3.26 mg Fe g^{-1}) are very narrow, while the Fe coverage reported by Kumar et al. (2008) was one order of magnitude larger than our value (26 mg Fe g^{-1}). Compared with natural soils, where the range of Fe concentrations is even much broader, our result is within the average (0.05–40 mg Fe g^{-1} of soil, Blume et al. 2009).

Table 2.1. Fe and ferrihydrite contents in the coated sand samples after different shaking treatments

Sample	mg Fe g^{-1}	mg FH g^{-1}	Remaining Fe after mechanical detachment (%)
untreated	2.31 ± 0.07	3.92	100
washed[a]	1.93 ± 0.07	3.29	84
1 min	1.43 ± 0.07	2.44	62
10 min[a]	1.02 ± 0.13	1.73	44
100 min	1.23 ± 0.07	2.08	53
1000 min[a]	1.56 ± 0.07	2.56	68

The corresponding amount of ferrihydrite in the coated sand was calculated as 1.7 times the measured Fe content. This factor is the relation between the molecular weight of the ferrihydrite (per Fe) and the Fe (95 and 55.85, respectively).
[a] Samples chosen to be further characterized after shaking (in Table 2.2)

Mechanical abrasion test

Results from the mechanical abrasion test showed that when applying the mildest abrasion process –simple rinsing with DI water– about 16 % of the attached Fe was removed from the coated sand (Table 2.1). A stronger detachment force –shaking the slurries of coated sand and water for 1, 10, 100, and 1000 min– resulted in different loss levels. The largest loss of about 56 % of the originally attached Fe was registered with the 10 min treatment. With increasing shaking-time the loss of Fe decreased to only 32 % after 1000 min of shaking (Table 2.1), instead of increasing. Due to these peculiar Fe contents, the washing water after 10 min and 1000 min shaking, along with the treatment only *washed* were further analysed. The total amount of Fe detached after shaking or washing was consistent with the Fe content measured in the sand, also reflected in the turbidity of the washing solution (Fig. 2.1a).

A marked decreasing particle size of the detached Fe colloids was observed along the shaking. *Washed* has the largest and most heterogeneous particle size, while 1000 min presents the smallest and homogeneous particle size. In between this particle sizes, the samples shaken for 10 min presents a heterogeneous range of sizes: large particles but also small ones close to the size of the 1000 min shaking (Fig. 2.1b).

Scanning electron images show a rough coating surface in all the samples given by the amorphous ferrihydrite structure (heavily aggregated due to water molecules chemisorbed at its surface; Zhao et al. 1994). However, the roughness of the coating surfaces among samples changed (Fig. 2.2). *Washed* samples present large,

irregular rounded aggregates of coating, and some sand surface areas are uncovered. A similar coating pattern with ferrihydrite was shown by Jerez and Flury (2006).

The 10 min sample looks similar when observed with a low resolution, but presents larger areas uncovered. When observed with a higher resolution, the surface of the sample presents a mixture of small and large rounded aggregates, and some visible uncovered areas. In contrast, 1000 min has a smooth and flat layer composed by homogeneously arranged tiny rounded aggregates visible at low and high resolution, and no uncovered sand surface is left.

The morphology of the obtained 2L-FH coating contrasts with patterns reported for crystalline Fe (hydr)oxides. Surfaces covered with goethite present only patches or scarce points of acicular-shaped crystals (in cauliflower-like aggregates). Coatings with hematite present crystals aggregated in spherule shapes, and both Fe minerals are distributed mainly in rough areas of the sand surface (Bedarida et al. 1973; Scheidegger et al. 1993; Ilg et al. 2008; Rusch et al. 2010). Szecsody et al. (1994) reported 2L-FH coating aggregates similar in shape to the ones we obtained, although the coating had isolated aggregates of Fe (hydr)oxide adhering to the surface. In our work, in contrast, the 2L-FH coating covers larger surface areas of the sand grains and has a completely overcast and homogeneous surface after 1000 min of shaking.

The zeta-potentials of the detached particles increased along with the shaking time: from 2.5 mV, when only washed, to 17 mV when shaken for 1000 min (Fig. 2.1b). Despite all the physical changes of the particles, these changes are not induced by pH, since the pH remains fairly constant around 5.30 ± 0.05 in all the samples. Nevertheless, the surface charge correlated positively with the particle size of the detached aggregates (R^2 = 0.934). The smaller the aggregates are, the larger is the exposed surface, and the positive charges along with it.

Table 2.2. Specific surface area (SSA) of the shaken coated sands, the concentration of 2L-FH coating the sand and its calculated SSA

Sample	SSA Coated sand (m^2 g^{-1})	Amount of coating (mg 2L-FH g^{-1})	SSA of FH in coating (m^2 g^{-1})
uncoated sand	0.06 (calculated)	–	–
washed	1.32 ± 0.01	3.29	385 ± 3
10 min	0.88 ± 0.01	1.73	476 ± 5
1000 min	1.26 ± 0.03	2.56	470 ± 11

The changes observed above point out to a detachment and fractioning process of the aggregates that conforms the FH coating layer of the sand due to the

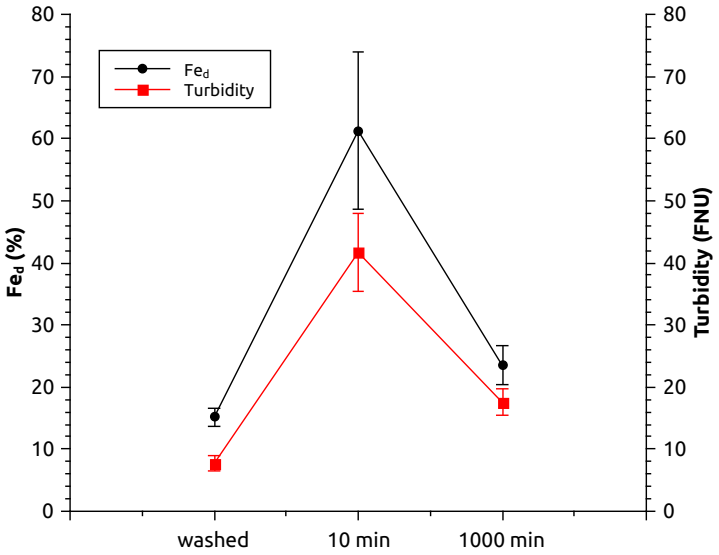

(a)

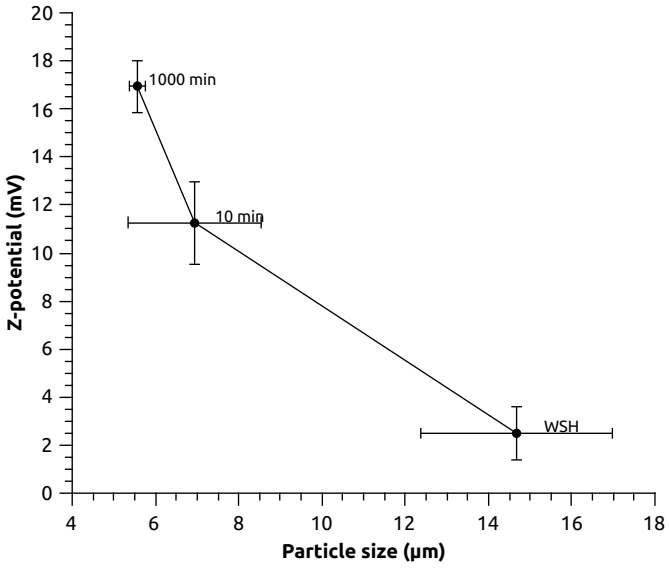

(b)

Figure 2.1. Characterization of the detached particles in the washing water collected resulting from the shaking process of the coated sands. **(a)** Percentage of total iron (Fe_d), plotted together with the turbidity (diluted 1:10) expressed in formazin nephelometric units (FNU) and **(b)** the correlation (R^2 = 0.934) of the particle size and the zeta-potential of the detached particles

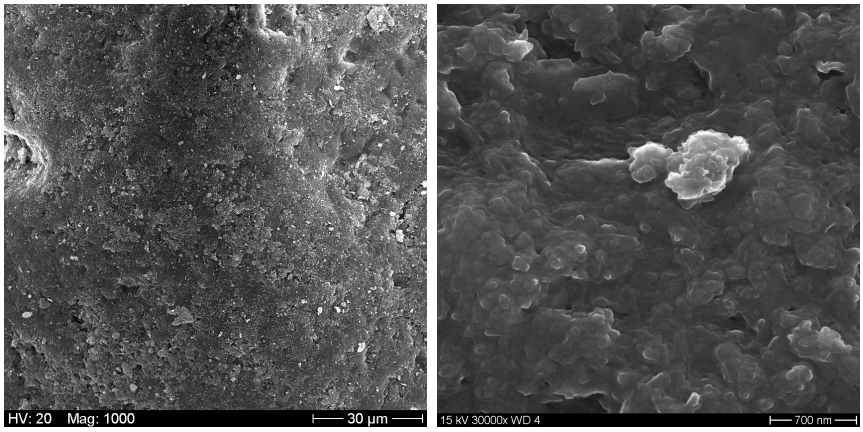

(a)

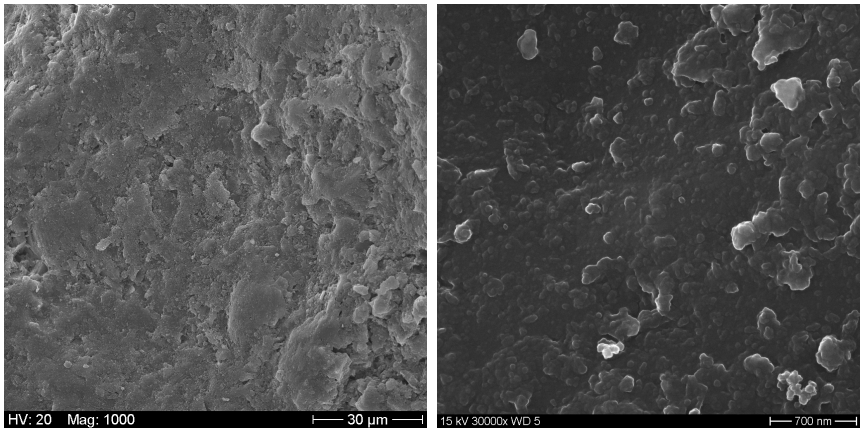

(b)

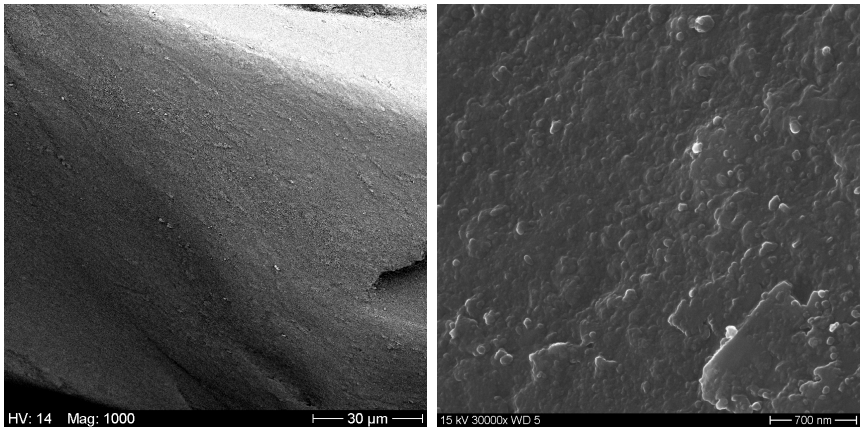

(c)

Figure 2.2. Scanning electron microscope images of the 2L-FH coated sand surfaces of the samples after **(a)** washing, **(b)** 10 min, and **(c)** 1000 min of shaking. Scales of 30 µm (*left*) and 700 nm (*right*). In the *washed* sample large aggregates and a rough surface can be observed. In 10 min sample the sizes of the aggregates are heterogeneous and the surface is rough, with some areas uncovered. In 1000 min sample the surface is smooth and homogeneous rounded aggregates cover the whole surface

grinding work by long term shaking of the sandy slurry. This collision effect could be markedly strong because of the low water to sand ratio, which provided a dense suspension. The large sizes of the aggregates when the samples were only washed are completely reduced after 1000 min of shaking. The intermediate point can be observed after 10 min of shaking, where a large amount of aggregates is already ground, but not all the smaller particles reattached. The 1000 min of shaking could provide the time to reattach homogeneously on the sand surface by charge attraction.

The amorphous 2L-FH cover enhances the SSA of the coated sands. The measurements indicate 15 to more than 20–fold increase of the coated samples SSA compared to the uncoated sand (Table 2.2). Similar data were reported by Chang et al. (2012, 1.06 $m^2 g^{-1}$). The measured SSA of the coated sands is directly related to the amount of attached 2L-FH in each sample; thus, *washed* presents the largest surface area due to its high amount of FH, followed by 1000 min, and 10 min with the lowest value.

The calculated values for the SSA of the 2L-FH (Table 2.2) are in line with literature data (200 to 500 $m^2 g^{-1}$; Schwertmann and Taylor 1989). Treatments had only small effects on the SSA. Both the 10 and the 1000 min samples showed even similar SSA, while *washed* had about 20 % lower. These observations support our above presented model: We consider that the original 2L-FH of the coating consists of large aggregates of loosely attached particles. The surfaces of these particles are accessible to N_2, except for those sites where these particles attach to each other tightly. Disaggregation should thus cause only a small increase of the N_2-accessible surface. Since only small particles, and not large aggregates, reattach to the sand surface, the SSA of the 2L-FH after 10 and 1000 min of shaking must be similar, as shown.

2.3.2. P-adsorption

The physical characteristics of the coating particles are reflected in their ability to adsorb phosphate. With smaller coating particle sizes after abrasion and a corresponding SSA increase, the adsorption of P rises.

The Freundlich model fitted the adsorption data better for the sample *washed*, but very similar to the Langmuir model for the 10 and 1000 min data (Fig. 2.3, Table 2.3), in line with Arias et al. (2006). In contrast, adsorption experiments with soils often show a generally better fit of the empirical Freundlich model. The

mechanistic basis of the Langmuir model is that the heat of adsorption at all sites which are involved in the adsorption process is similar. In heterogeneous systems like soils, that is not the case. Our system with only 2L-FH adsorbed to quartz is much simpler and we may consider the Langmuir equation as an appropriate model to describe our data. Thus, we accept the calculated adsorption maxima (q_{max}) as reasonable estimates for q_{max}, although our experimental P-adsorption maxima are in part much lower (Table 2.4).

Table 2.3. Fitting parameters for phosphate adsorption of the three coated samples

	Langmuir parameters		Freundlich parameters		
Sample	K_l	R^2	K_f	n	R^2
washed	1.88	0.92	3.62	0.16	0.97
10 min	0.51	0.94	3.57	0.34	0.94
1000 min	0.46	0.96	4.20	0.42	0.95

K_l is the Langmuir equilibrium constant, related to the binding strength, K_f is the Freundlich average affinity constant, and n is the adsorption intensity factor

The results range within the reported values (and even higher) for amorphous Fe (hydr)oxides. McLaughlin et al. (1981) reported 4.85 µmol P m^{-2} in a dry Fe gel and Wang et al. (2013b) found 2.96 µmol P m^{-2} with ferrihydrite. Some q_{max} of crystalline Fe (hydr)oxides range from 2.50 µmol P m^{-2} (Strauss et al. 1997) to 6.1–12 µmol P m^{-2} (McLaughlin et al. 1981; Ilg et al. 2008). The coated sand P adsorption capacity is attributable to the 2L-FH that covers the sand, because quartz has no adsorption capacity (Arias et al. 2006).

In spite of the wide range of P adsorption capacity of the natural soils, the experimental adsorption values obtained with the coated sand (140.17–197.92 mg P kg^{-1}) are related to reported values for fertile soils, such as Luvisols (158 mg P kg^{-1}, Rommel 2000). These experimental values indicate an acceptable adsorption level that could lead to a potential P pool in the coated sand produced. Concerning the availability of this P pool, it is a fact that the P adsorbed by Fe (hydr)oxides is not readily available for plants. However, Wang et al. (2013b) recently showed that the P desorption rate form ferrihydrite with citric acid is 32 % of the q_{max}, even larger than in goethite (25 % of the q_{max}). This implies that the secretion of organic acids by plant roots will directly improve the P bioavailability in the constructed Technosol, avoiding high levels of occlusion.

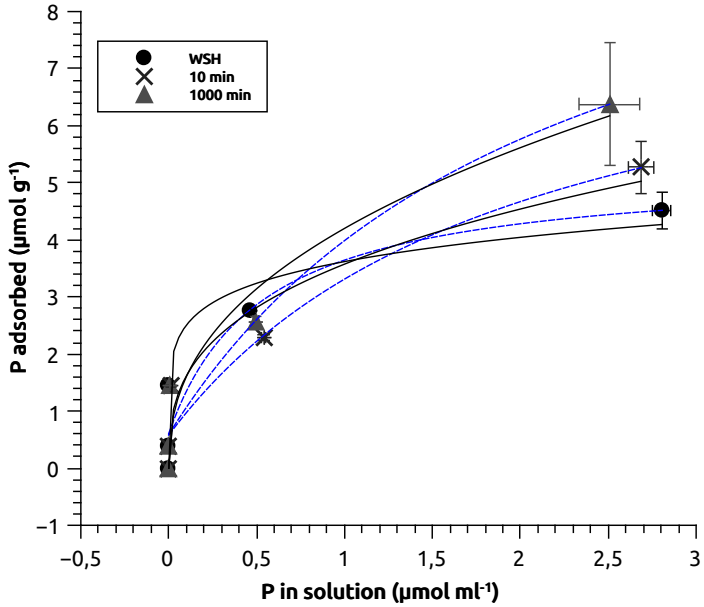

Figure 2.3. Phosphate adsorption Langmuir (*dash*) and Freundlich (*line*) isotherm plots of the 2L-FH coated sand samples washed and shaken for 10 and 1000 min

P adsorption and Fe detachment, pH, and zeta-potential

The detachment of Fe due to P adsorption was gradual and reached a maximum loss of 14 % of the coating on the 10 min sample. The 1000 min sample had the minimum loss (7 %) with the highest concentration of P experimentally loaded (Fig. 2.4a). Therefore, 1000 min coating is more stable against mechanical abrasion and withstands the reduction in the surface charge of the 2L-FH associated with P adsorption. The Fe detachment level at a zero concentration of P was considered as a result of a mild but constant mechanical abrasion, not related to the electrostatic forces from the P addition.

This is in line with the results of Scheidegger et al. (1993), who proposed that the formation of chemical Fe-O-Si-bonds (based on X-ray photoelectron spectroscopy, XPS) are responsible for strong binding forces of Fe-oxide particles to silica surfaces. However, in contrast to our results, Ilg et al. (2008) observed a strong detachment of goethite from quartz sand along with the addition of phosphate. The detachment of the Fe-colloids started at a zeta-potential of −20 mV and was complete at −30 mV, which was the lowest zeta-potential at the maximum phosphate-equilibrium concentration of 3.3 µM (pH 5.7–5.8). In our experiment, the zeta-potential remained beneath this critical value. Further, Scheidegger et al. (1993) observed that the extent of coating increased along with increasing temperature. With respect to our results, we may assume that the activation en-

ergy needed for the formation of strong bonds could be introduced by the intensive grinding process due to the mixing of the thickish slurry. However, this could not be tested experimentally in the frame of our recent work.

Table 2.4. Maximum P sorption values of the coated sand and the 2L-FH coating the sand

Sample	Coated sand						2L-FH		
	mg P kg^{-1}		µmol P g^{-1}		µmol P m^{-2}		g P kg^{-1}	µmol P m^{-2}	
washed	140.2	144.1	4.5	4.6	3.4	3.5	36.6	3.6	3.7
10 min	163.4	251.9	5.3	8.1	6.0	9.2	72.1	6.4	9.9
1000 min	197.9	336.4	6.4	10.8	5.1	8.7	62.1	5.2	8.8
	exp.	calc.	exp.	calc.	exp.	calc.	exp.	exp.	calc.

Experimental values (exp.) means the P sorption at the largest experimental P loading. Calculated (calc.) values were obtained with the Langmuir isotherm (q_{max})

As a consequence of the P adsorption, a pH increase was registered (Fig. 2.4c) related to inner-sphere complex formation involving P adsorption and release of OH^- (Celi et al. 1999; Ilg et al. 2008; Wang 2013a). However, the pH in the system is still low, compared to pH values in real Technosols.

As the pH affects directly the P adsorption capacity (low pH values enhance the P adsorption), in further Technosol designing steps we have to be aware of a pH shift introduced by the addition of compost and certain porous materials that are needed to guarantee the functioning of a Technosol. If other sands with higher pH are used in the future, the P adsorption capacity will directly decrease. However, on the other hand, this fact will lower the risk of Fe detachment from the coated sands. The pH could then be moderated by the organic matter and other amendments addition.

2.4. Conclusions

The coating method is quite effective and simple, uses less energy, resources, and time than traditional procedures. As it was performed is a novelty, it has not been reported before in the reviewed literature.

Shaking the sand after the 2L-FH coating process for 1000 min infringes important changes in the physical features of the coating aggregates by its detachment, fractioning, and reattachment. This model was supported by the results of particle size, SEM, zeta-potential, and SSA.

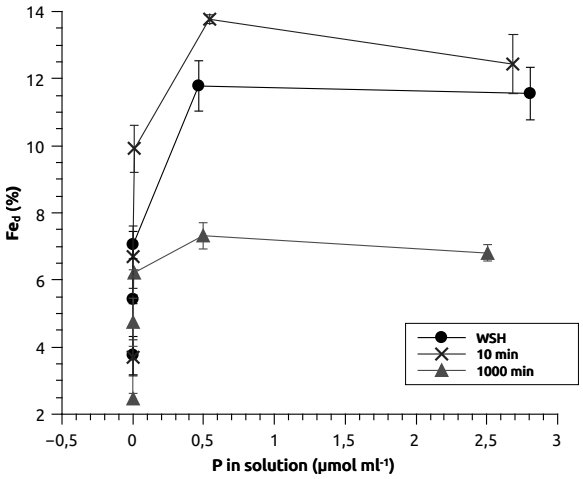

(a) Fe$_d$(%)

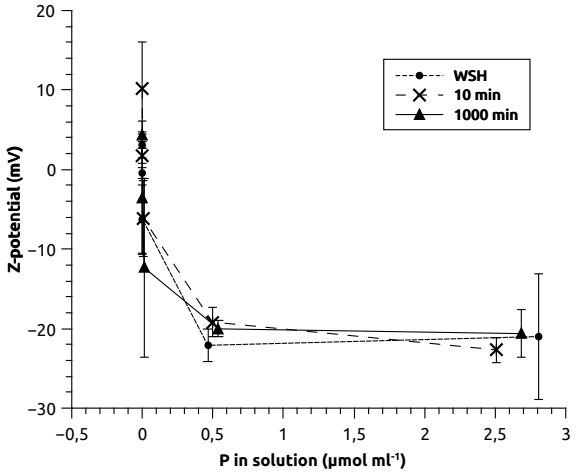

(b) zeta-potential

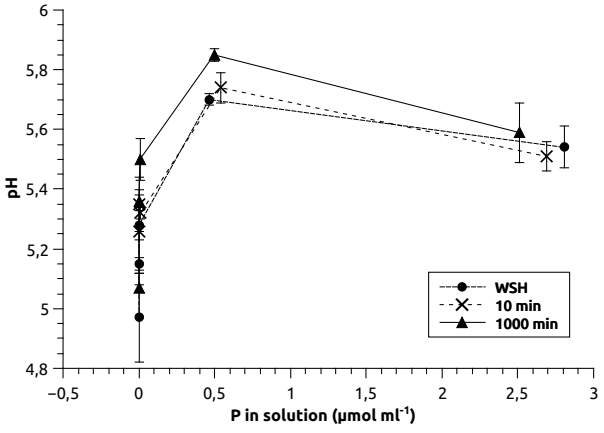

(c) pH

Figure 2.4. Phosphate in equilibrium in solution related to the **(a)** total Fe content (Fe$_d$) percentage, **(b)** zeta-potential, and **(c)** pH

These changes leaded to a stable sample in terms of low Fe (hydr)oxide detachment after mechanical abrasion and against the 2L-FH surface charge reduction associated with P adsorption. Thus, providing to this designed technogenic substrate promising features to (a) keep a stable Fe (hydr)oxide coating in spite of fertilization excess, avoiding leachates into the runoff water; (b) function as a sink of P which in medium-term could be plant available; (c) filter pollutants (such as As, Zn, or Cu) adsorbed due to its high sorption capacity related to its SSA, (d) reduce the erodibility of soils by increasing the macroaggregation.

In consequence, we propose the use of our coating method followed by a 1000 min shaking in order to get a stable coated sand.

This work is a solid first step in the development process of an Fe (hydr)oxide-coated sand aimed to be a technogenic substrate for a purpose-designed Technosol, conjugating the well known high hydraulic conductivity provided by the sand particle size and the adsorption features of the 2L-FH. It is the first time that the Fe fraction is planned to be included in a designed Technosol as an Fe (hydr)oxide coated sand.

However, still important aspects to obtain a completely functional and cost-effective technogenic substrate for a large-scale production need to be achieved. It would be necessary to replace the costly synthesis of the 2L-FH. One could search for other sources of Fe-minerals and test them with the same process. Additionally, to reduce costs and resemble as much as possible a natural substrate, sand preferably should have a heterogeneous particle size distribution and should be obtained form a local source.

3. Coating a dredged sand with recycled ferrihydrites to create a functional material for plant substrate[2]

Abstract

Purpose Urban greenery provides a series of benefits for the environment and inhabitants of cities. However, the substrate preparation mostly implies the mining and erosion of valuable natural soils (e.g. peat). Purpose-designed substrates, preferably made of waste materials, could avoid the extraction damage. The present work aims at improving the production and lowering the costs of a functional stably coated sand with ferrihydrite. This functional substrate combines the Fe (hydr)oxide sorptive capacities and the fast drainage of sand. Thus, secondary raw materials were tested: a dredged sand and three Fe (hydr)oxides; one from groundwater, an industrial intermediate product, and a mining by-product.

Materials and methods Three Fe (hydr)oxides were structurally characterized by XRD, XRF analysis, and SSA measurements. Further, amorphous Fe (hydr)oxide concentrations were determined. Sludges of these Fe (hydr)oxides in different concentrations were hand-mixed with a dredged and a mined sand, and dried at 35 °C. The stabilization of the coating was made by heavy shaking (250 rpm) the coated sand with water (3:1 *w:w*) for 0, 10 and 1000 min, washing and drying at 35 °C afterwards. Thereafter, the effectiveness of this treatment was determined by the Fe concentration and pH of the coated sand, along with the particle size of the detached aggregates during shaking, and the pH in the washing water. The morphology of the coating was observed by scanning electron microscopy.

Results and discussion All Fe (hydr)oxides were 2-line ferrihydrites with large SSA, and coated both sands. Only after 1000 min shaking, homogeneous and small ferrihydrite aggregates covered the sands surfaces (verified by SEM and particle size). The impurities of the ferrihydrites affected the stabilization of the coating. Calcium carbonates enhanced the aggregation and reattachment of the Fe aggregates to the sand during shaking, while phosphate reduced the reattachment by stabilizing the aggregates in the suspension.

Conclusions Two out of three ferrihydrites were suitable to develop a stable coating. To coat dredged sand with both ferrihydrites lowers the cost and production time to obtain a functional substrate. One ferrihydrite has a high pH due to its high $CaCO_3$ content, and sand coated with it may be used as an amendment for acidic clayey soils.

3.1. Introduction

The establishment of urban green areas is one of the strategies to counteract soil sealing and degradation of soil functions in cities. Important and diverse advantages

[2] This is a postprint version of an article published by Springer: Flores-Ramírez, E., Dominik, P., and Kaupenjohann, M. (2018b). Coating a dredged sand with recycled ferrihydrites to create a functional material for plant substrate. *Journal of Soils and Sediments*, (18)2: 534–545. DOI: 10.1007/s11368-017-1772-7. Republished with permission of Springer. The publication is available on SpringerLink.

are gained in the regulation of the ecosystem services provided from urban soils and urban green areas (Bolund and Hunhammar 1999; Weng et al. 2004; Morel et al. 2014).

However, large quantities of natural soil are often used to establish urban green infrastructure. For example, in the projected urban green area to be installed on the roof of the A7 highway cut-and-cover tunnel, in Hamburg, Germany, has been planned to use about 1×10^3 kg m^{-2} of natural soil for its 25 ha (Melchior 2016).

The soil is predominantly obtained from forested surrounding areas or agricultural lands, causing the degradation of the extraction area. For instance, in France, around 3×10^6 m^3 per year of natural soils are used for green infrastructure (Rokia et al. 2014). It is clear that the ecological impact of this practice must be reduced and alternative technologies and materials should be implemented. The rehabilitation or reclamation of one place should not imply the degradation of another.

One way to decrease the demand of natural soil for these needs is to construct purpose-designed soils, preferably from waste materials (Séré et al. 2008). They could specifically fulfil local needs for vegetation, according to the environmental and technical conditions based on current pedogenic knowledge. A soil composed mainly by materials of technical origin is classified as a Technosol (IUSS Working Group WRB 2015); in this case, a purpose-designed Technosol for greening. Additionally, costs of transportation to nearby areas and waste disposal can be considerably reduced using local and/or recycled materials.

In such direction, some researchers have assessed diverse substrates to obtain fertile mixtures for constructed soils using materials of natural or artificial origin mixed with an organic fraction: paper mill sludge (Séré et al. 2008), urban wastes, bricks, or demolition rubble (Nehls et al. 2013; Rokia et al. 2014).

Among the materials widely used as part of many substrate mixtures sustaining vegetation, quartz sand is a conventional material. However, in spite of its relative availability, sand has become scarcer in the last years, as it is a natural resource mostly mined (Gibbs 2011). Alternatively, sand recycled from crushed construction and demolition waste (Ulsen et al. 2013), or sand dredged from rivers can be used in order to reduce the extraction impact and to face scarcity. Dredging is a regular process to extract the river bottom sediments, thus providing large amounts of local material that needs to be disposed.

In a constructed Technosol, sand can provide an easy-to-handle main mineral fraction, which allows fast drainage and rootability in the soil profile. However, it has

a loose structure and a very low specific surface area (<0.1–3.0 $m^2\,g^{-1}$; Slater et al. 2006; Arias et al. 2006), which implies a low reactive surface area (Sposito 2008), important for the chemical reactivity of the soil solid phase. In natural soils part of these functions are given by the ubiquitous pedogenic Fe (hydr)oxide minerals (oxides, oxihydroxides and hydroxides). They enhance soil aggregation by cementing clay minerals and quartz particles (Wang et al. 1993; Duiker 2003), and adsorb oxyanions (PO_4^-, SiO_3^-, AsO_4^-, SeO_4^-; Ko et al. 2007), heavy metals (Lai and Chen 2001), organic molecules, and even viruses and bacteria (Lukasik et al. 1996; Scott et al. 2002).

Among these Fe (hydr)oxides, ferrihydrite is amorphous as a result of the fast oxidation during its formation and its content of structural and adsorbed water (Wang et al. 2013b). Ferrihydrite is conformed by nanocrystals (<10 nm; Michel et al. 2007) and it tends to aggregate to satisfy the high surface energies of nanoparticles (Nanda et al. 2003). Its small particle size confers a large specific surface area to the ferrihydrite (>200 $m^2\,g^{-1}$; Cornell and Schwertmann 2003), and hence, a high adsorption capacity (Zhao et al. 1994; Wang et al. 2013a).

When combining sand and ferrihydrite, we get an enhanced substrate highly functional to be part of a purpose-designed Technosol when mixed with compost and other water retaining particles. While providing soil structure stability and surface chemical reactivity of the soil solid phase, it could sustain plants in conditions of high risk of water stagnation, installed over a sealed bottom or in areas with a constant precipitation regime, for example.

With this aim, in a previous research, Flores-Ramírez et al. (2016) coated a mined sand with synthesized 2-line ferrihydrite (2L-FH). The Fe (hydr)oxide fraction of the coating improved the sand functionality by providing an adsorptive surface, mimicking natural soils. Once coated the sand, the best treatment to stabilize mechanically the coating was a long term heavy shaking with water. The sand treated had a low Fe detachment and was also stable against the 2L-FH surface charge reduction associated with P adsorption. Nevertheless, the procedure is not affordable nor practical to produce large amounts of substrate, mainly due to the time and high costs that the ferrihydrite synthesis requires.

However, ferrihydrite forms naturally or as a result of industrial processes. Fe (II) leached from soils and sediments into water bodies forms precipitates of ferrihydrite and lepidocrocite when it oxidises (Rhoton et al. 2002). Groundwater with dissolved Fe(II) is oxidized at waterworks to filter the precipitated Fe (hydr)oxides for drinking water (Lytle et al. 2004; Rhoton and Bigham 2005). Ferrihydrite is also

produced from the oxidation of pyrite present in the deposits of open pit mining. The outcome is an acidic sulphate-rich drainage known as acid mine drainage (Akcil und Koldas 2006). Also, the paint industry synthesizes Fe (hydr)oxides, such as goethite or hematite, where ferrihydrite is an intermediate step.

Objective Therefore, the aim of the present work is to test whether the replacement of the costly materials with available recycled Fe (hydr)oxides and sand obtained from the Elbe river (Germany) dredging is practicable to obtain a stable sand coating. This implies the structural and chemical characterization of the chosen Fe (hydr)oxides, as well as the characterization of the sands coated and stabilized with the new materials. A successful replacement would reduce the production time and cost in comparison to the previous research, to obtain a functional technogenic substrate.

3.2. Materials and Methods

3.2.1. Materials

Fe (hydr)oxides

Three Fe (hydr)oxides were chosen from different sources:

LX is an amorphous Fe (hydr)oxide that is an intermediate product of the commercial production of goethite by Lanxess AG®. The material is solid, but humid.

CM is a mining by-product. The Fe (hydr)oxides of this material result from the oxidation of the pyrite (FeS_2) present in the brown coal. The Fe(II) of the pyrite is subsequently oxidized and precipitates as amorphous Fe (hydr)oxide. In the process, H_2SO_4 is formed and $CaCO_3$ is added to rise the pH of the system. The material is solid but humid, and was obtained through FerroSorp ®.

WW are Fe (hydr)oxides obtained at the waterworks of the city of Hamburg (Germany). The large amount of dissolved ferrous iron (Fe (II)) in the groundwater is expressly oxidized at air contact at the waterworks, producing precipitable particles that can be filtered afterwards. The material was collected from the open air basins where the Fe (hydr)oxides concentrate and sediment by water evaporation. The material is a sludge.

After collection, all the materials were stored at 4 °C to avoid transformation into crystalline forms.

Sand

Two types of sand were used for the coating experiments:

Mined sand is a commercial mined sand (Sand Schulz®), used also in Flores-Ramírez et al. (2016). It has a specific surface area (SSA) of 0.06 $m^2\,g^{-1}$, a pH of 5.2, ($CaCl_2$ 0.01 M; Knick 761 Calimatic), and a charge of -38 mV. It is composed of SiO_2 >96 %, C, N, S ≪0.1 % (measured with the CNS analyzer Vario EL III Elementar), and therefore, it is free of carbonates.

The **dredged sand** was obtained from the sediments of the Elbe river. It has a SSA of 0.04 $m^2\,g^{-1}$, a pH of 7.01 ($CaCl_2$ 0.01 M), and a charge of -22 mV. It presents C 0.14 %, N 0.01 % and S 0.06 % (CNS analyzer Vario EL III Elementar), with 0.03 % of C associated to carbonates (measured after dry-heating at 500 °C for 5 h). However, as it is a fluvial sediment, the sand is heterogeneously mixed with fragmented shells, thus reacting positively to the carbonate test (HCl 10 %).

3.2.2. Methods

Fe (hydr)oxide characterization

Dense sludges of the Fe (hydr)oxide samples were lyophilized (Christ Alpha 2-4) to stop their transformation into crystalline forms. A fine dust of each sample was obtained after lyophilization.

Lyophilized Fe (hydr)oxides were characterized by (a) total Fe, (b) amorphous and crystalline Fe ratio, (c) specific surface area (SSA), (d) zeta-potential, (e) zeta-potential at different pH values, (f) crystallography and (g) chemical composition.

Total Fe was extracted with citrate-bicarbonate-dithionite (Fe_d) according to Mehra and Jackson (1958). The amorphous Fe (hydr)oxides were extracted with oxalate (Fe_o), according to Schwertmann (1964). The Fe concentrations (cFe) in the Fe_d and Fe_o extracts were measured along with Al and Ca concentrations by atomic adsorption spectrophotometry (AAS Perkin Elmer 1100B). The amount of crystalline Fe was calculated as the difference between Fe_d and Fe_o.

The specific surface area (SSA) of the Fe (hydr)oxide samples was quantified with a nitrogen gas adsorption isotherm of 11 points using the BET equation (Quantachrome Autosorb 1 surface analyzer).

The powder samples were ultrasonically dispersed (Elma Transsonic 820/H) in deionized water in order to measure their pH (Knick 761 Calimatic) and zeta-

potential (Malvern Z-Seizer 2000). Also, the dispersed samples were titrated at pH values of 4, 5, 6, 7, and 8 and the corresponding zeta-potentials were measured.

Diffraction patterns of the Fe (hydr)oxides were observed with X-ray powder diffraction (XRD; Panalytical PW 1710, Cu anode, with a measuring range of 5–80 °, at a scanning speed of 0.01 ° 2Θ min^{-1}), and their chemical composition was determined with X-ray fluorescence spectroscopy (XRF, Panalytical PW 2400, detection limit >5.0 mg).

The water content of the fresh samples was determined gravimetrically, heating for 12 h at 105 °C.

Sand characterization

The particle size distribution of the sands was obtained by wet sieving the following fractions: 0.06, 0.1, 0.2, 0.35, 0.63, and 2.0 mm for the dredged sand, and 0.06, 0.1, 0.2, 0.3, 0.4, 0.5, 0.6, 1.0, and 2.0 mm for mined sand (distribution given by Sand Schulz®).

Additionally, the Fe_d of the sands was measured (Mehra and Jackson 1958; Perkin Elmer 1100B AAS) and the values were subtracted from all the correspondent calculations.

Coating process

In Flores-Ramírez et al. (2016), a dense suspension of synthetic 2-line ferrihydrite (2L-FH) was homogeneously hand-mixed with mined sand and dried afterwards at 35 °C. We modified the process and substituted the 2L-FH with the three Fe (hydr)oxides collected to coat the mined and the dredged sands.

In order to achieve a wide range of Fe:sand coating ratios, two suspensions of each Fe (hydr)oxide, in a low and a high concentration of Fe were used:

LX 16.7 and 34.7 g L^{-1}; CM 17.0 and 31.4 g L^{-1}; WW 20.9 and 38.1 g L^{-1}. The differences in the concentrations between Fe (hydr)oxides were due to heterogeneity in the water content of their fresh samples.

Afterwards, 19.8, 39.6 and 79.2 ml of these sludges were added to cover 300 g of mined sand. Due to a smaller SSA of the dredged sand, only 13.3, 26.7, and 53.4 ml of the sludges were added. The suspensions added to both sands were hand-mixed until a visual homogenization was reached (5–7 min per sample). Then the mixtures were dried at 35 °C.

All the coated sand samples were dry sieved (63 µm) in order to exclude as much as possible the free or loose attached coating particles. The loaded Fe_d of the coated sands was measured afterwards.

Process of coating stabilization

In order to improve the mechanical stability of the Fe coatings, the method of Flores-Ramírez et al. (2016) was applied to selected samples, as following. Thirty grams of coated sand and 10 ml of deionized water in 100 ml Nalgene bottles (in triplicate) were horizontally shaken (250 rpm; Janke & Junkel KS501) for 0, 10 and 1000 min, respectively. All samples were washed with deionized water through a sieve (63 µm) until the effluent was visually clear. The first 200 ml of this washing water were collected to characterize the detached particles through pH (Knick 761 Calimatic), and particle size (only selected samples, by laser diffraction with Sympatec Helos H0541). The samples were dried at 35 °C afterwards.

After the shaking and washing process, the pH and the Fe_d of the coated sands were measured. The coating loss was calculated from the initial and final values of the Fe_d.

Morphology and topography of the coating surface of selected samples were observed with the scanning electron microscope (SEM) and the backscattered electron detector (BSE; Zeiss Leo 982). The samples were mounted dry and coated with a 25 nm carbon film using an Edwards-E12E4 Vacuum Coating Unit.

3.3. Results

3.3.1. Fe (hydr)oxides

Fe concentration

The three Fe (hydr)oxides present little variation in their total Fe concentration (Fe_d) but larger variation in their amorphous Fe concentration (Fe_o; Table 3.1), reflected in their Fe_o:Fe_d. LX has the highest Fe_d (62 %), with a Fe_o:Fe_d of 0.77. WW has 40 % Fe_d, although the lowest Fe_o:Fe_d ratio (0.40). CM presents 34 % of Fe_d and, with 0.82, the highest ratio of Fe_o:Fe_d.

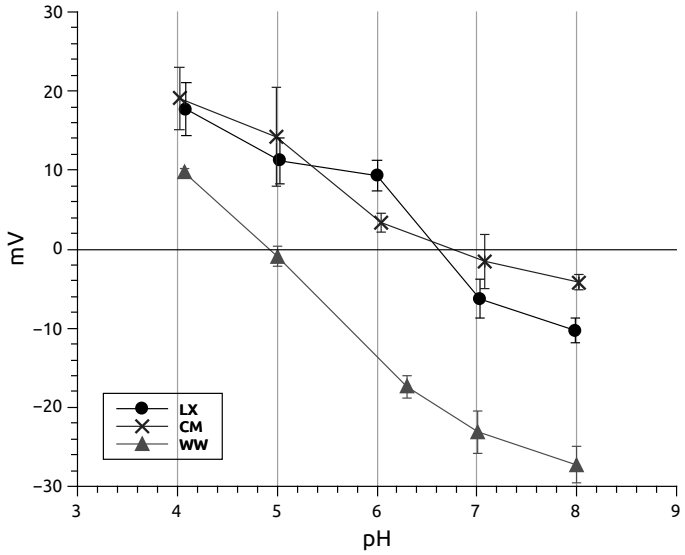

Figure 3.1. Zeta-potential of the Fe (hydr)oxides in relation with pH

Specific surface area

The sample with the largest SSA (Table 3.1) is LX ($341\,m^2\,g^{-1}$) followed by CM ($241\,m^2\,g^{-1}$) and WW ($199\,m^2\,g^{-1}$). Values are directly related to the Fe_o concentration of the materials.

Zeta-potential

All samples have increasing negative values with rising pH (Fig. 3.1), nevertheless, charge values of LX and CM do not drop drastically, reaching -10.3 mV and -12.2 mV, respectively. In contrast, WW drops to -27.3 mV. The point of zero charge (PZC) of LX and CM are close (pH between 6.6 and 7), in contrast with pH 5.0 for WW.

Structural and chemical composition

X-ray diffraction confirmed the amorphous nature of the collected Fe (hydr)oxides. The diffractograms show the typical pattern of a 2L-FH, the most amorphous of the two ferrihydrites (two-line and six-line). The pattern consists of two very broad peaks, the first between the interplanar spacing (d) of 2.2, 2.5 Å and the second with the maxima around 1.5 Å (Fig. 3.2).

The broad peaks of LX are more defined and pointy, while the ones of WW and CM are even broader. Also, the obtained diffractograms show diffuse diffraction bands, composed of several small peaks instead of clear lines, hindering the proper iden-

Table 3.1. General characteristics of the Fe (hydr)oxides

Characteristic	LX	CM	WW
Fe_d (%)	62	34	40
Fe_o (%)	48	28	16
SSA [$m^2 g^{-1}$]	341.41	241.85	199.97
Zeta-potential [mV]	11.5	-12.2	-17.4
pH	5.4	8.32	6.44

The z-potential reading was taken at the pH given

tification of crystal peaks. Only CM and WW present crystal peaks in the XRD diffractogram of other compounds. CM has several defined, large, and narrow peaks of calcite ($CaCO_3$), with interplanar spacings (d) at 1.599, 1.876, 1.918, 2.090, 2.282, 2.290, 2.488, 3.035, and 3.848 Å. The diffractogram of the sample also shows peaks that could correspond to maghemite (γFe_2O_3), magnetite (Fe_3O_4), wüstite (FeO), or other Fe oxides at interplanar spacings (d) between 1.434–1.618 Å. WW has a defined peak at position 2.429 Å identified as purpurite ([Mn, Fe]PO_4), and a smaller peak corresponding to quartz (SiO_2), with a d value of 3.384 Å.

The chemical composition of the samples (Table 3.2) is in line with the XRD. For instance, CM presents a high Ca concentration of 16.6 % of CaO, 3 % of SiO_2 and 2 % of SO_3. WW is the sample with more impurities, with a high percentage of P_2O_5 (7 %) and SiO_2 (5 %), followed by Ca, and Al. LX is the sample with less impurities.

3.3.2. Sand

The mined sand has a Fe_d concentration of 0.32 mg g^{-1}. It has a particle size distribution of 0.06–0.6 mm, with 94 % of particles between 0.1-0.4 mm.

The dredged sand has a Fe_d of 1.08 mg g^{-1}. It has a particle size distribution of 0.06–6.0 mm, with 86 % of particles between 0.1–0.6 mm. For further use the sand was sieved to exclude particles larger than 2 mm.

3.3.3. Coating process

A wide range of cFe was obtained from the different Fe:sand coating ratios (Table 3.3). The lowest and the highest cFe obtained are LX 1.07 and 4.80 mg g^{-1};

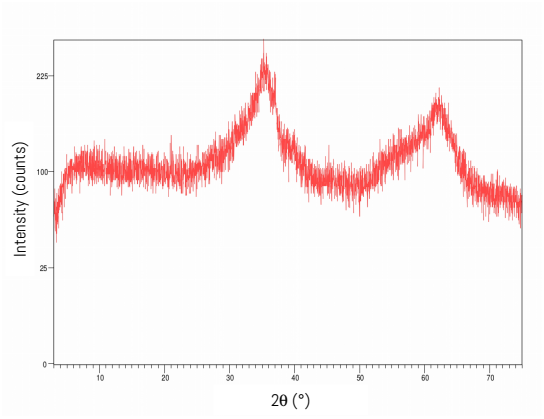

(a)

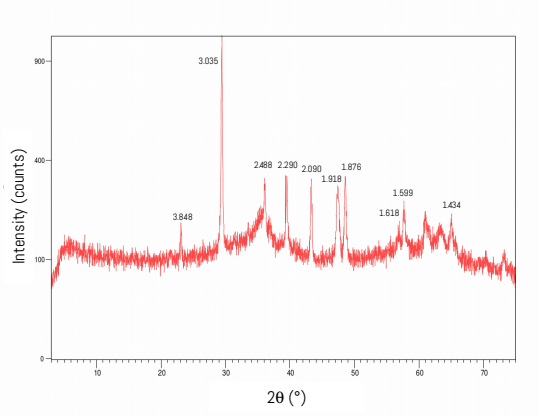

(b)

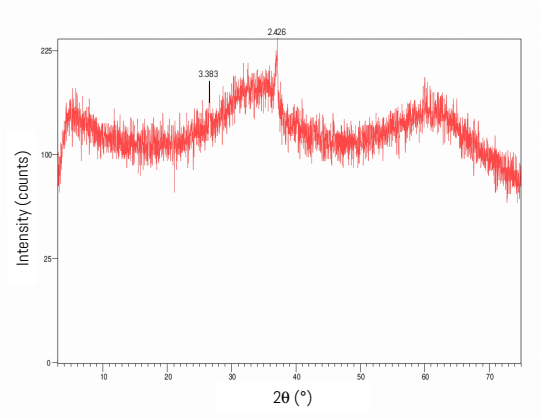

(c)

Figure 3.2. X-ray powder diffractograms depicted in 2Θ degrees of **(a)** LX, **(b)** CM, and **(c)** WW, with *d* values for peak heights in angstroms. The three of them present the typical pattern of a 2-line ferrihydrite, the most amorphous of the two ferrihydrites (*two-line* and *six-line*). LX has the most pointy hills, indicating its low level of impurities. CM has several defined peaks of calcite ($CaCO_3$) at 1.599, 1.876, 1.918, 2.090, 2.282, 2.290, 2.488, 3.035, and 3.848 Å. The diffractogram of the sample also shows *d* values that match with different Fe oxides (maghemite [γFe_2O_3], magnetite [Fe_3O_4], or wüstite [FeO]) in the range of 1.434–1.618 Å, but their peak intensity is <10 % and were not properly identified due to the diffusion of the diffraction bands. WW has a defined peak that can correspond to purpurite ([Mn, Fe]PO_4) at position 2.429 Å, and a smaller peak corresponding to quartz (SiO_2), at 3.384 Å

Table 3.2. Chemical composition of the Fe (hydr)oxides measured by X-ray fluorescence and through dithoinite extraction ($_d$) measured by atomic adsorption spectroscopy

Compound formula	LX Concentration [%]	CM Concentration [%]	WW Concentration [%]
Al_2O_3	0.06	1.68	3.23
SiO_2	0.08	3.382	5.34
P_2O_5	<d.l.	0.04	6.85
SO_3	2.64	2.22	0.64
CaO	0.09	16.61	3.53
MnO	0.27	0.96	2.35
Fe_2O_3	81.23	51.84	63.50
Sr	<d.l.	0.16	0.02
Na_2O	0.34	<d.l.	<d.l.
TiO_2	<d.l.	<d.l.	0.08
Zn	<d.l.	0.05	<d.l.
Al_d	<d.l.	1.40	1.71
Ca_d	<d.l.	16.36	2.51

<d.l.= value below the detection limit

CM 1.02 and 8.18 mg g^{-1}; WW 0.77 and 8.19 mg g^{-1}. The larger the volume and concentration of ferrihydrite suspensions added to the sands, the higher is the loaded coating.

3.3.4. Process of coating stabilization

For both types of sand were chosen representative low, medium and high cFe of the three coating ferrihydrites, to test the process of coating stabilization (Table 3.3).

Fe concentration of coatings

A decrease in the cFe after 10 min of shaking and an increase after shaking for 1000 min, is obtained in the cases of LX ferrihydrite coating mined sand (Table 3.3).

Instead, dredged sand coated with LX and both sands coated with CM present similar cFe values for 10 and 1000 min treatments.

In contrast, sands coated with WW present a very different pattern of cFe. The coating diminishes with every step of the shaking treatments, reaching nearly the absence of ferrihydrite in some samples, without distinction between sands or cFe of the initial coating.

Additionally, in spite of some high initial Fe loadings (up to 8.2 mg g^{-1}), after the washing treatment the Fe loading decreases in all the cases.

pH

After the washing and shaking treatments, the average pH of all mined sands coated with LX is 5.2 ± 0.1, and the one of the dredged sand is 7.2 ± 0.2.

The pH measured in the water used in the washing step of the mined sand is constant (5.4 ± 0.1) among all treatments (Table 3.3). However, the pH of the water used in the washing step of the coated dredged sand increases with each shaking time: *washed* (6.7 ± 0.4) < 10 min (7.8 ± 0.3) < 1000 min (8.5 ± 0.3). The average pH in the mined and dredged sands coated with CM are 9.1 ± 0.3 and 8.4 ± 0.7, respectively. The pH in the water used in the washing step did not change among treatments, and had an average of 9.1 ± 0.2.

The pH of the mined sand coated with WW treatments was lower (6.5 ± 0.2) than the coated dredged sand treatments (7.0 ± 0.2). The pH in the water used in the washing step of both sands coated with WW presented a stable pH of 7.2 ± 0.3 among all treatments.

Particle size of detached aggregates

The size range of the detached ferrihydrite aggregates of all measured treatments is 4–23 µm. The largest aggregates were detected in the treatments with high initial Fe loadings.

The size of the detached aggregates of all non-shaken samples are much larger than those of the shaken ones. The aggregates of 10 and 1000 min samples present similar sizes (Table 3.3).

The increasing cFe loss of WW coatings along each shaking treatment pointed to an insufficient Fe adsorption of the ferrihydrite on sand. Therefore, the particle size of its detached aggregates was not further analysed.

SEM images

All the observed aggregates of the three ferrihydrites covering the sands surfaces change in the same way in shape, size, and cover after been shaken (Fig. 3.3).

The aggregates of the original coating (observed on the non-shaken sample) are predominantly large and spheroid-shaped, with irregular borders, covering densely only certain areas of the sand surface.

After shaking for 10 min, a mixture of few large aggregates with abundant smaller ones can be observed in all the samples. Their borders are irregular, ranging from

Table 3.3. Fe concentrations of the coated sands before and after the shaking treatments (250 rpm)

FH	Sand	cFe(i) mg g^{-1}	Treatment (min)	cFe mg g^{-1}	cFe:cFe(i) -	pH -	Particle sizes (x=50 %) Average (µm)
LX	mined sand	1.07	0	0.91 *(0.04)*	0.85	5.14	7.41 *(1.00)*
			10	0.62 *(0.09)*	0.58	5.05	6.15 *(2.40)*
			1000	0.83 *(0.04)*	0.78	5.07	4.06 *(0.04)*
		2.21	0	1.76 *(0.14)*	0.80	5.27	
			10	1.20 *(0.02)*	0.54	5.19	
			1000	1.71 *(0.35)*	0.77	5.11	
		3.94	0	3.16 *(0.07)*	0.80	5.31	
			10	2.18 *(0.14)*	0.55	5.31	
			1000	2.57 *(0.05)*	0.65	5.21	
		4.80	0	4.08 *(0.11)*	0.85	5.39	22.89 *(2.63)*
			10	3.22 *(0.05)*	0.67	5.41	13.39 *(1.86)*
			1000	3.18 *(0.04)*	0.66	5.21	15.30 *(0.52)*
	dredged sand	1.35	0	0.81 *(0.16)*	0.60	7.08	
			10	0.54 *(0.34)*	0.40	7.45	
			1000	1.65 *(0.81)*	1.00*	7.35	
		2.42	0	2.92 *(0.07)*	1.00*	7.08	9.25 *(0.29)*
			10	1.64 *(0.23)*	0.68	7.46	4.67 *(0.54)*
			1000	1.01 *(0.51)*	0.41	7.18	4.19 *(0.30)*
		4.21	0	6.24 *(1.11)*	1.00*	6.92	
			10	2.10 *(0.39)*	0.49	6.93	
			1000	1.74 *(0.19)*	0.41	7.29	
CM	mined sand	1.58	0	0.91 *(0.14)*	0.60	8.71	
			10	0.56 *(0.04)*	0.35	8.62	
			1000	0.77 *(0.05)*	0.49	8.38	
		2.87	0	1.58 *(0.25)*	0.55	9.16	13.22 *(2.61)*
			10	0.88 *(0.00)*	0.31	9.17	6.11 *(0.23)*
			1000	1.26 *(0.00)*	0.44	9.14	6.45 *(0.51)*
		5.72	0	2.30 *(0.16)*	0.40	9.25	17.97 *(0.95)*
			10	1.97 *(0.19)*	0.34	9.29	8.30 *(0.25)*
			1000	2.05 *(0.34)*	0.36	9.29	11.02 *(3.1)*
		8.18	0	3.68 *(0.21)*	0.45	9.24	
			10	2.78 *(0.04)*	0.34	9.20	
			1000	1.55 *(0.19)*	0.19	9.20	
	dredged sand	1.02	0	0.62 *(0.18)*	0.61	8.10	
			10	0.90 *(0.11)*	0.88	7.03	
			1000	0.66 *(0.62)*	0.65	7.99	
		2.19	0	1.57 *(0.49)*	0.72	8.59	6.62 *(0.31)*
			10	1.27 *(0.46)*	0.58	8.50	3.78 *(0.05)*
			1000	1.05 *(0.11)*	0.48	8.57	6.86 *(0.25)*
		4.60	0	4.22 *(1.77)*	0.92	9.09	
			10	2.15 *(0.42)*	0.47	8.93	
			1000	2.65 *(0.35)*	0.58	9.12	
WW	mined sand	1.08	0	0.61 *(0.00)*	0.56	6.50	
			10	0.42 *(0.12)*	0.39	6.33	
			1000	0.00 *(0.02)*	0.00	6.23	
		2.26	0	1.33 *(0.04)*	0.59	6.57	
			10	0.61 *(0.11)*	0.27	6.33	
			1000	0.37 *(0.09)*	0.16	6.32	
		8.19	0	4.73 *(0.04)*	0.58	6.78	
			10	3.37 *(0.12)*	0.41	6.77	
			1000	0.75 *(0.05)*	0.09	6.70	
	dredged sand	2.58	0	1.74 *(0.30)*	0.67	6.92	
			10	0.56 *(0.12)*	0.22	6.87	
			1000	0.59 *(0.19)*	0.23	7.01	
		6.79	0	5.41 *(0.23)*	0.80	7.01	
			10	1.17 *(0.04)*	0.17	7.31	
			1000	0.49 *(0.30)*	0.07	7.06	

Where FH is ferrihydrite, the pH corresponds to the coated sands, cFe is the average Fe concentration of the sand, and cFe(i) is the initial Fe concentration of the sands before treatments. Standard deviation in brackets (n=3). * = values that exceed the measured cFe, but are in concordance with the calculated maximum

spheroid-shaped to flattened-shape. Some samples show scattered clusters all over the surface, while others have just few dense covered areas of coating.

The aggregates after shaking for 1000 min have homogeneous sizes. The majority has the size of the small aggregates observed in 10-min samples, some are slightly larger. All samples exhibit flattened aggregates forming a uniform cover on the whole sand surface.

Even in the samples coated with WW, where the cFe fades through the shaking treatments, the same strong changes of the aggregates in shape, size, and distribution are registered.

The changes of the aggregates observed with SEM are in line with the sizes of the ferrihydrite aggregates detached after shaking.

3.4. Discussion

3.4.1. Characterization of the Fe (hydr)oxides

The three Fe (hydr)oxides used to coat the sands are 2-line ferrihydrites, as indicated by the two broad peaks in the XRD diagrams (Fig. 3.2). While LX shows a quite defined pattern, CM and WW shows broader and less defined peaks as a result of their impurities, which increase their structural disorder (Cismasu et al. 2011). Although the three Fe (hydr)oxides present different SSA, their values are still in the same order of magnitude.

Among the three Fe (hydr)oxides, LX is the purest ferrihydrite, with the highest concentration of Fe_o (48 %), corresponding with the highest SSA. Although CM has a high Fe_o concentration (28 %) as well, it includes impurities commonly reported for mining by-products (Akcil und Koldas 2006; Cismasu et al. 2011). The most abundant observed is $CaCO_3$, which is amended during the production of CM, to reduce the acidity (mainly H_2SO_4 formed) aroused from pyrite oxidation. The latter is also the source of the sulphur in the sample.

WW has the lowest Fe_o concentration, the lowest SSA, but the largest amount of impurities. As WW was extracted from groundwater it presents impurities commonly found in fresh and seawater. In particular, dissolved species of silicates, phosphates and organic matter are quite common in such Fe (hydr)oxides, which corresponds with the measured chemical composition of WW (Table 3.2). The phosphorous, presumably in the form of PO_4, has been proven to coprecipitate

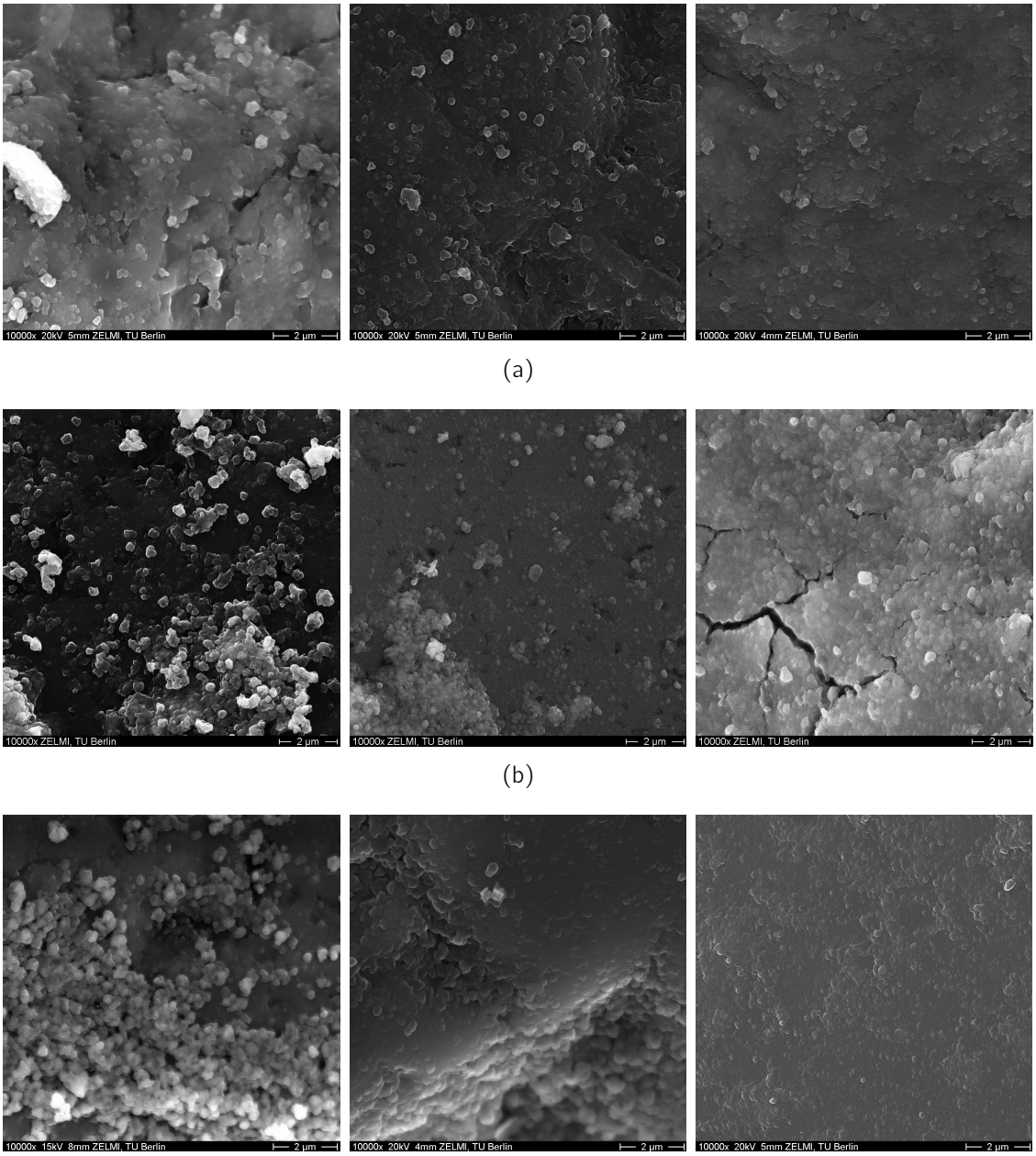

Figure 3.3. Scanning electron microscope images of dredged sand surfaces coated with **(a)** LX, **(b)** CM, and **(c)** WW. From *left* to *right* each image corresponds to the treatments: non-shaken, 10 min, and 1000 min. Scale of 2 µm. In the samples that were not shaken large aggregates can be observed. The aggregates are predominantly spheroid-shaped with irregular borders, covering densely certain sand surface areas. LX ferrihydrite has the most flattened aggregates, and WW the most spheroidal ones. Samples shaken for 10 min present heterogeneous sizes and shapes of aggregates, ranging from flattened to spheroidal with irregular borders, covering only certain areas. After 1000 min of shaking, the aggregates of the three ferrihydrite samples present homogeneous sizes and shapes. The whole sand surface is smooth, covered with rounded and flat aggregates. Sand coated with WW has a very thin layer, as the sand surface can be distinguished, which reflects its Fe loss due to the shaking treatments

along with the oxidation of Fe(II) and hydrolization of Fe (III) (Gunnars et al. 2002). Also, a certain content of purpurite ([Mn, Fe]PO_4 identified in the XRD may be present as the sample contains Mn. Calcium is also associated with phosphates (Rhoton and Bigham 2005), but it can also be related to organic matter (Gunnars et al. 2002), or adsorbed by complexation reactions with hydroxyl groups of the Fe (hydr)oxide surface (Dzombak and Morel 1990). These complexes may count for the high Ca content in the coating, as $CaCO_3$ is unlikely due to the low pH of the sludge. The measured Al could be based on the replacement of Fe in the Fe (hydr)oxide. The content of silicates results from detrital bedrock particles. The presence of other Fe (hydr)oxides in CM and WW is possible, as reported for ferrihydrites with similar origins (Ferris et al. 1989; Rhoton and Bigham 2005), and observed at the XRD, although hard to determine which ones due to the predominance of ferrihydrite.

Fe (hydr)oxide charges are pH dependent (Cornell and Schwertmann 2003) and all ferrihydrites have increasing negative charges when increasing the pH (Fig. 3.1). The $CaCO_3$ present in CM should be specifically adsorbed, modifying its zeta-potential, PZC, and it may also change the CM capacity of proton buffering, as reported (Appelo et al. 2002; Su and Suarez 1997). The zeta-potential of WW decreases drastically (-27 mV), in contrast with LX and CM, as a result of the deprotonation of the phosphates –adsorbed to the Fe–, along with the increasing pH.

The properties of a coated material and its chemical reactivity in the soil solid phase tend to depend almost entirely on the type and characteristics of the coating Fe (hydr)oxide (Sakurai et al. 1990). As all Fe (hydr)oxides are composed by amorphous ferrihydrite, the coated substrates will enhance the nutrient retention capacity (e.g. of PO_4; Guzman et al. 1994) of the designed Technosol due to the ferrihydrite reactive surface (Zhao et al. 1994; Wang et al. 2013b) and its high SSA. Also, ferrihydrite would foster the soil aggregation better than a crystalline Fe (hydr)oxide (Duiker et al. 2003), which is of capital importance for a loose material such as sand.

3.4.2. Coating process and coating stabilization

The coating of both sands is achieved with the three Fe (hydr)oxide suspensions in spite of the dredged sand heterogeneity and the impurities of CM and WW. Therefore, the repeatability of the coating as a first step in the process is reached.

Also, a wide range of low and high cFe on both sands is obtained to further test the coating stabilization process (Table 3.3).

The combinations of sands and ferrihydrites developed cFe of the coatings which differ from the ones obtained in the previous work after the shaking treatments (Table 3.3). In the previous work (Flores-Ramírez et al. 2016) the Fe loss was reduced after 1000 min of shaking in comparison with 10 min.

The washing treatment caused a decrease in the cFe of all the initial coatings, reaching in some samples more than 50 %, in spite of some high Fe loadings. This indicates that a large amount of ferrihydrite is weakly attached, probably due to a weak surface adsorption.

After the shaking treatments, only mined sand coated with LX shows the pattern obtained by Flores-Ramírez et al. (2016), as the materials used in both studies are equivalent: LX as the synthesized 2L-FH and the same mined sand used. However, the shaking treatments did not show explicitly a different impact on the cFe of the sands coated with CM and dredged sand coated with LX, but the Fe remains even after heavy shaking. In contrast, for both sands coated with WW, an overall drastic decrease of cFe along the increasing shaking time was observed (Table 3.3).

Nevertheless, while for the majority of shaken samples no explicit quantitative difference in the cFe along the treatment could be observed, the quality of the coating changes drastically in all coated substrates, without difference of sand or ferrihydrite origin. This is indicated by the morphology of the coating aggregates observed by the SEM images, and their sizes measured by laser diffraction.

The non-shaken samples exhibit larger coating aggregates than the shaken ones. The observed spheroid-shaped aggregates, with irregular borders, and the scattered distribution of the coating coincide with the characteristics of other coatings obtained by diverse methods and also with other Fe (hydr)oxides (Bedarida et al. 1973; Sakurai et al. 1990; Scheidegger et al. 1993).

On the contrary, the shape and distribution pattern observed in the samples shaken for 10 and 1000 min differ from the non-shaken samples. The 10 min samples have heterogeneous aggregate shapes and sizes, while after 1000 min of heavy shaking are quite homogeneous in size and shape. After this treatment, small and flattened aggregates cover the whole sand surface as observed with the synthesized ferrihydrite coating in the previous work (Flores-Ramírez et al. 2016). The heterogeneity of the 10 min aggregates shows an intermediate stage of sizes, shapes and

distribution of the coating aggregates between the non-shaken and the 1000 min treatments.

These results corroborate the approach that the ferrihydrite aggregates of the coatings are detached with the shaking force. Further, once floating in the suspension, they grind over the shaking time by friction, reaching small and homogeneous sizes. Then, the ground aggregates reattach on the whole sand surface, forming a homogeneous layer. Flores-Ramírez et al. (2016) propose that the weak bonding of the original coating may partly turn into a strong covalent bonding during shaking treatment, as necessary energy could be generated by friction in this process step. A covalent bonding among Fe-O-Si has been already confirmed by Scheidegger et al. (1993) and Ma et al. (2003). The aggregates arranged in a layer are more stable because more ferrihydrite can be bond directly to the quartz sand, unlike the clusters observed in the original coating. This can reduce the vulnerability of detachment by mechanical stress. Also, if the ferrihydrite coating is not arranged in clusters, its surface binding sites are more exposed, improving its adsorptive capacity.

In this model of aggregate detachment–reattachment by shaking, we propose that the cFe similarity of most samples between the treatments of 10 and 1000 min is caused by the large amount of $CaCO_3$ present in the dredged sand and CM (16 %). Carbonates are known to increase the stability of soil structure by formation of strong bonding involving Ca^{2+} bridges (Chan and Heenan 1999), and promoting the agglutination of colloids (Zehlike 2016). Thus, the carbonates of both materials could have adhered ferrihydrite colloids on the sand surface during the shaking, allowing only a moderate cFe decrease even at 10 min of shaking, when the largest Fe loss has been reported (Flores-Ramírez et al. 2016). Regarding the ferrihydrite loss registered in all the substrates coated with WW, it can be related to the PO_4 coprecipitated with the ferrihydrite. As the PO_4 is strongly associated with the ferrihydrite (Gunnars et al. 2002), the aggregates of the crystals can be very stable, and once detached in the suspension do not reattach to the sand surface and wash away with each shaking step. This effect could be also intensified due to the negative charge that WW presents (-17 mV at pH 6.4), lowering the attraction to the sand, though CM loaded and retained the ferrihydrite coating, even presenting a negative charge and a higher pH (-12 mV at 8.32). We can not discard the low ratio Fe_o:Fe_d (0.40) as another cause of the large loss of ferrihydrite in WW coatings, but the Fe_o was not determined in the shaken sands, and the crystallinity of the attached ferrihydrites can not be estimated. However, the three coats

of the used ferrihydrites presented the same pattern as the one obtained in the first research (SEM observations) with the pure synthesized ferrihydrite. With the current research we can only give hints of the mechanisms involved. In order to corroborate the role of each variable, a larger number of detailed variations and repetitions should be tested.

These cFe differences induced by the ferrihydrites impurities were clearly reflected on the coating layer observed by SEM. The sands coated with LX obtained a thin and smooth coating surface after 1000 min of shaking. CM had a thicker layer with even some visible cracks due to the $CaCO_3$ effect. WW had the thinnest layer (Fig. 3.3).

The size of the ferrihydrite aggregates corresponds positively with the initial Fe loading, therefore it depends on the available Fe, and further on the binding agents, such as $CaCO_3$, present in the suspension.

Both sands coated with LX and CM shaken for 1000 min retained a desirable ferrihydrite concentration, and have a positively modified homogeneous coating not observed in the samples shaken for 10 min. Although the amount of ferrihydrite used for coating is small, the use of CM ferrihydrite can favour an alternative use of the acid mining drainage sludge, disposed into ponds, pit lakes or tailings (Zinck 2006). In combination with dredged sand it may be an affordable product, although their $CaCO_3$ content is reflected in the alkaline pH of the coated sands. Further, despite CM is an Fe (hydr)oxide originating from the acid mine drainage, and therefore may contain heavy metals (Wieder 1989; Akcil and Koldas 2006), the material of this work reported amounts below the accurate detection limit when analysed with XRF (except for a low amount of Zn; Table 3.2). But even with a moderate content of heavy metals the risk level of pollution is low. It has been extensively reported that heavy metals are strongly bounded by specific adsorption to the Fe (hydr)oxides with a very slowly reversible desorption kinetic, in particular to the amorphous ones (Sauvé et al. 2000; Trivedi and Axe 2001). Moreover, the bioavailability of heavy metals and metalloids in soils in general, regulated by multiple factors, is overall low (Violante et al. 2010).

3.5. Conclusions and outlook

All Fe (hydr)oxides are composed of ferrihydrites and their quality strongly depends on their origin. Impurities have impacts on their characteristics and the suitability as components for an effective coating of sand.

Once the sand is coated, an improvement of the coating stability can be reached via shaking treatment. The best results were obtained after shaking the substrate for 1000 min. During this treatment ferrihydrite is detached, ground and rearranged on the sand surface. Smaller ferrihydrites particles are formed, which rearrange homogeneously on the sand surface, without distinction of ferrihydrite or sand origin. However, $CaCO_3$ and PO_4 influence the coating stability. Fe (hydr)oxides obtained from groundwater extraction process and cleaning process can contain plenty of PO_4, while $CaCO_3$ is a common constituent in dredged sand and it is related to the Fe (hydr)oxides from lignite mining materials, as it is used as an additive during processing. Species of PO_4 may interfere in the reattachment of the ferrihydrite onto the sand surface, leading to a substantial decrease of cFe through each shaking step, while $CaCO_3$ exhibits an adhering effect. However, more tests should be performed to discern which parameter of the measured ones have the largest effects on the coating stabilizing procedure.

Sands coated with the industrial intermediate product (LX), and the mining by-product (CM) ferrihydrites retained desirable Fe concentrations, and had a stable coating in spite of the high pH of the latter. Dredged sand coated with LX provides an appropriate functional substrate to be used in large amounts in a designed Technosol for greening purposes, with an adequate pH. Dredged sand coated with CM can be used as an amendment for acidic soils with a high content of clay, to improve their pH, aggregation, and adsorptive characteristics.

The use of coated sand made by recycled materials lowers the environmental and monetary impact of designed Technosols. Particularly, dredged sand is an easily available material in many cities, and the use of a mining by-product increases the environmental benefits as diminishes the pollutant charge of the mining process while obtaining a useful product.

The crucial benefit of the admixture of coated sand is the increase of the nutrient retention capacity, resulting from the surface characteristics of the ferrihydrites.

Further, the applicability of the coated sands is not limited to soils. Diverse materials coated with Fe (hydr)oxides are used as a filter for drinking or waste water to adsorb a large number of pollutants.

Nevertheless, further work has to be done in order to reach a large scale production. Therefore, it is necessary to shorten the shaking time, only to the breaking point when the ferrihydrite aggregates cover homogeneously the whole sand surface. Furthermore, it is desirable to reach a reduction of the coating and the coating stabilization process to one step by directly shaking heavily together the sand, the

ferrihydrite and the proper amount of water, avoiding one drying step. Also, it is pertinent to define which amount of Fe should be added to the sand in order to obtain the largest coating loads with the lowest loss. It is important to test the long term stability of the coating, and its resistance to diverse environmental factors. Further mechanical and acid detachment tests have to be performed.

4. Hydraulic properties of coarse porous materials to construct purpose-designed plant growing media[3]

Abstract

Among potential components to construct Technosols for urban greening purposes, the commercially available geogenic coarse porous materials (CPMs) are mainly used in practice because of their high porosity. However, the knowledge of the hydraulic behaviour of CPMs as well as of their mixtures with other substrates is limited, provoking their suboptimal usage.

Therefore, we determined the water retention characteristics, including the available water capacity (AWC) of six geogenic CPMs: porlith, expanded shale, expanded clay, tuff, pumice, and lava. In order to obtain the water retention characteristics of the CPMs as well as of their mixture with sand (1:4 per volume), the following methods adapted from soil physics were applied over a wide range of pressure heads: Equi-pF apparatus, ceramic tension plates, pressure plate extractors, WP4C apparatus, and water vapour adsorption. The results were used to parametrize the modified Kosugi model (using SHYPFIT 2.0).

Porlith and tuff have the highest AWC ($0.37\,m^3\,m^{-3}$) and $0.17\,m^3\,m^{-3}$, respectively) and are the only ones which can be recommended as effective water-retaining materials. Further materials exhibit an AWC less than $0.10\,m^3\,m^{-3}$. The CPMs exhibit a bimodal pore size distribution, which can be well described by the applied model, except for pumice and expanded shale. The mixtures present overall low AWCs up to $0.07\,m^3\,m^{-3}$ with the pure sand having less than $0.03\,m^3\,m^{-3}$.

For practical application a quite high ratio of CPM is needed, and the mixing material must be adapted to the hydraulic properties of the CPMs. The water inside the CPMs may be easily available for plant roots able to penetrate in the CPMs coarse pores.

4.1. Introduction

Urban green areas such as parks, gardens, green belts or allotments, help to mitigate the adverse ecological effects derived from the surface sealing in urban areas (Bolund and Hunhammar 1999; Scalenghe and Marsan 2009; Gessner et al. 2014; Morel et al. 2014; Jänicke et al. 2015).

However, the conservation and creation of traditional urban green areas face competitive disadvantages with other urban infrastructure projects. The scarcity of

[3]This is an Accepted Manuscript of an article published by Taylor & Francis: Flores-Ramírez, E., Abel, S., and Nehls, T. (2018a). Water retention characteristics of coarse porous materials to construct purpose-designed plant growing media. *Soil Science and Plant Nutrition*, (64)2: 181-189. DOI: 10.1080/00380768.2018.1447293. The publication is available on Taylor&FrancisLink

available areas, and their often low quality as plant habitats (e.g. highly compacted, polluted, sealed) are among such limitations. Frequently, in order to green such areas, expensive soil remediation techniques are used, or the polluted or sealing layers are removed.

As an alternative, Technosols (IUSS Working Group WRB 2015) specifically designed to function as plant growing media, can be installed *in situ* as secondary ready-to-use soils or soil layers on these areas (Séré et al. 2008). They can also be used to install secondary urban green on areas not intended to be vegetated before (Nehls et al. 2015), as it is the case for green façades and vegetated roofs.

These purpose-designed Technosols can be composed intentionally of a variety of materials, which in conjunction must fulfil the main functions of soils as plant habitats: provision of a stable rooting zone with adequate aeration, water storage, water drainage, favourable chemical soil conditions (e.g. CEC, pH, EC), as well as nutrient storage and availability.

For this aim, a large variety of materials have been investigated for the construction of Technosols for greening purposes. Some studies focussed on natural and processed natural substrates, such as brown coir (coconut fibre; Noguera et al. 1996), compost, peat (Vasenev et al. 2013), biochar (Abel et al. 2013), vermiculite, or clay pellets. Some authors pointed out the relevance of the reuse of recycled or waste materials, such as bricks (Nehls, et al. 2013; Farrell et al. 2013), paper mill sludge, rubber, concrete, rubble, or sewage (Séré et al. 2008; Rokia et al. 2014). However, due to strict legal regulations, the contamination of the recycled and waste materials must be previously tested according to the intended use. Additionally, the commercial availability of these materials is limited and their quality can vary largely. For these reasons, the use of uncontaminated and easily available natural porous materials, which are simply mined and crushed (e.g. porlith, tuff, pumice) or additionally processed (e.g. expanded clay, perlite) is a practicable and convenient option for immediate use.

Despite the material origin, its application will strongly depend on the local conditions and the main functions to be fulfilled. For instance, climate zones with high precipitation intensity require a Technosol design which ensures an efficient water drainage, avoiding stagnation, flash flooding and run off during heavy rain events. Simultaneously, the Technosol has to store enough readily available water for proper plant growth during drought periods. A sandy soil texture can ensure a high saturated hydraulic conductivity for drainage, though it has a very low available water capacity (AWC). Clay or silt would increase the AWC, but their small

particles lower significantly the hydraulic conductivity and may also clog the subsequent drainage system of the site. As a solution, the AWC in a sandy Technosol matrix has to be provided by porous materials with rather large grain sizes.

There are several mineral coarse porous materials (CPMs) commercialized as plant growing media that could be used. However, the description and quantification of their hydraulic properties are often insufficient up to now, are poorly described, constrained only to few parameters (Bilderback et al. 2005; Wallach 2008), or to narrow ranges of horticultural interest (up to pF 2.0; Wallach et al. 1992). In contrast, for organic materials used in horticulture, there are more studies available, describing their water retention charcteristics more in detail (Fields et al. 2016; Schindler et al. 2016a, 2016b).

In order to increase the knowledge-based design of Technosols that sustain vegetation, the objective of this work is to accurately characterize the hydraulic properties of six CPMs of natural origin in their commercial forms that can potentially increase the AWC of a sandy Technosol. Porlith, expanded shale, expanded clay, tuff, pumice, and lava were chosen due to their availability and use in the German market, their porosity, predictable qualities, lightweight, structural stability, not having extreme pH, and their large grain sizes. An accurate water retention capacity of these porous materials will allow to optimize their use within an appropriate ratio in composition with sand (or other materials), according to local climatic conditions (dryness, excess of precipitation).

4.2. Materials and methods

4.2.1. Materials

Six commonly used CPMs plus two mixing materials of natural origin, sand and silt, in their commercial presentation have been analysed:

Porlith is a consolidated smectite clay-schist scoria. It is a mineral by-product of the oil exploitation from an organic-containing Cenozoic sediment, deposited in a crater lake of volcanic origin (see Roth-Kleyer 2005). During exploitation process, the material was highly heated, resulting in a mixture of partially melted red claystone residue and porous lava-type material. The production process of porlith, as well as the resulting material, is comparable with the ones of bricks. Nowadays it is used as a growing medium. The pebbles used in this study had a diameter of 2–7 mm.

Pumice is a solidified lava with a low density due to the fast cooling process and the immediate depressurization and expansion after eruption (pebbles of 2–12 mm).

Tuff is formed naturally of consolidated volcanic ashes and lapilli, and was used in a grain size of 3–8 mm.

Lava is solidified magma, crushed to 5–15 mm grain size.

Expanded clay is produced by heating natural clay to temperatures of 1100–1200 °C in a rotating kiln. The gases produced by the heating expand the clay, creating small bubbles in its inner core, providing it with a foamy structure. Due to the rotation, the pebbles are roundish and have a lightweight ceramic shell (Hammer et al. 2000). Expanded clay is available in different sizes and densities. In this study it was used in a grain size of 4–8 mm.

Expanded shale (used in 2–7 mm grain size) is a shale light aggregate expanded by a thermal process with the formation of open pores (Bender 1986).

The **quartz sand** (SiO_2 >96 %), used for mixing with the porous materials has a particle size distribution of 0.06–0.6 mm, with 94 % of particles between 0.1–0.4 mm (Sand Schulz®).

The **silt** used in order to embed the CPM at certain hydraulic tests was obtained by grinding pure quartz sand. It has a maximum particle size of 0.2 mm.

Expanded clay and shale are of natural origin but further processed, while the rest of the materials are of natural origin, only mined and crushed, but not further processed.

4.2.2. Methods

General characterization

The pH (Knick 761 Calimatic pH-meter) and the electric conductivity (InoLab) were measured according to EN ISO 10523:2012 with the materials crushed to pass 2 mm. The densities (ρ) and porosities (ϕ) of the CPMs were characterized as follows. The bulk density (ρ_{bulk}) was measured with a pycnometer flask filled with the dry materials and weighed. The apparent density (ρ_{app}) of the CPM was measured dividing their mass by their apparent volume. The apparent volume excludes the large voids among CPMs. It was determined as the difference between the bulk volume (pycnometer or volumetric flask) and the volume that haloysite clay spheres (Dragonite^{TM}; 50–100 µm; ρ_{bulk} 1.85 g cm^{-3}) occupy of the CPMs inter-particle voids. Threfore, CPMs were mixed with Dragonite^{TM} and compated.

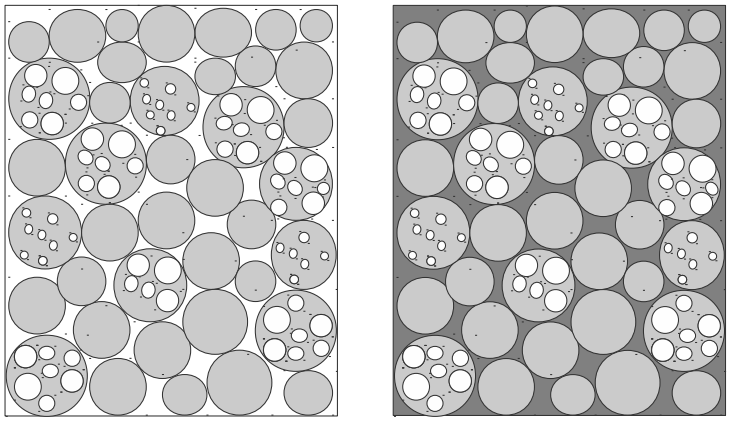

(a) ϕ_t (b) ϕ_{intra}

Figure 4.1. Graphic representation of the calculated porosities. The pores are represented in white. Two main pore domains are observed: the pores inside the CPMs, or intra-particle porosity (ϕ_{intra}), as well as the voids among particles, or inter-particle porosity (ϕ_{inter}). The **(a)** total porosity (ϕ_t) accounts for both and it was calculated by $1-\frac{\rho_{bulk}}{\rho_p}$. The **(b)** intra-particle porosity (ϕ_{intra}) excludes the ϕ_{inter} and was calculated by $1-\frac{\rho_{app}}{\rho_p}$

The compaction of the mixture was reached by vibration, refilling with Dragonite^{TM} until reaching a constant filling of the volumetric flask. The measurement of the CPM particle density (ρ_p) was performed with a Multi-Pycnometer (QuantaChrome MVP-1), and the materials were crushed in order to avoid encapsulated pores. Total porosity (ϕ_t) was calculated by $1-\frac{\rho_{bulk}}{\rho_p}$. It accounts for the voids among the CPM plus their intrinsec porosity (inter and intra-particle porosity, respectively; Fig. 4.1). The intra-particle porosity (ϕ_{intra}) was calculated by $1-\frac{\rho_{app}}{\rho_p}$.

Sample preparation

(1) *CPM as pure materials:* The pure CPMs were packed into steel cylinders of 100 and 385 cm^3 at their ρ_{bulk}. Besides, an additional set of samples were prepared mixing the CPM with silt in steel cylinders of 100 cm^3. This procedure was done in order to ensure capillary continuum and proper drainage within the limited timespan of the experiment.

(2) *Sand:* The sand was packed into steel cylinders of 100 cm^3 and compacted to a ρ_{bulk} of 1.48 $g\,cm^{-3}$ (94 % of proctor density in accordance with ASTM D698)

(3) *CPM mixed with sand:* The CPMs were mixed with sand (coarse texture matrix) with a ratio of 1:4 per volume. The samples were prepared by mixing the corresponding volume of 0.75 $m^3\,m^{-3}$ of sand at ρ_{bulk} of 1.48 $g\,cm^{-3}$ with 0.25 $m^3\,m^{-3}$ the CPMs, homogenously mixed and compacted afterwards.

Capillarity testing

The feasibility to determine the water retention characteristics of the CPMs with standard laboratory methods was tested in advance. In this context, the capillarity among CPMs, meaning the conductivity of water from one particle to the other, is a crucial prerequisite to ensure proper saturation and drainage of the material within the range of applied pressure heads. The capillary rise within the CPM was tested by packing each material into steel cylinders of 5 cm height (385 cm^3) placed in a 2 mm water table, and monitored for more than 24 h photographing the surface in a 2 min interval. Capillary rise was assumed as sufficient when 90 % of the surface was visibly wet. The fastest capillary rise was measured in expanded shale (70 min) and the slowest for expanded clay (1295 min), while for the other materials it was in between 150 to 365 min. As the capillarity was verified, we proceeded with further tests.

Water retention characteristics

We applied the following four different methods with specific features and measuring ranges in order to obtain detailed data needed to properly describe the water retention curve from saturation to wilting point of (a) the pure sand, (b) the pure CPMs, and (c) the CPMs mixed with sand.

(1) *Equi-pF, Streat Instruments lt.* This automated soil moisture release curve apparatus works with hanging water columns. It quantifies water retention characteristics at low pressure heads, including water saturation, air entry point, and field capacity. The resolution of pressure heads was 10 hPa, with two drying and one wetting loops. However, its measuring range is limited to a pressure head of pF 2.0.

(2) *Porous ceramic plate extractors, Eijkelkamp, Giesbeek* With this standardized method (ISO 11274) the water content of the materials was quantified at pF 1.8, and intermediate pressure heads pF 2.5, and 3.0. All measurements were done at least in triplicate.

(3) *Dewpoint Hygrometer WP4C apparatus* With this method the water content at permanent wilting point (pF 4.2) was determined using the chilled mirror dewpoint technique (www.ums-muc.de/assets-ums/00A4R.pdf). All measurements were done in triplicate.

(4) *Water vapour adsorption* Pressure heads higher than the permanent wilting point water ($>$ pF 4.2) were determined by measuring the water vapour adsorbed by the materials, controlling the relative humidity in a glass desiccator with a saturated

solution of K_2SO_4 at 20 °C (Wexler and Hasegawa, 1954). All measurements were done in triplicate.

The measurement of the pure CPMs was challenging. Although the capillarity among CPMs was verified at saturation, at higher pressure heads the capillarity is most probably insufficient to assure proper dewatering from the intrinsic pores. Further, the CPMs have a heterogeneous contact with the ceramic plate due to their large sizes. In order to ensure capillarity, the CPMs were mixed with silt at the pressure heads pF 1.8, 2.5, and 3.0 measurements. For the measurements of the permanent wilting point, and higher pressure heads, we applied methods which determine water content via dew point and thus are independent from capillary water transport. In contrast to the pure CPMs, the pure sand and CPM-sand mixtures have an adequate capillarity for proper dewatering. Altogether, the measurements obtained with the four methods mentioned above provided sufficient data to adequately describe the water retention characteristics of the materials.

For the composite samples with sand, as well as for the measurements in which CPMs were mixed with silt, the water content of the sand and silt was also measured and later subtracted in order to calculate the water content corresponding just to the water held by the CPMs, using the following equation:

$$\theta_{CPM} = [\theta_t - ((1-X) * \theta_{sa_i})/X] * (1-\phi_{inter}) \quad (6)$$

where θ_{CPM} is the volumetric water content of the CPM [$m^3\,m^{-3}$], θ_t is the total volumetric water content, X is the ratio of CPM mixed with sand or silt [$m^3\,m^{-3}$], and θ_{sa_i} is the volumetric water content of sand or silt at a corresponding pressure head. The term 1-ϕ_{inter} accounts for the correction of the inter-particle porosity among the CPMs packed in the steel cylinders. In order to emphasize the water retained exclusively inside the CPMs ϕ_{intra} when mixed with sand and silt at pF 1.8, ϕ_{inter} was not considered, and therefore set equal to 0. This approach was applied to the results obtained via the ceramic tension plate.

The water retention curve of the pure materials was derived using water content values obtained with the Equi-pF up to pF 2, and with the ceramic tension plates for pF 2.5 and 3.0. The AWC was set equal to water held in between pF 1.8 (field capacity, FC), and pF 4.2 (permanent wilting point, see, e.g., Blume et al. 2009)

Parameter estimation We used the experimental data to fit the parameters of the water retention function according to Peters-Durner-Iden (Peters, 2013, 2014; Iden and Durner, 2014) using the software SHYPFIT 2.0 (Peters and Durner 2006). The applied model describes the water retained in capillaries, the film water, and the adsorbed water. The model for capillary water retention is based on the model of Kosugi (1996) for a unimodal pore size distribution and on the modified Kosugi model (Durner 1994; Romano et al. 1999) for a bimodal pore size distribution, with the two distinct pore domains corresponding to the inter-particle pores and the intra-particle pores of the CPMs (Fig. 4.1).

The basic functions used are the unimodal function of Kosugi (1996) for sand, as well as the bimodal form of it for the CPM and the composite samples with sand. The unimodal Kosugi retention function is given by:

$$\Gamma(h) = \frac{1}{2} erfc \left[\frac{ln\left(\frac{h}{h_m}\right)}{\sqrt{2}\sigma} \right] \tag{7}$$

where h_m is the pressure head corresponding to the median pore radius, σ[-] is the standard deviation of the log-transformed pore-size distribution density function, and $erfc$[-] denotes the complementary error function. The bimodal functions are weighted sums of the unimodal functions:

$$\Gamma(h) = \sum_{i=1}^{2} w_i \Gamma_i \tag{8}$$

where Γ_i are the weighted subfunctions, expressed by unimodal functions, and w_i [-] are the weighting factors for the subfunctions ($0 < w_i < 1$).

4.3. Results and discussion

4.3.1. General characterization

The general characteristics of the materials are summarized in Table 4.1. The CPMs have appropriate pH and EC values to be used as fertile plant substrates. The pH of the materials ranges from 5.2–7.7, favouring the availability of most macro-nutrients, promoting biological activity, and preventing mobilization of toxic metals (Bradham et al. 2006; Schaetzl and Thompson 2015). The values are in

line with the ones reported by Roth-Kleyer (2007) for similar materials. The low values of EC ($<$1 dS m^{-1}) for all materials indicate their low salinity and sodicity.

The ρ_{bulk} of sand adjusted to 1.48 g cm^{-3} at the composite sample preparation has a corresponding ϕ_t of 0.43. The ρ_{bulk} of the pure CPMs presents lower values ranging from 0.41–0.88 g cm^{-3}. Their ρ_p are high (2.15–3.05 g cm^{-3}), and therefore the corresponding ϕ_t of the CPMs reaches 0.76 and 0.81 for porlith and expanded clay, respectively, as the highest values, and 0.65 for tuff as the lowest (Table 4.1).

The values for ϕ_t measured in this study are in line with reported results. For example, Asdrubali and Horoshenkov (2002) report a ϕ_t of 0.74–0.84 for expanded clay, and Beardsell et al. (1979) report a ϕ_t of 0.58 for volcanic scoria (similar to tuff). Comparing ϕ_t of the CPMs with non-mineral materials their values are lower (even of expanded clay). Wood fibres, for example, exhibit a quite high ϕ_t of 0.93 (Gruda and Schnitzler 2004), and Beardsell et al. (1979) report a ϕ_t of 0.77 for pinebark and 0.95 for peat.

The high ϕ_t of the CPMs of our study specifically reflects the large particle size and the shape of the CPMs, which results in large inter-particle pore sizes. Consequently, the high ϕ_t is not effective if the CPMs are included in mixtures with fine textured fractions, where smaller particles would easily fill the large voids among the CPMs, lowering ϕ_t. This is the case for the composite samples of CPMs and sand, where the addition of sand decreases considerably the ϕ_t. Such effects have to be considered when CPMs are assessed as plant substrate components which are planned to be mixed with smaller particles. Instead, the ϕ_{intra} is a more adequate reference to describe the effective porosity of CPM pebbles in mixtures. Porlith and pumice present the highest ϕ_{intra} of the CPMs, with 0.55 and 0.61, respectively, while further materials range between 0.42 and 0.46 (Table 4.1).

4.3.2. Water retention characteristics

Water retention characteristics of the pure materials

Figure 4.2 shows the water retention curves of the CPMs (pure sand included) and the corresponding fitted unimodal or bimodal retention functions.

Sand As pore sizes are directly related to the water potential (Kutílek and Nielsen 1994), the relatively low air entry point and a steep slope of the water retention curve of sand is related to a narrow inter-particle pore size distribution.

Table 4.1. General characteristics of the CPMs and the sand

Material	Size mm	pH	EC $\mu S\,cm^{-1}$	ρ_{bulk} $g\,cm^{-3}$	ρ_{app} $g\,cm^{-3}$	ρ_p $g\,cm^{-3}$	ϕ_t $cm^3\,cm^{-3}$	ϕ_{intra} $cm^3\,cm^{-3}$
Porlith	2–7	5.7	2.5	0.65	1.24	2.77	0.76	0.55
Expanded shale	2–7	7.4	109.9	0.78	1.42	2.41	0.68	0.42
Expanded clay	4–8	7.7	807.0	0.41	1.24	2.15	0.81	0.42
Tuff	3–8	6.9	81.5	0.88	1.47	2.55	0.66	0.42
Pumice	2–12	7.3	173.9	0.57	0.81	2.12	0.73	0.61
Lava	5–15	7.5	49.5	0.86	1.65	3.05	0.72	0.46
Sand	0.1–0.5	5.2	2.0	1.48	-	2.60	0.43	-

EC= electric conductivity, ρ_{bulk}= bulk density, ρ_{app}= apparent density, ρ_p= particle density, ϕ_t=total porosity and ϕ_{intra}= intra-particle porosity (only the pores of the materials, without the surroundings)

Sand has no intra-particle porosity, and its inter-particle pores are predominantly in the range >50 µm, so that only very little water is held at pF >1.8, namely <0.03 $m^3\,m^{-3}$. In comparison with naturally textured sands (0.16–0.19 $m^3\,m^{-3}$; Ad-Hoc-Arbeitsgruppe Boden 2005) such value is comparably low and it is attributed to the well-sorted particle size distribution of the used sand (mainly between 0.1 and 0.4 mm).

CPMs All CPMs show a first air entry point that indicates an abrupt drainage of a pore domain in the range of >0.3 mm (draining at pF <1; Kutílek and Nielsen 1994), corresponding mainly to the large inter-particle voids, and may also include visible large pores of lava and expanded shale (pictures included in Fig. 4.2). Only porlith and tuff show a clearly pronounced second air entry point implying a higher amount of smaller pores in the range between 3 µm and 30 µm related to their ϕ_{intra}. For expanded clay and lava this is less pronounced. Expanded shale shows no distinctive inflection of a secondary air entry point, but a constant water release rate at pressure heads >1.0, which indicates a wide pore size distribution of its ϕ_{intra}. Pumice up to pF 2.0 shows no secondary air entry point.

Due to the coarse grained texture of the materials, it can be assumed that the water in the large inter-particle pores held at FC is negligible, whereas the water at this point is mainly retained by the intra-particulate pores. Despite all materials are commercialized either as amendments to increase the water retention capacity (WRC) of soils, or as soilless medium substrates (Gül and Sevgican 1993; Beattie and Berghage 2004; Sailor and Hagos 2011; Sailor et al. 2008; Roth-Kleyer 2007), only porlith has a high water content at FC (0.44 $m^3\,m^{-3}$), followed by tuff (0.23 $m^3\,m^{-3}$). Further CPMs have values ≤0.11 $m^3\,m^{-3}$ (Table 4.2). Porlith and

tuff also present the highest values of AWC (0.37 and 0.17 $m^3 m^{-3}$, respectively), while the rest of the CPMs do not exceed 0.10 $m^3 m^{-3}$.

Porlith has a high AWC of 0.38 $m^3 m^{-3}$ which is in a comparable magnitude with the one for bricks (up to 0.4 $m^3 m^{-3}$; Blume and Runge 1978; Nehls et al. 2013). These comparable water retention characteristics can be attributed to similarities of the structure of these two materials.

For tuff, the measured FC (0.23 $m^3 m^{-3}$) exceeds the reported values of 0.10 $m^3 m^{-3}$ (Da Silva et al. 1993) and 0.12 $m^3 m^{-3}$ (Wallach et al. 1992). The tuff studied in this work has, accordingly, more pores able to retain water in the range of the AWC.

Expanded clay, expanded shale and pumice have a similarly low FC and AWC compared to tuff and porlith. The expanded clay has a ceramic cover, which is likely to disrupt the capillary continuum and thus hinders the uptake of water (see the structure of the material in Fig. 4.2). Expanded shale shows a low and narrow amount of pores retaining water in between pF 1.8 and pF 3.0, draining almost completely at pF $>$ 3.0.

Regarding pumice, previous research on its porosity shows that it has a wide pore size spectrum and that shape and connectivity of the pores depends on the origin of the pumice (Whitham and Sparks 1986; Lura et al. 2004). Gunnlaugsson and Adalsteinsson (1994) report that the majority of pumice ϕ_{intra} is composed by closed, occluded or dead-end pores not available for water storage. This particular porosity may also be present in our studied material, and it can be reflected in the high variance of the WRC (Fig. 4.2) at pF$\leq$2.5 (SD = 0.007 $m^3 m^{-3}$), and pF 3.0, with a SD = 0.053 $m^3 m^{-3}$. For higher suctions (pF $>$ 4.0), the values are more consistent as the materials were crushed prior measurement.

Lava has a very low AWC. Its water retention characteristics are quite similar to the ones of the sand of our study. The low AWC is mainly attributed to its large pore sizes $>$50 µm, some of them clearly visible, as depicted in Fig. 4.2.

In order to test the equivalence of the two experimental setups (pure CPMs, measured with Equi pF apparatus vs. CPMs mixed with silt, measured with ceramic pressure plates) as well as the accuracy of the applied model fitted to the experimental data, the water content of the CPMs at pF 1.8 of both setups was compared. The differences in the water content values calculated between the two methods are smaller than 0.055 $m^3 m^{-3}$ for all CPMs, except for pumice and expanded shale. This high difference points to an inconsistency between the two

applied setups. Since for the parametrization of the water retention model we used the outcomes of both setups, this inconsistency results in a high uncertainty of the model. Thus, for pumice and expanded shale, the water retention curve can be given only for rather low suctions. In Fig. 4.2, the mentioned uncertainty is symbolized by the dash dotted line. The difference in the experimental setups points to the need for a specially adapted method which accounts for a higher representative volume of CPMs.

Table 4.2. Available water capacity (AWC), field capacity (FC), and parameters of unimodal (applied just for sand) and bimodal Peters-Durner-Iden model (2015) fitted to the data of pure materials and the materials mixed with sand

Material	Parameter									
	h_{m1}	σ_1	h_{m2}	σ_2	θ_r	θ_s	w_1	RMSE	AWC	FC
Porlith	6.99	0.286	284.20	0.205	0.17	0.76	0.50	$2.37{\cdot}10^{-3}$	0.37	0.44
Exp. Shale	6.25	0.200	3.36	0.830	0.11	0.68	0.66	$4.88{\cdot}10^{-2}$	0.08	0.09
Exp. Clay	2.69	0.200	120.70	1.091	0.00	0.81	0.18	$3.34{\cdot}10^{-2}$	0.09	0.10
Tuff	908.42	0.208	3.54	0.567	0.11	0.66	0.73	$1.43{\cdot}10^{-2}$	0.17	0.23
Pumice	2.68	0.355	2.68	0.338	0.15	0.73	0.60	$4.12{\cdot}10^{-2}$	0.09	0.11
Lava	3.49	0.499	56.97	0.207	0.07	0.72	0.04	$0.84{\cdot}10^{-2}$	0.06	0.07
Sand	20.45	0.691	-	-	0.02	0.43	-	$7.03{\cdot}10^{-3}$	0.03	0.03
Porlith + Sand	29.38	2.791	29.38	0.200	0.11	0.46	0.80	$0.69{\cdot}10^{-2}$	0.08	0.13
Exp. Shale + Sand	176.51	1.248	27.68	0.307	0.04	0.42	0.86	$0.44{\cdot}10^{-2}$	0.06	0.08
Exp. Clay + Sand	27.68	0.200	27.68	0.201	0.09	0.47	0.75	$0.15{\cdot}10^{-2}$	0.06	0.09
Tuff + Sand	26.07	0.297	186.78	1.856	0.07	0.43	0.25	$0.58{\cdot}10^{-2}$	0.10	0.13
Pumice + Sand	26.92	1.678	22.19	0.401	0.02	0.48	0.85	$0.23{\cdot}10^{-2}$	0.07	0.09
Lava + Sand	121.15	1.170	24.17	0.305	0.01	0.44	0.86	$0.33{\cdot}10^{-2}$	0.05	0.05

For simplification, θ_s was set equal to ϕ_t and thus not fitted. The parameter h_0 was set to $10^{6.8}$ cm, which is the suction at oven dryness for 105 °C (Schneider and Goss 2012). h_i and σ_i are shape parameters. The first can be related to the air entry point and the latter can be related to the inclination. w is a weighing factor

Water retention characteristics of the mixtures

The water retention characteristics of the composite samples show just slight differences when compared to the sand. The data indicate two pore size domains for the composite samples: a highly pronounced pore size domain related to the sand matrix, and a secondary pore size domain, introduced by the CPMs. The latter is discernible by a moderate, but constant water release at pressure heads within the range of the AWC (pF 1.8–4.2), with the corresponding pore sizes between 0.2 and 50 µm.

The overall increase of AWC is quite moderate (maximum 0.07 $m^3\,m^{-3}$; Table 4.2); however, the increase can be clearly related to the added CPMs, as AWC for the

pure sand is $<0.03\,m^3\,m^{-3}$. In order to emphasize the effective contribution of CPMs to the increase of AWC, it is necessary to quantify the water retained in their ϕ_{intra}.

Water content of the CPM ϕ_{intra} This retained water calculated with Equation 6 shows a moderate to high water retention of CPMs at FC, with porlith and tuff being the most effective ones (Fig. 4.3). We found that the FC and the AWC for pebbles mixed with silt are higher than for those mixed with sand, except for expanded clay. This may be due to an additional porosity created in the contact zone between the surface of the CPMs and the mixing material, which occurs in a higher extent for silt than for sand. The calculation of this additional porosity was not included in Equation 6, and cannot be reliably determined by the methods applied.

For expanded clay, the sandy matrix is not able to drain the water from the shell fine pores, while in the silt matrix this is possible. Therefore, the water in the inner pore system can drain when embedded in silt, but is insulated when embedded in sand. The water insulated in the CPM of the composite samples can be favorable. It could solve the problem of the low field capacity and could store water, which otherwise would drain fast and would be lost for plants, notwithstanding the prevention of flash flooding due to heavy rain events. The roots of the plants can colonize the CPMs to obtain the water and the nutrients stored there, as it has been proved in the case of bricks (Nehls et al. 2013). Therefore, the capacity of the substrates to be rooted should be tested in further works.

4.3.3. Resume for practical use

Despite the moderate retaining water performance of four out of six of the analysed CPMs, most of them are widely used (Roth-Kleyer 2007) as the main components of green roof substrates where they are readily available (Sailor et al. 2008; Ampim et al. 2010; Sailor and Hagos 2011). However, they are mostly used in mixtures with organic material and other mineral components, improving their performance.

In the design of a Technosol profile with the purpose of sustaining vegetation, a mixture of sand and porlith or tuff, which considerably increases the AWC, can accomplish the function of a good quality subsoil layer. In order to construct a proper topsoil, a further addition of organic material (e.g., compost) is needed. The addition of organic material increases the overall AWC, along with the nutrient

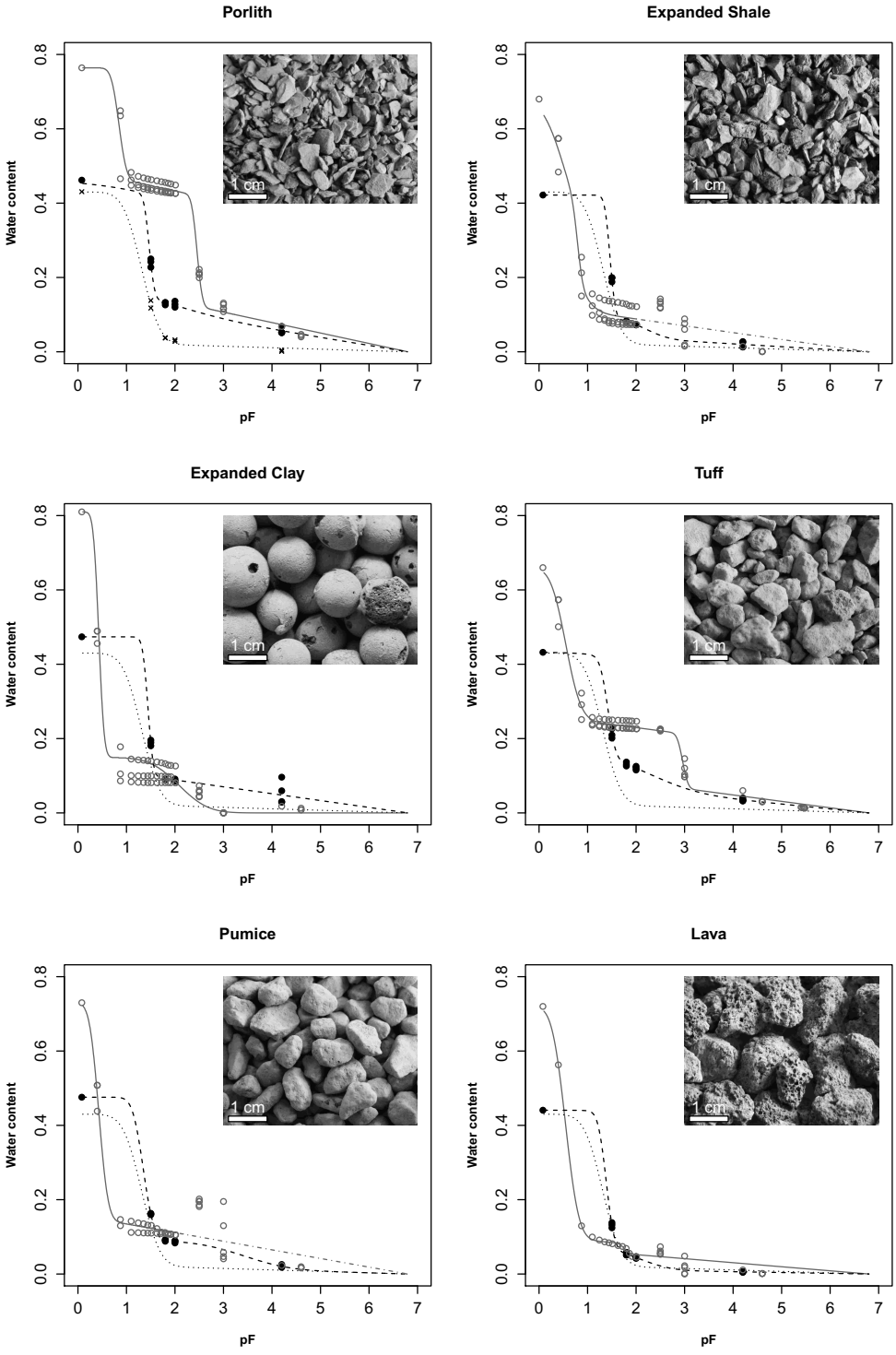

Figure 4.2. Observed water retention data and fitted retention curves for the sand, composite samples and pure CPMs. Sand: (×) measured, (····) fitted, Sand mixed with CPM: (•) measured, (– –) fitted, CPMs: (○) measured, (—) fitted (uncertainty is symbolized by –·–·). The graph of porlith (upper left) shows the measured points for sand. In the graphs can be observed the inflections of the air entry point(s), and the water held in the range of available water content (AWC) from pF 1.8 to pF 4.2

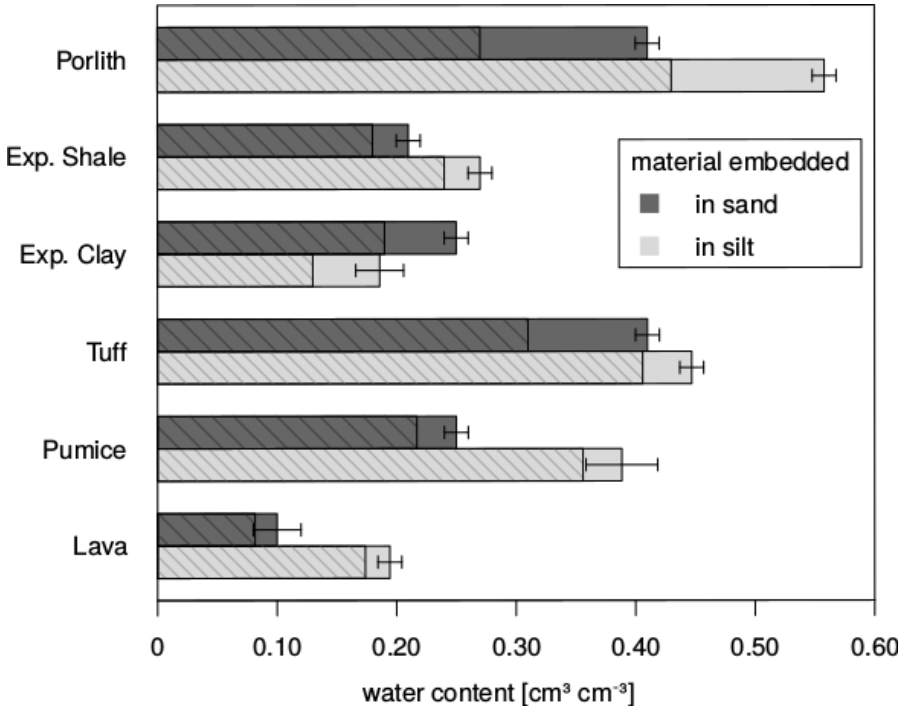

Figure 4.3. Volumetric water content of the CPMs intra-particle porosity (ϕ_{intra}) held at matric force of pF 1.8 (considered as field capacity) and AWC (cross hatched columns) when embedded in sand compared when embedded in silt. The pebbles of the CPMs were embedded in silt to ensure capillary contact when measured with ceramic tension plates at matric forces ranging from 1.8–3. Therefore, the water content of the pure sand and silt was obtained and subsequently subtracted with Equation 6. The result is the water stored specifically inside the pebbles. The differences between the water contents measured for the CPMs embedded in silt and sand demonstrate the higher importance of a good capillary contact for saturation then for dewatering

retention capacity, and improves the texture. In contrast, mono-substrates of CPMs commonly used for certain horticultural purposes (e.g., for germination, in pots, or in green roofs) hinders soil aggregation and provokes excessive aeration due to the large size of the materials.

With the knowledge of potential AWC of each CPM, an optimization of the composite substrates in terms of the overall AWC can be conducted. The results obtained in this work indicate this can be achieved by a higher mixing ratio CPM:sand. For instance, a soil with a FC of about $0.30\,m^3\,m^{-3}$ (recommended by the German Landscape Research, Development, and Construction Society, FLL 2002 as a minimum for green roof substrates) can be reached mixing porlith with naturally textured sand (FC 0.16–$0.19\,m^3\,m^{-3}$; Ad-Hoc-Arbeitsgruppe Boden 2005) at a

ratio of 1:1. Additionally, the soil can be complemented with organic material to reach even higher water contents.

4.4. Conclusions

The CPMs are commonly used and commercialized for greening purposes due to their high porosity. The AWC is high for porlith, moderate for tuff, but low for pumice, lava, expanded clay and expanded shale. Hence, the water retention characteristics of sandy soils can just be weakly improved by the addition of the last four mentioned. Tuff and porlith positively affect the hydraulic characteristics of sandy soils; however, the applied ratio between sand and CPM has to be adapted in order to gain the optimum in AWC.

Nevertheless, a high water content in the intra-particle pores of the CPM when mixed with sand was calculated for most CPMs, despite the low overall AWC in the mixtures. Such retained water could be available for plant roots entering the CPMs.

The pore sizes of the CPMs show a bimodal distribution for pure materials as well as the composite samples with sand. There are two distinctive pore sizes, one for the interparticle pores among the CPMs or within the embedding sand matrix, and the other for the intra-particle pores of the CPMs.

We conclude that the behavior of the components must be known in detail and that the commercialized mixtures have to be investigated in a high resolution, probably using the here introduced methods in order to adjust the mixtures according to the purpose.

5. Synthesis

The aim of the work was to design a Technosol which copes with the problem of water stagnation in areas with high precipitation. This is the case for the *Hamburger Deckel* project, in which a sandy-loam as fertile substrate was suggested for the installation of the Technosol.

A designed Technosol that ensures a high hydraulic conductivity, and simultaneously retain water and nutrients for proper plant growing was therefore planned. The materials selected to fulfil those functions were sand, ferrihydrite and coarse porous materials. The sand was selected to be the mayor fraction of the Technosol to provide the high hydraulic conductivity, the ferrihydrite improves the low chemical reactive specific surface of the sand, and the coarse porous materials retain plant-available water.

Instead of only amend the ferrihydrite to the sand, it is stably incorporated to the sand surface by a coating. The technique of sand coating with a ferrihydrite is quite effective and simple, and uses less energy, resources and time than traditional procedures. The process developed to further stabilize the ferrihydrite coating, consisting in a heavy shaking of the already coated sand for 1000 min, infringes important changes in the physical features of the coating aggregates by its detachment, fractioning and reattachment. This model was supported also by the outcomes obtained with the recycled ferrihydrites (observed mainly by scanning electron microscope and the particle size of the coating aggregates).

A direct benefit of the stabilization process of the ferrihydrite coating on the sand is the low Fe (hydr)oxide detachment after mechanical abrasion. Also, the coated sand was tested against the ferrihydrite surface charge reduction associated with P adsorption. Therefore, for practical use, the main benefit is the nutrient retention capacity. This is particularly the case when applied as a component in growing media, where high content of organic matter frequently induces an excess of nutrients and leaching might occur. The coated sand regulates and operates as a temporal sink for those nutrients which in medium-term can be detached and assimilated by the plants. Besides, also the leaching of pollutants can be decreased with the application of ferrihydrite-coated sand. Therefore, it can be also used for soil remediation of contaminated areas.

Moreover, all these benefits are equally obtained by the sands coated with recycled ferrihydrites, proving the feasibility to obtain the same characteristics using other materials. However, some of the applied ferrihydrites have certain characteristics

which differ from each other. Particularly, the pH is of major interest. Ferrihydrites with high $CaCO_3$ content and high pH can be used as an amendment for acidic soils, while other ferrihydrites strengthens optimal soil pH for plant growth in neutral soils. Overall, soil reaction of the Technosol can be directly controlled by the application of the right material.

The characterized coarse porous materials, intended to store available water when mixed with sand, showed a low water retention capacity at the applied mixing ratio. Only porlith and tuff showed moderate to high water contents as pure materials, while expanded clay, expanded schist, pumice, and lava did not. A theoretical optimal water retention capacity can be achieved applying a ratio of 1:1 of sand and porlith for the substrate.

The observations in water retention pointed to a bimodal pore size distribution with two distinctive pore sizes, which could be effectively described with the applied water retention model. The bimodal distribution of pore sizes was also evident in the mixtures with sand. The larger inter-particle pores, namely the pores among the coarse porous materials or within the embedding sand, drained faster than the smaller intra-particle pores of the coarse porous materials, leading to the shape of the observed water retention curve. Regarding the water content separately for inter-particle and intra-particle porosity, the intrinsic porosity of the coarse porous materials feature a high water content when mixed with sand, despite the low overall AWC in the mixtures. The water retained in the intra-particle porosity can be available and be uptaken by plant roots entering the coarse porous materials.

Therefore, it was obtained a detailed knowledge about the behaviour and composition of the materials intended to integrate the Technosol, to guarantee its optimal design. After the obtained good performances of the materials developed, a fully functional mixture of the materials can be successfully achieved.

6. Conclusions and Outlook

6.1. Conclusions

A separated characterization and development of each independent component selected for the designed Technosol, allows to know in detail their functioning. This strategy enables, therefore, to distinguish the individual impacts of the components and reduces multifactorial correlations. When few components are mixed later on in order to create an optimal growing media, a better monitoring and interpretation of the overall characteristics, including pedogenesis, are allowed.

The desired stable combination of ferrihydrite and sand was successfully obtained by a newly developed coating-and-stabilization process, which is simple and efficient. The coated sand provides high hydraulic conductivity and a large chemical reactive surface to the substrate in which it is used, as projected. The Fe fraction can now be incorporated in a stabilized form in predictable quantity and quality through an artificial and controlled process. The resulting alkaline or acidic pH of the sands coated with the recycled ferrihydrites widen the possibility of uses. The multifunctionality of the coated sand overcomes its applicability only for soils.

Despite the assumption of high potential to retain plant-available water of the porous materials characterized, their performance was low. Nevertheless, with two of the materials a theoretical optimal water retention capacity can be achieved. The general scarce or incomplete knowledge about the commercial materials that are currently used in many greening facilities was therefore evinced. The widespread commercialisation and application should thus be intensively discussed to avoid ineffective input of resources and energy for the production of a material with only a moderate ability to store water.

Further, a need to expand the appropriate analysing methodology for the technogenic materials was also evinced when the water retention of one of the porous materials could not be measured with the methodologies applied. Structural differences between natural soils and technogenic materials (e.g. inner porosity, large coarse grain sizes, or the artificial layering not related to natural pedogenesis) may complicate the examination when using analysing tools intended only for the fine-earth fraction of natural soils.

Based on the experimental data obtained in this work, a mixture of ferrihydrite-coated sand with a certain ratio of one of the two coarse porous materials will

effectively drain water excess, retain simultaneously plant-available water, and will count with a large chemical reactive surface area given by the Fe (hydr)oxide addition. Therefore, its further installation sustaining vegetation is pursued. In contrast with the projected sandy-loamy substrate to be installed in the *Hamburger Deckel* park, the pedological functionality of the present designed Technosol not only solves the stagnation risk (a common problem shared by many urban areas), but it also contributes with the sustainable secondary upcycling of resources, avoiding the extraction of natural soil.

As similar local versions of the materials used can be found worldwide, the design of this Technosol can be transferred to many urban areas. It can also be used to reclaim or remediate degraded areas where large amounts of substrate are needed as the mining areas. In extensive or intensive roof greening it will also reduce clogging risks. However, its applicability must only be preceded by a positive weight charge evaluation.

Ferrihydrite-coated sands can be used to filter water entering aquifer-recharge wells, road embankments, or to generate infiltration spots for areas with water stagnation risk. In soils they can work as an optimized vehicle to immobilize heavy metals and As (Miretzky and Cirelli 2010), or to reduce P leaching from agricultural areas (Rhoton and Bigham 2005) to adjacent water bodies, for example.

By a simple design, with just few materials and also incorporating recycled resources, a highly functional Technosol with greening purposes could be achieved with a considerable reduction of costs and energy inputs, with the potential to be further improved. Less is more.

This work encourages to consider the convenience of an adequate and simple design-and-construction of Technosols with greening purposes as a priority in the sustainable planning of the urban areas.

6.2. Outlook and further work

The present purpose-designed Technosol and the ferrihydrite-coated sand developed offer a drastic reduction of resources and energy input joined with functionality when compared with, for example, highly industrialized or scarce natural materials (e.g. water-absorbent polymers, peat moss) used in some horticultural substrates. Therefore, beyond the ecological advantages, a commercial benefit can also be obtained from the substitution of materials, either mined or further processed.

A practical implementation will render account for the technical difficulties that should be solved along with the conceptual questions. With a successful experimental implementation, not only the outcomes could be verified, and pedological functioning could be tested and monitored, but it will be possible to counteract the still generalized idea that only natural soil can efficiently perform functions to sustain vegetation.

However, in order to reach a larger production scale, and to expand their utility, the production processes of materials have to be further improved. Considering the ferrihydrite-coated sand, it is necessary to reduce the time and energy demand of the complete coating-and-stabilization process to make an industrial production feasible. It is needed to get information about which impurities hinder or foster the coating stabilization, as it is also important to investigate the boundaries of the stability of the coating ferrihydrite (e.g. mobilization of Fe(III) due to eventual highly acidic conditions).

Most of the commercially available coarse porous materials characterized in this work presented a low performance despite the advantages like immediate use, availability and standard quality. Therefore, further use of recycled materials should be preferred, with the environmental advantages already mentioned. Unpolluted defective bricks, for example, can be obtained from the factories, and therefore the risk assessment of the material could be reduced.

Finally, the present work joins forces with the developing researches whose shared aim is to develop techniques or materials geared to lower environmental impacts and promote secondary upcycling of resources. With further knowledge and optimization, affordable green cities can be built up in a future not far away.

7. List of publications

The following publications are included in this Dissertation:

- Publication I, page 15:
  Flores-Ramírez, E., Dominik, P., and Kaupenjohann, M. (2016). Novel ferrihydrite sand coating process as a first step for designed technosols. *Journal of Soils and Sediments*, 1-11. DOI: 10.1007/s11368-016-1450-1
- Publication II, page 35:
  Flores-Ramírez, E., Dominik, P., and Kaupenjohann, M. (2018b). Coating a dredged sand with recycled ferrihydrites to create a functional material for plant substrate. *Journal of Soils and Sediments*, (18)2: 534–545.
  DOI: 10.1007/s11368-017-1772-7
- Publication III, page 57:
  Flores-Ramírez, E., Abel, S., and Nehls, T. (2018a). Water retention characteristics of coarse porous materials to construct purpose-designed plant growing media. *Soil Science and Plant Nutrition*, (64)2: 181-189.
  DOI: 10.1080/00380768.2018.1447293

References

Abel, S., Peters, A., Trinks, S., Schonsky, H., Facklam, M., and Wessolek, G. (2013). Impact of biochar and hydrochar addition on water retention and water repellency of sandy soil. *Geoderma*, 202:183–191.

Ad-Hoc-Arbeitsgruppe Boden (2005). *Bodenkundliche Kartieranleitung, 5. Auflage*. E.Schweizerbartsche Verlagsbuchhandlung.

Akcil, A. and Koldas, S. (2006). Acid mine drainage (AMD): causes, treatment and case studies. *Journal of Cleaner Production*, 14(12):1139–1145.

Albanese, S. and Cicchella, D. (2012). Legacy problems in urban geochemistry. *Elements*, 8(6):423–428.

Altieri, M. A., Companioni, N., Cañizares, K., Murphy, C., Rosset, P., Bourque, M., and Nicholls, C. I. (1999). The greening of the "barrios": Urban agriculture for food security in Cuba. *Agriculture and Human Values*, 16(2):131–140.

Ampim, P. A., Sloan, J. J., Cabrera, R. I., Harp, D. A., and Jaber, F. H. (2010). Green roof growing substrates: types, ingredients, composition and properties. *Journal of Environmental Horticulture*, 28(4):244.

Appelo, C., Van der Weiden, M., Tournassat, C., and Charlet, L. (2002). Surface complexation of ferrous iron and carbonate on ferrihydrite and the mobilization of arsenic. *Environmental Science & Technology*, 36(14):3096–3103.

Arias, M., Da Silva-Carballal, J., Garcia-Rio, L., Mejuto, J., and Nunez, A. (2006). Retention of phosphorus by iron and aluminum-oxides-coated quartz particles. *Journal of Colloid and Interface Science*, 295(1):65–70.

Asdrubali, F. and Horoshenkov, K. (2002). The acoustic properties of expanded clay granulates. *Building Acoustics*, 9(2):85–98.

Beardsell, D., Nichols, D., and Jones, D. (1979). Water relations of nursery potting-media. *Scientia Horticulturae*, 11(1):9–17.

Beattie, D. and Berghage, R. (2004). Green roof media characteristics: the basics. In *Second Annual Greening Rooftops for Sustainable Communities Conference, Awards and Trade Show*, pages 2–4.

Bedarida, F., Flamini, F., Grubessi, O., and GM, P. (1973). Hematite goethite surface weathering scanning electron-microscopy. *American Mineralogist*, 58(7-8):794–795.

Bender, F. (1986). Untersuchungsmethoden für Metall-und Nichtmetallrohstoffe, Kernenergierohstoffe, feste Brennstoffe und bituminöse Gesteine, Band 4 der Reihe Angewandte Geowissenschaften. *Angewandte Geowissenschaften*, 4:422.

Bendt, P., Barthel, S., and Colding, J. (2013). Civic greening and environmental learning in public-access community gardens in Berlin. *Landscape and Urban planning*, 109(1):18–30.

Bilderback, T. E., Warren, S. L., Owen, J. S., and Albano, J. P. (2005). Healthy substrates need physicals too! *HortTechnology*, 15(4):747–751.

Blume, H.-P., Brümmer, G. W., Horn, R., Kandeler, E., Kögel-Knabner, I., Kretzschmar, R., Stahr, K., and Wilke, B.-M. (2009). *Scheffer/Schachtschabel: Lehrbuch der Bodenkunde*. Springer-Verlag.

Blume, H.-P. and Runge, M. (1978). Genese und Ökologie innerstädtischer Böden aus Bauschutt. *Journal of Plant Nutrition and Soil Science*, 141(6):727–740.

Bolund, P. and Hunhammar, S. (1999). Ecosystem services in urban areas. *Ecological economics*, 29(2):293–301.

Borggaard, O. (1983). The influence of iron oxides on phosphate adsorption by soil. *European Journal of Soil Science*, 34(2):333–341.

Brabec, E., Schulte, S., and Richards, P. L. (2002). Impervious surfaces and water quality: a review of current literature and its implications for watershed planning. *CPL bibliography*, 16(4):499–514.

Bradham, K. D., Dayton, E. A., Basta, N. T., Schroder, J., Payton, M., and Lanno, R. P. (2006). Effect of soil properties on lead bioavailability and toxicity to earthworms. *Environmental Toxicology and Chemistry*, 25(3):769–775.

Bradshaw, A. D. (1997). *Restoration Ecology and Sustainable Development*, chapter What do we mean by restoration?, pages 8–14. Cambridge University Press, New York, NY.

Burghardt, W. (2006). Soil sealing and soil properties related to sealing. *Geological Society, London, Special Publications*, 266(1):117–124.

Burghardt, W., Morel, J. L., and Zhang, G.-L. (2015). Development of the soil research about urban, industrial, traffic, mining and military areas (SUITMA). *Soil Science and Plant Nutrition*, 61(sup1):3–21.

Capra, G. F., Ganga, A., Grilli, E., Vacca, S., and Buondonno, A. (2015). A review on anthropogenic soils from a worldwide perspective. *Journal of soils and sediments*, 15(7):1602–1618.

Celi, L., Lamacchia, S., Marsan, F. A., and Barberis, E. (1999). Interaction of inositol hexaphosphate on clays: Adsorption and charging phenomena. *Soil Science*, 164(8):574–585.

Chan, K. and Heenan, D. (1999). Lime-induced loss of soil organic carbon and effect on aggregate stability. *Soil Science Society of America Journal*, 63(6):1841–1844.

Chang, Y.-Y., Lim, J.-W., and Yang, J.-K. (2012). Removal of As (V) and Cr (VI) in aqueous solution by sand media simultaneously coated with Fe and Mn oxides. *Journal of Industrial and Engineering Chemistry*, 18(1):188–192.

Cismasu, A. C., Michel, F. M., Tcaciuc, A. P., Tyliszczak, T., and Brown Jr, G. E. (2011). Composition and structural aspects of naturally occurring ferrihydrite. *Comptes Rendus Geoscience*, 343(2):210–218.

Cornell, R. M. and Schwertmann, U. (2003). *The iron oxides: structure, properties, reactions, occurrences and uses*. John Wiley & Sons.

Da Silva, F., Wallach, R., and Chen, Y. (1993). Hydraulic properties of sphagnum peat moss and tuff (scoria) and their potential effects on water availability. *Plant and Soil*, 154(1):119–126.

De Sousa, C. A. (2003). Turning brownfields into green space in the City of Toronto. *Landscape and urban planning*, 62(4):181–198.

Duiker, S. W., Rhoton, F. E., Torrent, J., Smeck, N. E., and Lal, R. (2003). Iron (hydr)oxide crystallinity effects on soil aggregation. *Soil Science Society of America Journal*, 67(2):606–611.

Durner, W. (1994). Hydraulic conductivity estimation for soils with heterogeneous pore structure. *Water Resources Research*, 30(2):211–223.

Dzombak, D. A. and Morel, F. M. (1990). *Surface complexation modeling: hydrous ferric oxide*. John Wiley & Sons.

Earth Pledge (2005). *Green roofs: ecological design and construction*. Schiffer Pub Limited.

Farrah, S. and Preston, D. (1991). Adsorption of viruses by diatomaceous earth coated with metallic oxides and metallic peroxides. *Water Science and Technology*, 24(2):235–240.

Farrell, C., Ang, X. Q., and Rayner, J. P. (2013). Water-retention additives increase plant available water in green roof substrates. *Ecological Engineering*, 52:112–118.

Ferris, F., Tazaki, K., and Fyfe, W. (1989). Iron oxides in acid mine drainage environments and their association with bacteria. *Chemical Geology*, 74(3-4):321–330.

Fields, J. S., Owen, J. S., Zhang, L., and Fonteno, W. C. (2016). Use of the evaporative method for determination of soilless substrate moisture characteristic curves. *Scientia Horticulturae*, 211:102–109.

Fleischer, M., Chao, G., and Kato, A. (1975). New mineral names: Ferrihydrite (MF). *American Mineralogist*, 60:485–486.

Flores-Ramírez, E., Abel, S., and Nehls, T. (2018a). Water retention characteristics of coarse porous materials to construct purpose-designed plant growing media. *Soil Science and Plant Nutrition*, 64(2):181–189.

Flores-Ramírez, E., Dominik, P., and Kaupenjohann, M. (2016). Novel ferrihydrite sand coating process as a first step for designed technosols. *Journal of Soils and Sediments*, pages 1–11.

Flores-Ramírez, E., Dominik, P., and Kaupenjohann, M. (2018b). Coating a dredged sand with recycled ferrihydrites to create a functional material for plant substrate. *Journal of Soils and Sediments*, 18(2):534–545.

Forschungsgesellschaft Landschaftsentwicklung Landschaftsbau FLL (2002). Guidelines for the planning, execution and upkeep of green-roof sites. *Forschungsgesellschaft Landschaftsentwicklung Landschaftsbau, Bonn, Germany*.

Gessner, M., Hinkelmann, R., Nützmann, G., Jekel, M., Singer, G., Lewandowski, J., Nehls, T., and Barjenbruch, M. (2014). Urban water interfaces. *Journal of Hydrology*, 514:226–232.

Gibbs, S. (2011). Sand shortage, myth or reality? *Modern Casting*, 101(7):28–31.

Gruda, N. and Schnitzler, W. (2004). Suitability of wood fiber substrate for production of vegetable transplants: I. Physical properties of wood fiber substrates. *Scientia horticulturae*, 100(1):309–322.

Gül, A. and Sevgican, A. (1993). Suitability of various soilless media for long-term greenhouse tomato growing. In *II Symposium on Protected Cultivation of Solanacea in Mild Winter Climates 366*, pages 437–444.

Gunnars, A., Blomqvist, S., Johansson, P., and Andersson, C. (2002). Formation of Fe (III) oxyhydroxide colloids in freshwater and brackish seawater, with incorporation of phosphate and calcium. *Geochimica et Cosmochimica Acta*, 66(5):745–758.

Gunnlaugsson, B. and Adalsteinsson, S. (1994). Pumice as environment-friendly substrate-a comparison with rockwool. In *International Symposium on Growing Media & Plant Nutrition in Horticulture 401*, pages 131–136.

Guzman, G., Alcantara, E., Barron, V., and Torrent, J. (1994). Phytoavailability of phosphate adsorbed on ferrihydrite, hematite, and goethite. *Plant Soil*, 159(2):219–225.

Hammer, T. A., van Breugel, K., Helland, S., Holand, I., Maage, M., Mijnsbergen, J. P., and Sveinsdóttir, E. L. (2000). Economic Design and Construction with Structural Lightweight Aggregate Concrete. *Euromat 99, Materials for Buildings and Structures*, 6:18.

Haraldsen, T. K. and Pedersen, P. A. (2003). Mixtures of crushed rock, forest soils, and sewage sludge used as soils for grassed green areas. *Urban Forestry & Urban Greening*, 2(1):41–51.

Hernández-Lamas, P., Rubio Gavilán, A., and Bernabeu-Larena, J. (2016). Parks and roads build the cities: the M-30 and Madrid-Río project, building landscape. In *Back to the Sense of the City: International Monograph Book*, pages 415–428. Centre de Política de Sòl i Valoracions.

Huot, H., Simonnot, M.-O., and Morel, J. L. (2015). Pedogenetic trends in soils formed in technogenic parent materials. *Soil Science*, 180(4/5):182–192.

Huot, H., Simonnot, M.-O., Watteau, F., Marion, P., Yvon, J., De Donato, P., and Morel, J.-L. (2014). Early transformation and transfer processes in a Technosol developing on iron industry deposits. *European Journal of Soil Science*, 65(4):470–484.

Iden, S. C. and Durner, W. (2014). Comment on "Simple consistent models for water retention and hydraulic conductivity in the complete moisture range" by A. Peters. *Water Resources Research*, 50(9):7530–7534.

Ilg, K., Dominik, P., Kaupenjohann, M., and Siemens, J. (2008). Phosphorus-induced mobilization of colloids: model systems and soils. *European journal of soil science*, 59(2):233–246.

IUSS Working Group WRB (2015). *World reference base for soil resources 2014 (update 2015), international soil classification system for naming soils and creating legends for soil maps*. FAO, Rome.

Jambor, J. L. and Dutrizac, J. E. (1998). Occurrence and constitution of natural and synthetic ferrihydrite, a widespread iron oxyhydroxide. *Chemical Reviews*, 98(7):2549–2586.

Jangorzo, N. S., Watteau, F., and Schwartz, C. (2013). Evolution of the pore structure of constructed Technosols during early pedogenesis quantified by image analysis. *Geoderma*, 207:180–192.

Jänicke, B., Meier, F., Hoelscher, M.-T., and Scherer, D. (2015). Evaluating the effects of façade greening on human bioclimate in a complex urban environment. *Advances in Meteorology*, 2015.

Jerez, J. and Flury, M. (2006). Humic acid-, ferrihydrite-, and aluminosilicate-coated sands for column transport experiments. *Colloids and Surfaces A: Physicochemical and Engineering Aspects*, 273(1):90–96.

Katsumi, T. (2015). Soil excavation and reclamation in civil engineering: Environmental aspects. *Soil science and plant nutrition*, 61(sup1):22–29.

Ko, I., Davis, A. P., Kim, J.-Y., and Kim, K.-W. (2007). Arsenic removal by a colloidal iron oxide coated sand. *Journal of Environmental Engineering*, 133(9):891–898.

Kosugi, K. (1996). Lognormal distribution model for unsaturated soil hydraulic properties. *Water Resources Research*, 32(9):2697–2703.

Kumar, A., Gurian, P. L., Bucciarelli-Tieger, R. H., and Mitchell-Blackwood, J. (2008). Iron oxide-coated fibrous sorbents for arsenic removal. *American Water Works Association*, 100(4):151–164.

Kutílek, M. and Nielsen, D. R. (1994). *Soil hydrology: texbook for students of soil science, agriculture, forestry, geoecology, hydrology, geomorphology and other related disciplines.* Catena Verlag.

Lai, C. and Chen, C.-Y. (2001). Removal of metal ions and humic acid from water by iron-coated filter media. *Chemosphere*, 44(5):1177–1184.

Lai, C., Lo, S., and Chiang, H. (2000). Adsorption/desorption properties of copper ions on the surface of iron-coated sand using BET and EDAX analyses. *Chemosphere*, 41(8):1249–1255.

Lehman, A. (2006). Technosols and other proposals on urban soils for the WRB (World Reference Base for Soil Resources). *International agrophysics*, 20(2):129.

Lehmann, A. and Stahr, K. (2007). Nature and significance of anthropogenic urban soils. *Journal of Soils and Sediments*, 7(4):247–260.

Lo, S.-L., Jeng, H.-T., and Lai, C.-H. (1997). Characteristics and adsorption properties of iron-coated sand. *Water science and technology*, 35(7):63–70.

Lorenz, K. and Lal, R. (2009). Biogeochemical C and N cycles in urban soils. *Environment International*, 35(1):1–8.

Lukasik, J., Farrah, S. R., Truesdail, S. E., and Shah, D. (1996). Adsorption of Microorganisms to Sand Diatomaceous Earth Particles Coated With Metallic Hydroxides. *KONA Powder and Particle Journal*, 14(0):87–91.

Lura, P., Bentz, D. P., Lange, D. A., Kovler, K., and Bentur, A. (2004). Pumice aggregates for internal water curing. In *Proceedings of International RILEM Symposium on Concrete Science and Engineering: A Tribute to Arnon Bentur*, pages 22–24. RILEM Publications SARL Evanston.

Lytle, D. A., Magnuson, M. L., and Snoeyink, V. L. (2004). Effect of oxidants on the properties of Fe (III) particles and suspensions formed from the oxidation of Fe (II). *American Water Works Association*, 96(8):112–124.

Ma, M., Zhang, Y., Yu, W., Shen, H.-y., Zhang, H.-q., and Gu, N. (2003). Preparation and characterization of magnetite nanoparticles coated by amino silane. *Colloids and Surfaces A: Physicochemical and Engineering Aspects*, 212(2):219–226.

Makhelouf, A. (2009). The effect of green spaces on urban climate and pollution. *Journal of Environmental Health Science & Engineering*, 6(1):35–40.

McLaughlin, J., Ryden, J., and Syers, J. (1981). Sorption of inorganic phosphate by iron and aluminium containing components. *European Journal of Soil Science*, 32(3):365–378.

Mehra, O. and Jackson, M. (1958). Iron oxide removal from soils and clays by a dithionite-citrate system buffered with sodium bicarbonate. In *National conference on clays and clays minerals*, volume 7, pages 317–327.

Melchior, S. (2016). Bodenmanagement und bodenkundliche Baubegleitung auf den Deckeln der Bundesautobahn 7 in Hamburg. *Bodenschutz*, 3(42234):93–96.

Michel, F. M., Ehm, L., Antao, S. M., Lee, P. L., Chupas, P. J., Liu, G., Strongin, D. R., Schoonen, M. A., Phillips, B. L., and Parise, J. B. (2007). The structure of ferrihydrite, a nanocrystalline material. *Science*, 316(5832):1726–1729.

Miretzky, P. and Cirelli, A. F. (2010). Remediation of arsenic-contaminated soils by iron amendments: a review. *Critical Reviews in Environmental Science and Technology*, 40(2):93–115.

Morel, J. L., Chenu, C., and Lorenz, K. (2014). Ecosystem services provided by soils of urban, industrial, traffic, mining, and military areas (SUITMAs). *Journal of Soils and Sediments*, pages 1–8.

Nanda, K., Maisels, A., Kruis, F., Fissan, H., and Stappert, S. (2003). Higher surface energy of free nanoparticles. *Physical review letters*, 91(10):106102.

Nehls, T., Rokia, S., Mekiffer, B., Schwartz, C., and Wessolek, G. (2013). Contribution of bricks to urban soil properties. *Journal of Soils and Sediments*, 13(3):575–584.

Nehls, T., Schwartz, C., Kim, K.-H. J., Kaupenjohann, M., Wessolek, G., and Morel, J.-L. (2015). Letter to the editors. Phyto-P-mining—secondary urban green recycles phosphorus from soils constructed of urban wastes. *Journal of Soils and Sediments*, 15(8):1667–1674.

Noguera, P., Abad, M., Puchades, R., Noguera, V., Maquieira, A., and Martinez, J. (1996). Physical and chemical properties of coir waste and their relation to plant growth. In *International Symposium Growing Media and Plant Nutrition in Horticulture 450*, pages 365–374.

Oberndorfer, E., Lundholm, J., Bass, B., Coffman, R. R., Doshi, H., Dunnett, N., Gaffin, S., Köhler, M., Liu, K. K., and Rowe, B. (2007). Green roofs as urban ecosystems: ecological structures, functions, and services. *BioScience*, 57(10):823–833.

Peters, A. (2013). Simple consistent models for water retention and hydraulic conductivity in the complete moisture range. *Water Resources Research*, 49(10):6765–6780.

Peters, A. (2014). Reply to comment by S. Iden and W. Durner on "Simple consistent models for water retention and hydraulic conductivity in the complete moisture range". *Water Resources Research*, 50(9):7535–7539.

Peters, A. and Durner, W. (2006). SHYPFIT 2.0 User's Manual. Technical report, Institut für Geoökologie, Technische Universität Braunschweig.

Peters, A., Iden, S. C., and Durner, W. (2015). Revisiting the simplified evaporation method: Identification of hydraulic functions considering vapor, film and corner flow. *Journal of Hydrology*, 527:531–542.

Rhoton, F. and Bigham, J. (2005). Phosphate adsorption by ferrihydrite-amended soils. *Journal of environmental quality*, 34(3):890–896.

Rhoton, F., Bigham, J., and Lindbo, D. (2002). Properties of iron oxides in streams draining the loess uplands of Mississippi. *Appl Geochem*, 17(4):409–419.

Rokia, S., Séré, G., Schwartz, C., Deeb, M., Fournier, F., Nehls, T., Damas, O., and Vidal-Beaudet, L. (2014). Modelling agronomic properties of Technosols constructed with urban wastes. *Waste Management*, 34(11):2155–2162.

Romano, N. and Santini, A. (1999). Determining soil hydraulic functions from evaporation experiments by a parameter estimation approach: Experimental verifications and numerical studies. *Water resources research*, 35(11):3343–3359.

Rommel, J. (2000). *Einfluß linearer Alkylbenzolsulfonate auf Mobilität und biologische Verfügbarkeit von Cadmium und Kupfer in Böden*. Shaker.

Rossiter, D. G. (2007). Classification of urban and industrial soils in the world reference base for soil resources (5 pp). *Journal of Soils and Sediments*, 7(2):96–100.

Roth-Kleyer, S. (2005). Substrate für Retentionsbodenfilter. *Neue Landschaft*, pages 29–34.

Roth-Kleyer, S. (2007). Vegetationstrag und Dränschichten für Dachbegrünungen. *Neue Landschaft*, pages 39–45.

Rusch, B., Hanna, K., and Humbert, B. (2010). Coating of quartz silica with iron oxides: Characterization and surface reactivity of iron coating phases. *Colloids and Surfaces A: Physicochemical and Engineering Aspects*, 353(2):172–180.

Sailor, D. J. and Hagos, M. (2011). An updated and expanded set of thermal property data for green roof growing media. *Energy and buildings*, 43(9):2298–2303.

Sailor, D. J., Hutchinson, D., and Bokovoy, L. (2008). Thermal property measurements for ecoroof soils common in the western US. *Energy and Buildings*, 40(7):1246–1251.

Sakurai, K., Teshima, A., and Kyuma, K. (1990). Changes in zero point of charge (ZPC), specific surface area (SSA), and cation exchange capacity (CEC) of kaolinite and montmorillonite, and strongly weathered soils caused by Fe and Al coatings. *Soil Science and Plant Nutrition*, 36(1):73–81.

Santamouris, M., editor (2001). *Energy and Climate in the Urban Built Environment*. Routledge: London.

Sauvé, S., McBride, M., Hendershot, W., et al. (2000). Adsorption of free lead (Pb) by pedogenic oxides, ferrihydrite, and leaf compost. *Soil Science Society of America Journal*, 64(2):595–599.

Scalenghe, R. and Ferraris, S. (2009). The first forty years of a Technosol. *Pedosphere*, 19(1):40–52.

Scalenghe, R. and Marsan, F. A. (2009). The anthropogenic sealing of soils in urban areas. *Landscape and Urban Planning*, 90(1):1–10.

Schaetzl, R. J. and Thompson, M. L. (2015). *Soils*. Cambridge University Press.

Scheidegger, A., Borkovec, M., and Sticher, H. (1993). Coating of silica sand with goethite: preparation and analytical identification. *Geoderma*, 58(1):43–65.

Schindler, U., Lischeid, G., and Müller, L. (2016a). Hydraulic Performance of Horticultural Substrates—3. Impact of Substrate Composition and Ingredients. *Horticulturae*, 3(1):7.

Schindler, U., Müller, L., and Eulenstein, F. (2016b). Measurement and evaluation of the hydraulic properties of horticultural substrates. *Archives of Agronomy and Soil Science*, 62(6):806–818.

Schneider, M. and Goss, K.-U. (2012). Prediction of water retention curves for dry soils from an established pedotransfer function: Evaluation of the Webb model. *Water Resources Research*, 48(6).

Schwertmann, U. (1964). Differenzierung der Eisenoxide des Bodens durch Extraktion mit Ammoniumoxalat-Lösung. *Zeitschrift für Pflanzenernährung, Düngung, Bodenkunde*, 105(3):194–202.

Schwertmann, U. and Cornell, R. M. (2008). *Iron oxides in the laboratory: preparation and characterization*. John Wiley & Sons.

Schwertmann, U. and Taylor, R. M. (1989). *Minerals in soil environments*, chapter Iron oxides, pages 379–438. Soil Science Society of America.

Scott, T., Sabo, R., Lukasik, J., Boice, C., Shaw, K., Barroso-Giachetti, L., El-Shall, H., Farrah, S., Park, C., Moudgil, B., et al. (2002). Performance and cost-effectiveness of ferric and aluminum hydrous metal oxide coating on filter media to enhance virus removal. *KONA Powder and Particle Journal*, 20(0):159–167.

Séré, G., Ouvrard, S., Magnenet, V., Pey, B., Morel, J. L., and Schwartz, C. (2012). Predictability of the evolution of the soil structure using water flow modeling for a constructed technosol. *Vadose Zone Journal*, 11(1):0–0.

Séré, G., Schwartz, C., Ouvrard, S., Sauvage, C., Renat, J.-C., and Morel, J. L. (2008). Soil construction: A step for ecological reclamation of derelict lands. *Journal of Soils and Sediments*, 8(2):130–136.

Slater, L., Ntarlagiannis, D., and Wishart, D. (2006). On the relationship between induced polarization and surface area in metal-sand and clay-sand mixtures. *Geophysics*, 71(2):A1–A5.

Sposito, G. (2008). *The chemistry of soils*. Oxford university press.

Strauss, R., Brümmer, G., and Barrow, N. (1997). Effects of crystallinity of goethite: II. Rates of sorption and desorption of phosphate. *European Journal of Soil Science*, 48(1):101–114.

Su, C. and Suarez, D. L. (1997). In situ infrared speciation of adsorbed carbonate on aluminum and iron oxides. *Clays and Clay Minerals*, 45(6):814–825.

Sumner, M. E. (1999). *Handbook of soil science*. CRC press.

Szecsody, J. E., Zachara, J. M., and Bruckhart, P. L. (1994). Adsorption-dissolution reactions affecting the distribution and stability of CoIIEDTA in iron oxide-coated sand. *Environmental science & technology*, 28(9):1706–1716.

Thirunavukkarasu, O., Viraraghavan, T., and Subramanian, K. (2003). Arsenic removal from drinking water using iron oxide-coated sand. *Water, Air, & Soil Pollution*, 142(1):95–111.

Trivedi, P. and Axe, L. (2001). Ni and Zn sorption to amorphous versus crystalline iron oxides: macroscopic studies. *Journal of Colloid and Interface Science*, 244(2):221–229.

Tzoulas, K., Korpela, K., Venn, S., Yli-Pelkonen, V., Kaźmierczak, A., Niemela, J., and James, P. (2007). Promoting ecosystem and human health in urban areas using Green Infrastructure: A literature review. *Landscape and urban planning*, 81(3):167–178.

Ulsen, C., Kahn, H., Hawlitschek, G., Masini, E., Angulo, S., and John, V. (2013). Production of recycled sand from construction and demolition waste. *Construction and Building Materials*, 40:1168–1173.

United Nations Population Division (2014). World Urbanization Prospects: highlights. Technical report, United Nations.

Vasenev, V., Anan'eva, N., and Ivashchenko, K. (2013). The effect of pollutants (heavy metals and diesel fuel) on the respiratory activity of constructozems (artificial soils). *Russian Journal of Ecology*, 44(6):475–483.

Veihmeyer, F. and Hendrickson, A. (1931). The moisture equivalent as a measure of the field capacity of soils. *Soil Science*, 32(3):181–194.

Violante, A., Cozzolino, V., Perelomov, L., Caporale, A., and Pigna, M. (2010). Mobility and bioavailability of heavy metals and metalloids in soil environments. *Journal of soil science and plant nutrition*, 10(3):268–292.

Wallach, R. (2008). *Soilless Culture: Theory and Practice*, chapter Physical Characteristics of Soilless Media, pages 41–116. Academic Press, San Diego.

Wallach, R., Da Silva, F., and Chen, Y. (1992). Hydraulic characteristics of tuff (scoria) used as a container medium. *Journal of the American Society for Horticultural Science*, 117(3):415–421.

Wang, H., White, G., Dixon, J., and Turner, F. (1993). Ferrihydrite, lepidocrocite, and goethite in coatings from east Texas vertic soils. *Soil Science Society of America Journal*, 57(5):1381–1386.

Wang, X., Li, W., Harrington, R., Liu, F., Parise, J. B., Feng, X., and Sparks, D. L. (2013a). Effect of ferrihydrite crystallite size on phosphate adsorption reactivity. *Environmental science & technology*, 47(18):10322–10331.

Wang, X., Liu, F., Tan, W., Li, W., Feng, X., and Sparks, D. L. (2013b). Characteristics of phosphate adsorption-desorption onto ferrihydrite: comparison with well-crystalline Fe (hydr) oxides. *Soil Science*, 178(1):1–11.

Weng, Q., Lu, D., and Schubring, J. (2004). Estimation of land surface temperature–vegetation abundance relationship for urban heat island studies. *Remote sensing of Environment*, 89(4):467–483.

Wexler, A. and Hasegawa, S. (1954). Relative humidity-temperature relationships of some saturated salt solutions in the temperature range 0 to 50°C. *Journal of Research of the National Bureau of Standards*, 53(1):19–26.

White, A. F. and Brantley, S. L. (1995). Chemical weathering rates of silicate minerals: an overview. *Chemical Weathering Rates of Silicate Minerals*, 31:1–22.

Whitham, A. G. and Sparks, R. S. J. (1986). Pumice. *Bulletin of Volcanology*, 48(4):209–223.

Wieder, R. K. (1989). A survey of constructed wetlands for acid coal mine drainage treatment in the eastern United States. *Wetlands*, 9(2):299–315.

Wong, J. (1995). The production of artificial soil mix from coal fly ash and sewage sludge. *Environmental Technology*, 16(8):741–751.

Xu, Y. and Axe, L. (2005). Synthesis and characterization of iron oxide-coated silica and its effect on metal adsorption. *Journal of colloid and interface science*, 282(1):11–19.

Yakovlev, A., Kaniskin, M., and Terekhova, V. (2013). Ecological evaluation of artificial soils treated with phosphogypsum. *Eurasian soil science*, 46(6):697.

Zehlike, L. (2016). Aggregation kinetics of TiO 2 and Ag nanoparticles in soil solution. Master's thesis, Technische Universität Berlin.

Zhang, F.-f., Liu, C.-j., Hu, Y.-h., and Qin, J. (2009). A screening of the substrates for Sedum polytrichoides mat producing for roof-greening. *Journal of Shanghai Jiaotong University (Agricultural Science)*, 27(3):215–218.

Zhao, J., Huggins, F. E., Feng, Z., and Huffman, G. P. (1994). Ferrihydrite: Surface structure and its effects on phase transformation. *Clays and Clay Minerals*, 42(6):737–746.

Zinck, J. (2006). Disposal, reprocessing and reuse options for acidic drainage treatment sludge. In *Proceedings in International Conference on Acid Rock Drainag ICARD, St Louis, MO, USA*, pages 2604–2617.